University of Strathclyde Glasgow

Tribology of Bio-implants

A thesis submitted to the University of Strathclyde for the degree of

Doctor of Philosophy

Shayan Sharifi

Department of Mechanical and Aerospace Engineering,

University of Strathclyde,

Glasgow, UK.

October 2013

Declaration of Authenticity and Author's Rights

This thesis is the result of the author's original research. It has been composed by the author and has not been previously submitted for examination which has led to the award of a degree.

Shayan Sharifi

24/10/2013

Declaration

This thesis is based on experiments which were carried out in the Department of Mechanical and Aerospace Engineering at the University of Strathclyde, and were under the supervision of Professor Margaret Stack. The study lasted from October 2010 to September 2013. Some of this thesis has been published as listed below;

Journal publication:

- Micro-abrasion of Y-TZP in tea
  Sharifi, S., Stack, M., Stephen, S., Li, W. and L. Wang
  Wear, Volume 297, Issues 1-2, 15 January 2013, Pages 713-721.

- A comparison of the tribological behaviour of Y-TZP in tea and coffee under micro-abrasion conditions
  Sharifi, S. and M.M. Stack
  J. Phys. D: Appl. Phys. 46 (2013) 404008 (11pp).

- Tribo-corrosion of steel in artificial saliva: application to dental implants
  D. Holmes, S. Sharifi and M.M. Stack
  Submitted to Tribology International.

Dedication

I would like to dedicate this work to my father. I can never thank him enough for the support he has provided to my family and I. I owe this work and my time in Glasgow to him.

Acknowledgements

I would like to express my sincere gratitude and appreciation to my supervisor, Professor Margaret Stack, for introducing me to the challenging and interesting field of tribology. Her guidance, support, dedicated supervision and patience during this work have been a constant encouragement to me whilst I completed this study. Also, I would like to thank the members of the MAE Tribology Group, University of Strathclyde, especially Dr Ghaith Abdulrahman.

I would like to acknowledge the invaluable help and support from members of the Mechanical and Aerospace Engineering Department at the University of Strathclyde, particularly from Professor Donald Mackenzie, Mr Jim Doherty, Mr Gerard Johnston, Mr James Kelly, Mr Chris Cameron and Dr Fiona Sillars.

Lastly, I owe my gratitude to my family for their constant encouragement and support, to my girlfriend Catherine for her patience and kindness, and to my good friends in Glasgow, Mohammad, Soroush, Jafar, Daryan, Roya, Bryce, Shahin, Farbod and Farnaz.

Shayan Sharifi

Tribology of Bio-implants

Shayan Sharifi

Submitted for the degree of

Doctor of Philosophy

Abstract

The service life of bio-materials used as implants depends on many factors. One of the factors which may significantly reduce the implant's service life duration is wear. Many tribologists have attempted to propose a model to predict wear behaviours involving a wide range of material properties and operating conditions, but it is still believed that there is no way of predicting tribological performances of surfaces with absolute certainty. As a result, laboratory tests on wear of different bio-implants are the most trusted method to evaluate the wear performance of such components in this era.

Bio-tribological techniques are developing constantly as long-term clinical results from various designs and materials are needed and wear testing is a critical gating item for preclinical evaluation. Recently, for abrasive wear tests, sphere-on-disc technique in micro-scale has been used to study the performance of different materials under abrasive wear. However, the possibility of occurrence of different wear mechanisms simultaneously in a tribological environment is high. Therefore, methods have been developed to combine

different types of wear mechanisms with a variety of sliding conditions such as tribocorrosion testing.

Wear processes which occur in the oral cavity can lead to dental defects which may require a restoration or replacement of damaged tissues. In the first part of this work the tribological behaviour of Y-TZP, as a dental restoration material, in popular caffeine based soft drinks, tea and coffee, under micro-abrasion conditions is investigated. The results suggested that the tea environment is less detrimental to Y-TZP implants than that of coffee. It was also suggested that Y-TZP implants will last up to twice as long when drinking coffee with milk compared to plain coffee, and up to four times as long compared to coffee with sugar. Evidence from the experiments showed that viscosity and acidity exacerbate the effects of load and exposure time.

The work continues with investigating the tribocorrosion and wear performance of 316L grade stainless steel as an orthodontic material in artificial saliva using a micro-abrasion-corrosion apparatus. The results showed that linearity in the relationship between load and wear volume is limited to certain ranges. Also, the observed differences between the corrosion potentials at the various loads with and without particles indicated that the stability of tribo-films is critically dependent on the tribological conditions in such environments.

Wear is also one of the main limiting factors on the life of total hip joint replacements. As bio-implants in the human body can be exposed to simultaneous chemical/electrochemical and mechanical stresses such as tribocorrosion, the evaluation of such surface degradation were carried out as a combined mechanism of corrosion and mechanical wear. The later part of this work considers and compares the tribological behaviour of a titanium alloy (Ti-6Al-4V) with a CoCr alloy (CoCrMo) as common bearing materials in artificial hip joints, coated with DLC coating under micro-abrasion-corrosion conditions. The results analysis suggested that the combination of DLC coating and CoCrMo can exhibit a better performance for hip replacement applications. Also, the role of adhesion between the coating and substrate on material removal was pointed out.

In order to understand the wear mechanisms involved in each set of experiments, wear mechanism maps were developed to describe the influences of different parameters.

Table of contents

List of tables

List of figures

1

General introduction

1.1Introduction

The service life of bio-materials used as implants depends on many factors. One of the factors which may significantly reduce the implant's service life duration is wear. Wear has been identified as one of the major problems associated with implant loosening, stress-shielding and ultimate implant failure. This is because most materials used in medical devices are subjected to high stresses and high cyclic loading in an aggressive body environment [1]. These parameters can provide a situation which leads to a wear process followed by total failure of the implant, regardless of the material category of the bio-material used. A wear process is the loss of material from a surface, transfer of material from one surface to another or the movement of material within a single surface [2]. The American Society for Testing and Materials (ASTM) has defined wear more accurately as 'damage to a solid surface, generally involving progressive loss of material, due to relative motion between that surface and a contacting substance or substances' [3].

To predict the wear performance of bio-materials used as implants, a variety of experimental arrangements have been used, either by investigating the mechanisms by which wear occurs or simulating the practical applications [4]. There have been attempts to propose a universal model to predict wear. In 1956 Archard and Hirst produced their

definitive paper on the wear of metals under unlubricated conditions, in which mild and severe wear were first defined in terms of observable characteristics. Many tribologists have also applied Archard's equation [5] into their experiments and attempted to complete the equation by adding new parameters. More than one hundred parameters can be found in the literature and most of them are derivatives of Archard's equation. Yet they are only applicable to the specific approaches which tribologists have followed [6]. Meng and Ludema [7] identified nearly 200 'wear equations' involving a wide range of material properties and operating conditions, but it is still believed that there is no way of predicting tribological performances of surfaces with absolute certainty. Therefore, laboratory tests of different bio-materials shall continue until a universal model to predict wear is found and widely accepted.

1.2 Micro-scale wear tests

Surfaces in relative motions always face tribological challenges. Miniaturisation in technology is on-going and dictates the necessity of investigating tribological phenomena at micro and nano scales. The advantage of micro and nano-tribology is that the tribological performance of the surfaces in a relative motion is dominated by the surface properties. This is because the interacting surfaces have a relatively small mass and interaction takes place under lightly loaded conditions [8].

In the case of bio-implants, the most trusted data on the bio-compatibility of a material must come from the actual use of that material in practical clinical examples in humans [9]. For obvious economic reasons, and also safety in case of bio-implants, running complete mechanical assemblies with lubricants contaminated by particulate materials is not practical. The results are often difficult to interpret and are accompanied by extensive collateral damage [10]. Bio-tribological techniques are developing constantly as long-term clinical results from various designs and materials are needed, whilst wear testing is a critical gating item for preclinical evaluation [11]. A variety of experimental arrangements have been used to study wear in micro scale, either by investigating the mechanisms by which wear occurs or by simulating the practical applications [12]. Recently, for abrasive wear tests, a sphere-on-disc technique in micro-scale has been used to study the performance of different materials under abrasive wear. In this type of test a rotating ball is

forced against the test material in the presence of an abrasive slurry. This type of tests is conducted in two main ways: either a fixed ball or a free ball [13]. However, the possibility of the occurrence of different wear mechanisms simultaneously in a tribological environment is high. The importance of an increased wear loss rate, which is attributed to the synergism of wear mechanisms, have inspired the tribologists to attempt to simulate wear systems which consist of wear mechanisms taking place simultaneously. In tribocorrosion tests, for example, methods have been developed to combine corrosion as a wear mechanism with a variety of sliding conditions, such as unidirectional motion, reciprocating motion, fretting and spinning contacts [4]. The techniques used for the current study, in order to evaluate the wear performance of different bio-materials, are micro-abrasion and micro-abrasion-corrosion.

1.3 Thesis outline

Chapter one begins the thesis with a general introduction to the present work. It introduces the challenge of wear in bio-tribology and gives a brief description of each following chapter.

Most types of wear in materials are the consequence of the friction occurring between interactive surfaces. Wear rate and the force of friction are proportional to the normal applied load and independent of the apparent area of contact. Therefore, mechanisms proposed for friction must clearly have some relevance to wear. As a result, it seemed necessary to describe the nature of friction in different materials and the factors that can influence the frictional behaviour of materials. This is addressed in chapter two (Literature review) along with one of the most important factors in the field of tribology; the properties of a surface. The chapter continues with wider definitions of a wear process and classifications of wear using more commonly accepted terms. Different techniques of wear testing, measurement and evaluation are also reviewed.

A wear process can occur when interacting surfaces are in a relative motion. Wear processes which occurred in the oral cavity can lead to dental defects which may require a restoration or replacement of damaged tissues. A dental restorative material should have the capability to recreate the lost function or restore aesthetic appearance [14]. Due to the required biocompatibility, chemical stability, aesthetics, and processing technologies,

ceramics and more specifically zirconia-based ceramics have been widely used in dental practice for the last two decades. It has been reported that abrasive wear is the main wear process in the oral cavity [15]. According to Antunes and Ramalho [16], the abrasive properties of dental restorations are more important than their hardness and the ball cratering technique is an appropriate test to assess these properties. The abrasive wear rate can also be influenced by the properties of the environment. In chapters three and four of this study, the tribological behaviour of Y-TZP in popular caffeine based soft drinks, tea and coffee, under micro-abrasion conditions is investigated. This involves considering wear mechanisms and generating a body of data as a reference for the wear behaviour of Y-TZP in such conditions.

Although the demands for ceramic dental restorations are growing [17], the use of stainless steel for dental crowns, retainers and implants, especially in developing countries, is very common due to economic reasons [18]. The British Society of Paediatric Dentistry (BSPD) has also recommended the use of stainless steel (pre-formed) crowns for the restoration of primary molars with multi-surface lesions, extensive caries (cavities) and those where pulpal treatment has been performed [19].The American Society of Testing and Materials (ASTM) has recommended type 316L for implant fabrication. However, corrosion is a form of wear that can have severe detrimental effects on this material. The importance of corrosion is emphasised in many studies as the interactions between body fluids, and the surface oxide layer may result in adverse biological reactions. This is because ion release can disturb cellular metabolism as well as the failure of the implant [20]. In chapter five the tribocorrosion and wear performance of 316L grade stainless steel as an orthodontic material in artificial saliva using a micro-abrasion-corrosion apparatus is investigated.

Wear is also one of the main limiting factors on the life of a total hip joint [21], [22]. The service life of the current implants is limited to 15 years which is not very pleasant when it comes to patients under 60 years of age. A longer lifetime can be expected if the wear volume of the materials used is decreased significantly [22], [23]. Several research groups have reported excellent bio-compatibility and tribological properties of diamond-like carbon (DLC) as a potential candidate for coatings in orthopaedic applications such as hip replacements [24], [25]. As bio-implants in the human body can be exposed to simultaneous chemical/electrochemical and mechanical stresses such as tribocorrosion, the evaluation of such surface degradation should be carried out as a combined mechanism of

corrosion and mechanical wear [26]. Chapter 6 of this work considers and compares the tribological behaviour of a titanium alloy (Ti-6Al-4V) and a CoCr alloy (CoCrMo) as common bearing materials in artificial hip joints. They are coated with DLC coating and tested under micro-abrasion-corrosion conditions.

Chapter seven ends the thesis with conclusions drawn from the work carried out. It also proposes ideas for further research on wear issues through experimenting and other methods.

2

A literature review on tribology

2.1 Introduction

In today's dynamic world failures and stoppages are associated with interacting moving parts and more specifically with interacting surfaces. The examples for this phenomenon can be observed everywhere, from gears and bearings in machinery to artificial joints in robots and human body. To define, many of the problems are 'tribological'.

Although men throughout the ages found that lubricants and smoother surfaces can facilitate motion and reduce friction, the subject of 'tribology' was first defined and brought to attention in the 1960s. The word 'tribology' is derived from the Greek word *tribos* which means rubbing. The meaning of tribology can therefore be 'the science of rubbing'. Yet, the scientific definition of tribology is in fact 'the science and technology of interacting surfaces in relative motion and of related subjects and practices' [27].

Tribology emerged from attempts to find the best solution to the problem of carrying load across an interface with an acceptable rate of friction and wear. A number of procedures have been proposed to face this problem. The most common procedures are [28]:

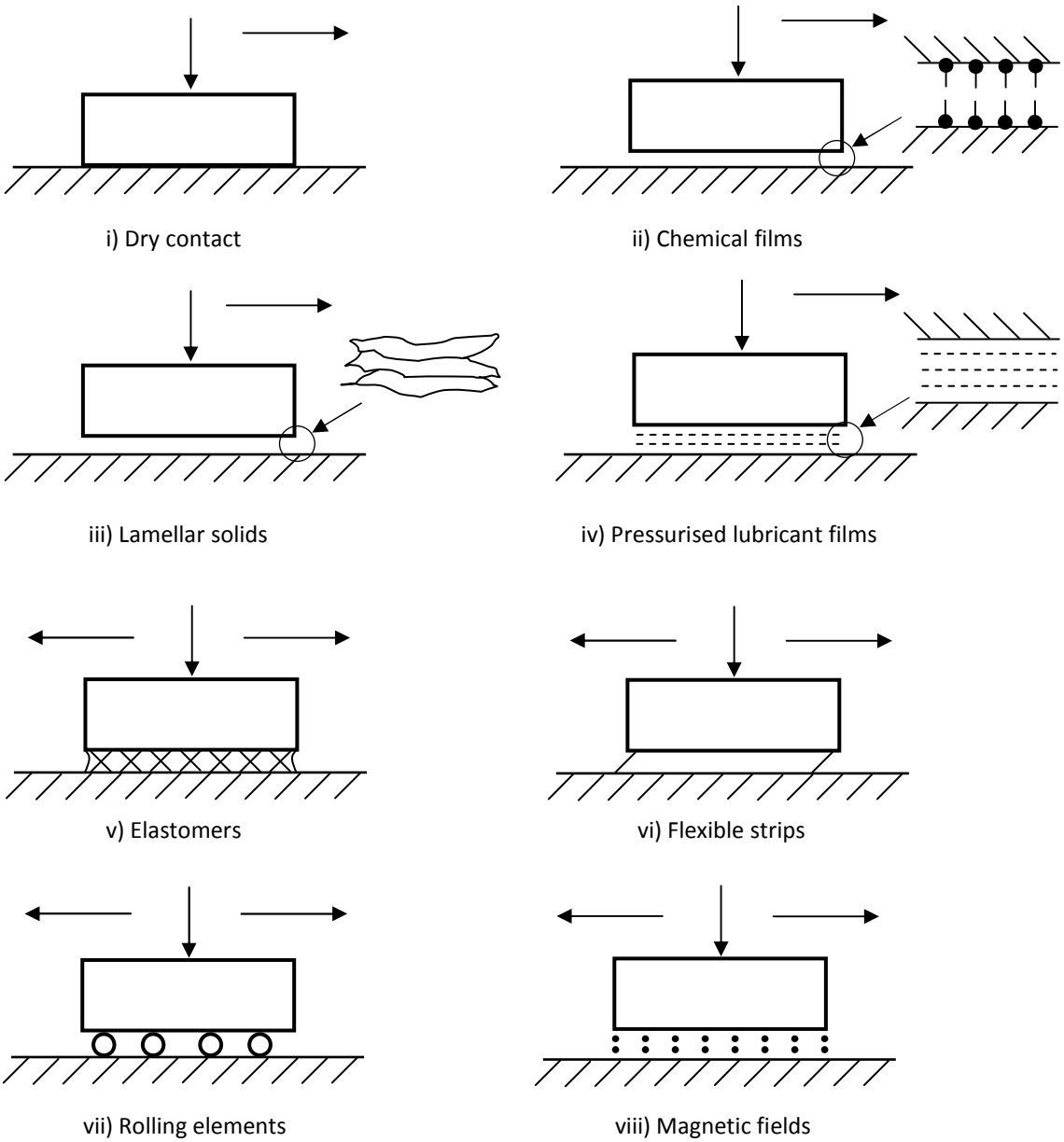

Figure 2.1 – Solution models to face tribological problems

i) Dry contact: This method is normally used for the contacting materials possessing low coefficient of friction and wear resistant.

ii) Chemical films: The chemical films or coatings could be applied to the sliding surfaces to reduce the intimate contacts.

iii) Lamellar solids: Materials with layer structure of low resistance to transverse shear can carry heavy normal loads. Weak bonding between planes at right-angles facilitates sliding.

iv) Pressurised lubricant films: The contacting surfaces can be separated by a continuous film of fluid with a built-in pressure to withstand the applied load.

v) Elastomers: The contacting surfaces can be separated by bonding elastomers when the range of transverse displacement is small.

vi) Flexible stripes: This is an alternative procedure where the degree of transverse displacement is of fairly small amplitude.

vii) Rolling elements: This is a widely used method to facilitate movement between two surfaces.

viii) Magnetic fields: This procedure creates a gap between two interacting surfaces to avoid direct contacts.

2.2 Surface studies and characterisation

The listed methods are simplified solutions to be used with respect to some influential factors. These include environmental conditions, the load to be carried, velocity and limitations which are due to friction and wear. One of the most important factors in the field of tribology is the surface properties. Surfaces are ubiquitous and the roles of them in science and technology cannot be emphasised enough, especially in micro and nano-systems. A surface is the layer organically grown out of a solid with its own special physico-chemical characteristics and functional significance [29]. Surfaces can be produced in different ways. Cutting, rolling, extrusion and drawing, electro-spark erosion, grinding and other abrasive operations are common. Naturally, the texture of a surface layer has different geometric properties to the base of a surface layer with an amorphous or micro-crystalline structure. A surface texture may contain a series of irregularities with different amplitudes and frequency of occurrence. These can even be caused by particles and molecular films which are deposited from the environment. Therefore, to achieve an expected tribological performance from a surface, the study of the topographic features of a surface is a necessity. The texture of a surface is normally defined by the characteristics of the finishing processes by which they are produced. Having a finished surface does not mean that the roughness has been omitted. It means that the amplitude of the hills and valleys fluctuates less. This is because the asperities are far larger compared to molecular dimensions. The distribution of the asperities could be either directional or homogeneous depending on the finishing process characteristics of a surface. The measurement of its

geometrical features and textures falls under micro-metrology category. This can be done optically or mechanically.

According to the definition, tribology is the science and technology of interacting surfaces in relative motion. As well as understanding the surface properties of a single body, it is therefore just as important to choose the appropriate pair or the antagonistic body in order to gain the ideal interactions at the contact point of several surfaces. This is the point where the mission of tribology begins. It should be noted that this does not mean that the interacting surfaces should necessarily both be in a solid phase. The mechanics of contact of the bodies should be well-understood. This involves an understanding of the depth of the surface layer and the nature of the associated deformations and stresses. These can be induced by an applied loading to bodies of a wide variety of geometric shapes. In many engineering contacts, where the bodies are solid materials, they are defined by circular arcs such as wheels on tracks and rolling elements. Also, a method to simplify the solid bodies in contact, where they are not defined as circular arcs, is to consider their surface asperities as very small spherically shaped protuberances. This gives us the opportunity to resolve any load which is inducing a deformation into a normal and a tangential component. Then, the total effect can be studied by superimposing the two parameters. Although this seems an interesting method, it cannot be always the case as the surface asperities are not always homogenous. The applied load is also not always centralised or distributed identically all over the surface. Yet this method is still valid for surfaces with a fairly low surface roughness. There are other methods to measure the area of contact [30]:

i) Using two large model surfaces with asperities greater than one inch in radius where one of them is covered by ink to reflect the point of contact to the other.
ii) Using electrical resistance by considering the electrical constriction resistance between the surfaces. This method is limited to surface oxides.
iii) Adhesion and separation of sticky surfaces. This method is conducted in a vacuum environment where two clean metal surfaces are touched together while applying a small load and then pulled apart.
iv) Acoustic transmission through the contact region between the surfaces.
v) Using optical equipment to see the interference, phase contrast and total reflectance.

Another factor to be considered is the thermal effects in a sliding situation. Assuming the generated heat is a continuous process during the sliding process, the highest temperature occurs at the point of heat release, which is the contact surface. The overall geometry of the surface asperities is the most effective factor in this situation. In a similar story to the applied load, the contact points (asperities) can be treated as an independent heat source. A mean value can also be used to obtain the temperature distribution for the general contact region. It is simpler for curved surfaces, as the contact spots will be close enough together to be regarded as a single heat source. Moreover, the factor that determines whether a body is stationery or moving should be taken into account. The points mentioned above emphasise the importance of having a good understanding of the contacting surfaces' characteristics and, as a result, the importance of the science of tribology.

The simplest method to decrease or even to eliminate the effects of friction and wear is to totally separate the interacting surfaces by means of a viscous fluid either hydro-dynamically or hydro-statically. The general effects of a lubricant in reducing friction are depicted in figure 2.2 which shows the relation between friction and Sommerfeld number [2].

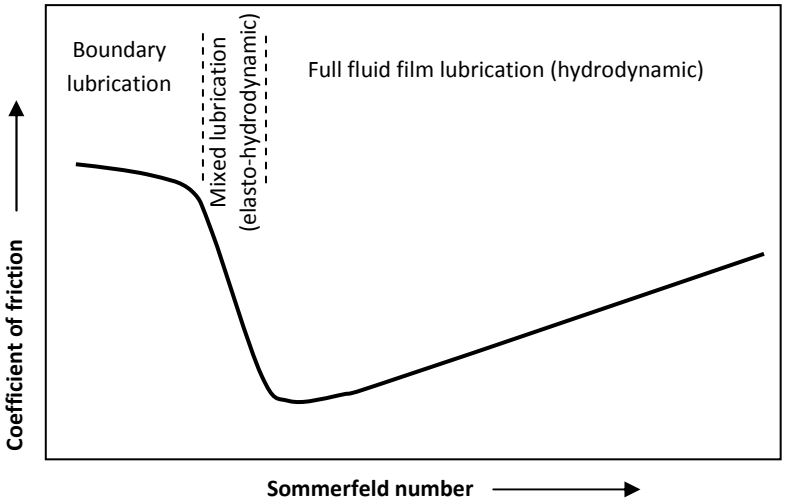

Figure 2.2 – Relation between friction and Sommerfeld number

The Sommerfeld number is ZN/p where Z is the lubricant viscosity, N the rotational speed of the bearing and p is the nominal pressure on the bearing surface. Although lubricants

and lubrication are not included in the scope of this research, using lubricants is not always an option because of two main reasons [28]:

i) The lubricants cannot always separate the solid surfaces effectively, particularly when hydro-dynamically lubricated equipment is in the stopping and starting states.

ii) When for some specific reasons the use of a fluid lubricant is not appropriate.

Therefore, while it is not possible to separate the interacting surfaces, acquiring further information about the tribological properties of surfaces and their topography is necessary. One of the properties to be considered is the hardness of a surface. It is advised for an interactive surface to choose a material that has a hardness several times greater than the contact pressure. If the contact pressure becomes greater than some fraction of the hardness, the likelihood of occurrence a transition from mild to severe wear is very high. For example, for metals this value is around one-third of the hardness. Another important tribological property is mutual solubility. When a pair of materials is chosen to have a surface interaction, particularly for boundary lubricated or un-lubricated sliding, extra care should be taken to choose materials with low mutual solubilities. This is because a high degree of mutual solubility exhibits a very poor tribological performance. Also, the crystal structure of solid surfaces plays an important role in tribological behaviour of the material. Hexagonal close packed crystal structures, for instance, have good tribological properties throughout metals.

In normal atmospheric environments, most metals acquire an oxide film immediately with a thickness of 5 to 50 molecules. This can be beneficial in most cases. Oxidation is a fast process which can be retarded only by the protection of the oxide layer itself [31]. Generally, oxidation takes place when a naked surface is exposed to an environment which it can react with and form a coherent oxide film on the surface. This process slows down over time, but the speed is determined by the characteristics of the corrosion process. Figure 2.3 shows the corrosion-time relation for a system in which a protective reaction product forms [32]. This film can protect the metal from inter-metallic contacts, although it is limited to small loads. The wear behaviour of the acquired films can be divided into two major regimes, mild and severe. Mild regime occurs when the applied load is small and the formed debris is fine and mainly consists of oxide. In this regime the surface shows a high electrical contact resistance and the subsequent surface has a burnished appearance.

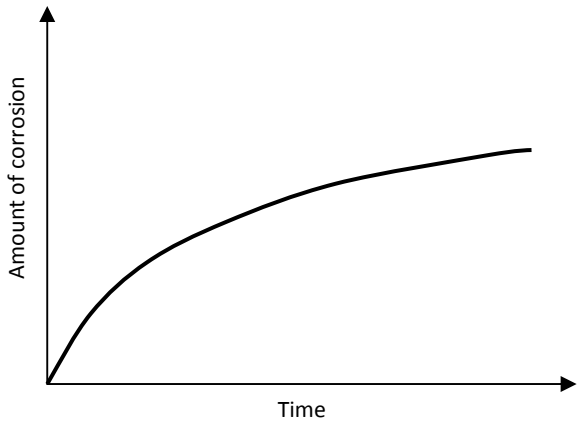

Figure 2.3 – Corrosion-time relation for the formation of oxide films

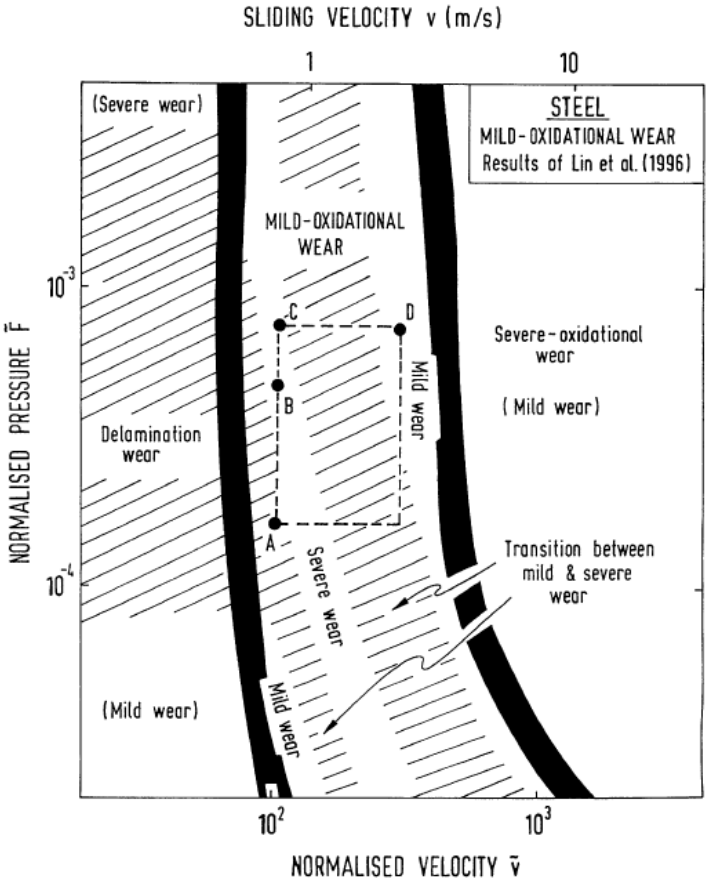

Figure 2.4 – A wear map illustrating transitions from mild to severe wear

When the load is increased, a transition from mild to severe regime takes place. Figure 2.4 illustrates a transition from mild to severe wear due to increased load [33] (Wear maps are reviewed in section 2.9). In severe wear regime, while the contact resistance is low, the

formed debris is made of coarse metallic particles and the subsequent surface will be rough. The transition is caused by deeper penetration and metallic adhesion. This behaviour is highly dependent on the material properties. For example, the acquired film on aluminium is brittle and provides little protection whereas the formed film on steel is tough and tenacious and provides significant protection. Deposition of a protective coating could change the whole story. The importance and role of a deposited coating will be discussed in consecutive sections.

As it mentioned earlier, the effects of temperature are very important, especially in the tribological performance of crystalline solids. An increase in temperature generally reduces hardness and as a result increases the wear rate. Higher temperatures increase the possibility of mutual solubility. And most importantly, temperature is one of the most effective factors in the formed structure of crystalline solids. It also affects the rate of oxidation and the type oxide formed. At low ambient temperatures the oxide layers form only at asperity contacts whereas at high ambient temperatures may not stay limited to the real area of contact [12]. Therefore, to study the surrounding environment prior to material selection is vital in tribology.

'Self-lubricating materials' possess desirable tribological characteristics intrinsically. They are normally categorised into three groups [34–36]:

i) Lamellar solids: In this type of materials the atoms are bonded in parallel and spaced sheets. These materials form a strong adherent transferred film on the surface being lubricated and after a period of work, the interface will consist of lubricant on lubricant. Subsequently, both surfaces develop a preferred orientation which reduces the interaction between the surfaces. The examples of these materials are graphite and molybdenum disulphide.

ii) Inorganic solids: The materials in this category are generally used in high temperature applications. An example of this category is lead monoxide. Although this material has poor performance in degrees below 250^{o}C, it shows excellent lubricating properties in the range of 250 – 650^{o}C. It can be used in ceramic bonded films. Another example of this group is calcium fluoride which is used for temperatures higher than 700^{o}C.

iii) Polymers: The use of these materials can be very advantageous in tribological applications. Polymers can deform into mating parts. They also absorb

vibrations and reduce noises. In addition to their low cost, they can be made in complex shapes and forms. The examples of this group are poly-tetra-fluoro-ethylene (PTFE) and phenolic laminates.

Self-lubricating materials can operate in a wider range of temperatures than fluids with higher chemical stability. They can be used in equipment where cleanliness is important, such as food processing, so that the design could be simplified and the complicated passageways for lubricants can be eliminated. More importantly, they can provide permanent lubrication for parts which are inaccessible after assembly.

Although self-lubricating materials cannot solve all problems relating to tribology, as their major drawback is generating debris, they can make a great contribution to by simplifying designs. Designs with fewer moving parts can eliminate some tribological problems and save money and time. Therefore, before finding a solution, finding ways to eliminate such problems seems logical.

Surface interactions can change the properties of the surfaces. There have been attempts to develop methods to preserve surface properties by applying coatings or developing new materials with enhanced tribological properties such as composites. Surface studies and surface treatments are to meet the design requirements and the required surface characteristics. This is done to face two main incidents in surface interactions: friction and wear. A wide range of studies are allocated towards characterising and developing the knowledge of mechanisms in the interface when friction or wear is occurring. One of the main issues with findings in tribology research is the output of the research cannot be used directly by designers, because it is more convenient for researchers to express the results in terms of non-dimensional parameters. Thus, to provide advice to the industry on how to benefit from existing knowledge, institutions and societies have been setup internationally to provide knowledge in a form that is readily accessible and understood by engineering designers [37]. As the main trigger for introducing the science of tribology was the economic pressure it should be mentioned that, in the expanding technical civilisation, the major causes of material wastages and energy dissipation are wear and friction, respectively. Any improved control of these two phenomena could lead to considerable savings. In this chapter, these two phenomena will be reviewed thoroughly. But first, a brief history of the science of tribology, from Dowson's book [38], from the early ages until the recent century will provide a better understanding of the subject.

2.3 History of tribology

2.3.1 The early civilisations to the middle ages (3500 B.C. – 1450 A.D.)

Archaeological studies show that the early civilisations, specifically in Mesopotamia and Egypt, had a relatively good understanding of tribological interactions; they started using drills, potter's wheel, wheeled vehicles, lubricants and transportation of heavy stone statues and blocks on sledges. Then, Greeks and Romans found the advantages of rolling over sliding and started using plain metal bearings in their devices. The first milling and lathe equipment were developed in this era. It is likely that they had not recognised the accurate aspects of tribology, yet they began to widely employ pulleys, gears, and rolling-element bearings in their equipment [39]. Even horseshoes emerged in this era. The subsequent developments until Middle-Ages from the tribological point of view were not substantial since the form of many materials and machinery in the medieval period originated from earlier times. Yet, the development of water and wind-mills, the use of studded ploughs, wheels, and magnetic compasses and the replacement of sand and water clocks with mechanical clocks all took place in this period.

2.3.2 The Renaissance (1450 – 1600)

What we know on tribology prior to the renaissance is generally based of archaeological studies. From the end of the middle ages, the tribological developments can also be traced more accurately as printing facilitated the expansion of scientific sources.

The first scientific approach towards friction was established by one the greatest tribologists of all times, Leonardo da Vinci. Guillaume Amontons developed the three laws of friction in 1699, which were approved by Charles-Augustin de Coulomb in 1781. However, the contributions of Da Vinci remained unrecognised until 278 years after his death when Bonaparte ordered the transfer of valuable art collections to France in 1796. Leonardo studied the frictional resistance of both horizontal and inclined surfaces and noted the reduced friction in lubricated sliding. These became known as the first and the second laws of friction. He introduced the coefficient of friction for the first time with the estimated value of 0.25. Leonardo also had a touch on basic design of plain bearing where he proposed to employ a split adjustable bush or a designated block to prevent a moving shaft from jumping out of the bearing. He recognised that the amount of wear in a bearing is affected by the magnitude of the load and he tried different types of lubrication systems

and even low-friction bearing alloys in bearings. In 16th century the main interest in tribology was towards pumps and mining equipment and the use of iron and steel bearings. A few valuable books were published by Biringuccio, Agricola, Besson and Ramelli in this field which were clear evidence of their tribological skills and the growing interest in low-friction bearings and hydraulic machinery.

2.3.3 Towards and during the Industrial Revolution (1600 – 1850)

The progress in this period was the continuation of the great achievements during the Renaissance; mainly centred in England and France. The growing urban population increased the demands for piston-pumps to supply water. Also, the economic pressure for fast transportation of heavy loads required manufacturing to need more efficient and reliable bearings. Stevin [40], the Belgian engineer who introduced decimals, designed a sailing chariot which could travel 68 km in 2 hours while carrying 28 men. This was a great achievement and inspired Hooke to work on rolling friction. He suggested that the use of softer metal bearings for shafts and gudgeons and employing seals and effective lubricants for a better bearing operation. Jacob Rowe developed the rolling bearing supports for wheeled vehicles and used a combination of different materials including wood, cast iron, brass, wrought iron and steel to reduce wear. He also implemented friction-wheels on wheeled vehicles, which distribute the axial loads, and claimed that by using this mechanism, a single horse can do the work of two. This was the first official attempt to reduce costs by a tribological innovation.

Specific work on friction was initiated in France by Amontons in 1699 and his findings are today known as the laws of ‘dry’ friction. He found out that friction is proportional to the load and applying pork fat as a lubricant narrows down this proportion. He also suggested that the general value of 0.33 as a constant coefficient of friction (not in the exact name). In the same period in England, John Desaguliers focused on the concept of cohesion between surfaces and the idea of interlocking asperities and tried, though unsuccessful, to find a mathematical approach to quantity of friction in engines. His findings were basically a confirmation of Amontons’ work in France. He even came up with the same value of the coefficient of friction. He also noted that the force of friction may increase between two well-polished surfaces as the surfaces of the bodies come to a closer contact, increasing the attraction of cohesion. In 1750 Leonhard Euler, the famous Swiss mathematician, suggested a valuable mathematical approach towards friction. He was the person who proposed μ as

the symbol of the coefficient of friction. He subtly addressed both static and kinetic frictions and found out the kinetic friction must be smaller than static friction. Sir Isaac Newton also had a touch on friction when he was considering the circular motion of fluids. He pointed out that the resistance of the fluids against flowing which today is known as Newton's law of viscous flow [41] referring to internal friction or viscosity; although he did not use the exact same words. In 1757, John Ladd invented a double reduction chain and sprocket wheel system connecting to the axles of wagons and carriages, which he claimed it as 'a new method of applying friction wheels which takes of a part of the friction and save them much longer from wearing out'. Richard Helsham, 1767, who was a professor of physics and natural philosophy in University of Dublin, published his work based on opposing asperities riding over each other. It showed that resistance caused by a given roughness to a given weight is independent of the magnitude of the surfaces. This was in accord with Amontons second law. C. Varlo, 1772, presented rolling bearings and proposed that a rolling globe which rolls upon a surface, as not to penetrate, would roll forever without stopping. In his statement he dismissed any anxiety over excessive heating by saying 'where there is no friction, there can be no heat'. In 1774, Semen Kirilovich Kotel'nikov, a Russian scientist and one of the Euler's pupils, published a book on the mechanics of equilibrium and the movement bodies and clearly introduced the concept of a 'coefficient of friction', without using the same terminology. He wrote: 'if we denote the friction content *F* and the applied force *P* as unknowns, in the ration μ:1, then friction $F = \mu P$'.

The most comprehensive study of friction in this era was carried out by Charles Augustin Coulomb. In 1781, Coulomb designed an apparatus to evaluate the resistance to motion using different kinds of materials in dry and lubricated conditions. The factors he was investigating were:

1. The nature of the materials in contact and their coatings.
2. The extent of the surface area.
3. The normal load
4. The length that the surfaces remained in contact.

What Coulomb was doing was confirming the previous findings and extending them to kinetic and rolling friction in a way that made the researchers feel all the problems of this topic have been unravelled. He found out that friction is proportional to load and independent of the size of the contacting surfaces. He also proposed that cohesion has a

very small influence on friction which is often negligible. He found a range of coefficient of friction from 0.15 to 0.90, emphasising the role of lubricants to facilitate uniform motion in machines. Also, his findings led to introducing the third law of friction.

'Laws of dry friction:

- **Amontons' First Law:** The force of friction is directly proportional to the applied load.
- **Amontons' Second Law:** The force of friction is independent of the apparent area of contact.
- **Coulomb's Law of Friction:** Kinetic friction is independent of the sliding velocity.'

Interestingly without any knowledge of Coulomb's work, Samuel Vince, a professor of astronomy and physics in Cambridge University, published a paper in 1785 with similar results. He stated in his paper that the kinetic friction of hard bodies is independent of sliding speed.

By the beginning of the Industrial Revolution, due to the spread of mining industry, drainage was one of the big issues; although some simple pumps had been designed by the time to resolve the problem, further development was a necessity. For a long time, miners were using the steam engine drainage piston pumps designed by Thomas Newcomen in 1712; until the winter of 1763, when James Watt was asked to repair one of them. He used a separate condenser to prevent the heat loss which increased the efficiency and the power output of the pump dramatically. Further development in science of friction was mainly associated with the industrial demands in late eighteenth century. Yet the combination of shafts and ball-metal bushes by Robert Hooke was a significant inflection point in the earlier era. The major advances in the principles of hydrodynamic lubrication were not significant until the late nineteenth century by Osborne Reynolds, although the laws of viscous flow were studied a long time ago by Newton. During the Industrial revolution, due to developments in accurate machining and particularly in grinding, the work on rolling-element bearing was continued for different purposes i.e. horse-drawn carriages, locomotive and carriage axles, wind and watermills. By the beginning of the nineteenth century the basic development of steam engines for pumping, milling, general industrial purposes, locomotives and steamships was complete. The main influential reason of developing bearings was the structural change of complete replacement of wood by iron in existing and new forms of machinery and taking advantage of using dissimilar metals in sliding pairs. George Rennie in 1829 conducted an impressive series of experiment and tabulated his results, listing the coefficient friction of a wide range of materials in dry

conditions. Also, he investigated the friction of axles at different speeds, with and without lubricants and created a list of properties of different lubricants. He did not attempt to formulate a theory of friction however. Not very long after publishing Rennie's results, Arthur Jules Morin, a young captain in French army attempted to extend Coulomb's findings in rolling friction, by suggesting that the resisting to rolling is proportional to load and inversely to the radius of the roller. His rival, Arsene Dupuit (1839), had a different theory and believed Morin's results had many numerical errors. Dupuit claimed that rolling friction has an inversely proportion to the square root of the radius of the roller. A year later, Morin revealed his new data and questioned the sensitivity of Dupuit's dynamometer. Half a century later Hertz (1881) provided contact stress analysis to show that Dupuit's theory was more accurate. In the same era, Isaac Babbitt (1839) in the United States presented the possibility of enhancing the mechanical properties of bearing materials by using alloys. The alloy patented by Babbitt consisted of 89% tin, 9% antimony and 2% copper; showing the suitability of low-shear-strength alloys. The lubricants used in this era were mainly from animals and vegetables and it was only towards the end of the period that mineral oils were extracted from shale and coal. However, it was in this period that the science of fluid mechanics and basic understanding of fluid-film lubrication were starting to be developed.

2.3.4 Mineral oil and scientific studies of lubrication (1850 – 1925)

Lubricants were barely studied before this period. While mineral oil was found in large quantities in different parts of the world in nineteenth century, its quantity and price made it the preferred sort of lubricant. Gustav Adolph Hirn published the results of his experiments on lubricants in France. He tested fats, 12 natural oils, water, air, and even mineral oil when it was still widely believed that mineral oil was an unsuited lubricant. He discovered that the coefficient of friction is directly related to the viscosity of the lubricant. He also found out that in a lubricated condition, when the temperature and the viscosity are constant, the coefficient of friction is directly proportional to speed. He subtly proposed that lubricated bearings must be running continuous for a certain period of time to reach a lower and steady value of friction. He suggested that mineral oil could be a suitable lubricant for heavy machines and he was the first person who demonstrated the possibility of using air as a lubricant and prepared the foundation of gas-bearing studies.

In 1879, Robert Henry Thurston, the first president of the American Society of Mechanical Engineers, conducted a series of experiments and published his work reporting coefficients of friction under realistic operating conditions for a wide range of lubricants. This became a reference for the lubrication of machinery. He pointed out the facts of loss of power from 5 to 90 percent due to overcoming friction in machinery. The influence of lubrication in a tribological system is illustrated in figure 2.2. Then, he published a book covering the significance of studying and applying tribological concepts, properties of lubricants and the importance of using appropriate machine elements and instruments with consideration the effects of friction. In Russia, in 1883, Nikolai Pavlovich Petrov realised that it was viscosity and not density which governed the lubricating characteristics of an oil in a given temperature. While he was trying to find a solution for the problems experienced with bearings on the railways, he carried out a comprehensive study of journal friction. In his report he stated that in cases where mediate (lubricated) friction is occurring, the two solid surfaces are totally separated by the liquid film. Instead of using the contemporary concepts of interlocking asperities, he focussed on simple hydrodynamics theories. It was Petrov who confirmed the hydrodynamic nature of mediate friction in journal bearings for the first time and proposed a few empirical equations, which were later known as Petrov's laws. However, what he missed was the action of pressure generation in fluid-film bearings, which was left to Beauchamp Tower in England (1883) to discover. He was appointed by the Institution of Mechanical Engineers' Committee to conduct a series of tests on friction at high velocities. He discovered that in an oil-fed bearing the oil-film is subject to a pressure due to the load and the pressure is variable at different points of the structure. He realised that it is best to provide the bearing with adequate quantities of lubricants, e.g. allowing the rotating shaft to dip into an oil-bath, to achieve repeatable friction measurements. Also, the lubricant should be supplied on the unloaded side of the bearing. The work of Tower provided the basis of the famous analytical study of Osborne Reynolds.

In 1886 Reynolds submitted a paper to the Royal Society on the theory of lubrication, which could be an excellent example to emphasise how careful experimental work can be the launch pad for further engineering development. Like Petrov, he recognised the importance of quantifying viscosity and its relation to the temperature. He pointed out that the film thickness should decrease in the direction of surface motion if load-carrying pressures were to be generated within the film. He presented a mathematical analysis for fluid-film lubrication and introduced an equation, known as Reynolds equation. He calculated that for

a bearing with the length of *l,* the maximum load-carrying capacity per unit width can be attained when the inlet film thickness is about 2.2 times the minimum film thickness. In his paper he also mentioned wear in relation to his theoretical findings and stated that continuous running in one direction may lead to the partial bedding in of the arc journal bearings. He recognised that wear may occur as a result of initial metallic contact, leading to abrasion and the introduction of metallic particles into the oil to blacken it.

After the great achievements of Reynolds, the study of lubricant was carried on with referring to his findings in different parts of the world. In the United States, Albert Kingsbury carried out his experiments on air-lubricated journal bearings. He measured the pressure at various places in the air film in both circumferential and axial directions and studied the effects of speed and published the results of his work in 1897. In Germany, Richard Stribeck (1902) continued experiments on journal friction using various loads and speeds. In 1914, Ludwig Gümbel worked on hydrodynamic problems associated with ship performance to rationalise his suggested results. The comprehensive work in Germany however was done by Arnold Johannes Wilhelm Sommerfeld in 1904 in Aachen. He brought up the cavitation phenomenon and utilised the analytical relationships of Reynolds to cover the lubricating film rupture due to cavitation. In the United Kingdom, W. J. Harrison started to analyse gas bearings in 1913 and extended his work to dynamic loading by 1919. He first solved Reynolds equation for a 360^{o} journal bearing by an incompressible fluid. He compared the differences between journal torques based upon power loss measurements and direct readings of bearing torques. He also considered plane inclined surface bearings and small fluctuations of the load. Martin in 1916 focussed on the gear lubrication and found out that, since the surface roughness of gears were larger than the thickness of the fluid films (by the time), the lubrication of gears was not satisfactory. He suggested that the minimum film thickness, effective radius of curvature, load per unit width, viscosity and mean surface speed should be all taken to account in this matter. In 1917, Lord Rayleigh analysed externally pressurised thrust bearings and the he tried to optimise their structures. T. E. Stanton also in the United Kingdom established his own approach to carry out a research on friction in 1923. He published a paper on the friction of surfaces in rolling contact, in combined rolling and sliding contact in the partially lubricated and completely lubricated and in dry conditions.

In addition to paying attention to the nature of lubricants and their effects on tribology during the period 1850 to 1925, the modern forms of rolling-element bearings also emerged in this era. Ball-bearings were designed and constructed by Benjamin in 1898. Also, in concern with dry friction studies, Kimbell (1877) in America after conducting a series of experiments reported that kinetic friction could be greater or less than static friction. This depends on the nature of the surfaces, the loads, sliding velocities and use of lubricants. Captain Douglas Galton (1878) studied the friction of railway brakes in England and found out the coefficient of kinetic friction in this case is highly dependent on the sliding speed, fixed velocity, or skidding. Furthermore, the sealing of pistons in steam and internal combustion engines were extensively developed in this period. John Ramsbottom invented his piston and piston ring in 1854 which is very similar to present-day piston rings.

2.3.5 Towards tribology (1925 – the present)

It is extremely difficult to mention the tribological achievements in the twentieth century chronologically as the progress in this field was rapid and simultaneous in different parts of the world. Therefore, a brief history of each tribological subject will be discussed.

To have a better understanding of dry contact of engineering surfaces and wear, surface topography became important to the tribologists. Profilometry using a fine diamond stylus became an attractive method and the widest application since it was first introduced by Abbott and Firestone in 1933 at the University of Michigan.

Dry friction was comprehensively studied from geometrical, mechanistic, molecular, adhesive, deformation and ploughing approach points of view. Tomlinson (1929) found a linear relation the surface interacting atoms and the normal load and the tangential force of friction. In 1940, Ernst and Merchant tried to rationalise the relation between surface roughness and the contact asperities angle. Bowden et al. (1943) in Australia ran a series of experiments on adhesion and ploughing and found out that adhesion plays an important role in determining the friction between metals. In 1957 Courtney-Pratt and Eisner discovered that the combination normal loads and shear stresses determine the real area of contact before sliding occurs. Also, the mechanism of rolling and bearings and the influence of both elastic and plastic deformations were widely developed in different parts of the world, including plain bearings, rolling bearings, hydrostatic bearings and gas bearings. Therefore, the selection of materials began to be carried out very carefully. Non-

metallic and polymeric bearings including partially lubricated and self-contained, which could perform without additional lubricants, were developed. De Hart in 1959 reviewed the basic forms and operating characteristics of ball-, roller-, self-acting, and externally pressurised liquid- and gas-lubricated bearings and produced a guidance chart to facilitate bearing selection. In 1964, Neale developed a set of logical procedures towards reliable bearing selection and design for a wide range of loads and speeds. The use of mineral oils as process fluids and effective lubricants developed impressively. By adding particular additives and producing synthetic and solid lubricants for hostile environments and machinery, the pace of developing special purpose equipment significantly increased.

The progress in lubricant technology, tribological materials, theoretical and experimental attack on problems of dynamically loaded bearings and piston rings, and wear facilitated the rapid development of internal combustion engines and reciprocating machinery. After major achievements in steam-turbines and rotor dynamics in the 1920s, no significant attempts were made to change this phenomenon until after the Second World War. Once again the field of bearing-influenced rotor dynamics became the area of interest to predict the thresholds of unstable operations. The stability of the system, critical speeds and the amplitude of vibration at various speeds were studied. Also, in larger rotor systems, e.g. aerospace components, the stiffness and damping coefficient were taken into account. During the third quarter of the twentieth century, due to the increasing demands for high-speed trains, road cars, constructional equipment and aircrafts, the importance of tribology and the tribological behaviour of high-friction materials were highly appreciated when it came to surface contacts, breaking systems and vehicle dynamics.

Although the term *wear* was long recognised in mechanical devices, it was in this era that the importance of wear was fundamentally governed and discussed. In 1969, the Organisation for Economic Cooperation and Development (OECD) defined wear as ‘the progressive loss of substance from the operation surface of a body occurring as a result of relative motion at the surface’. The description induces a negative impression regarding a wear process whereas it could have beneficial effects in many processes including grinding, polishing, writing with pencil or chalk and many more. Prior to this period the classification of wear processes were rather descriptive of the results such as pitting, fretting, scuffing and scoring. The classification however became more analytical by the recognition of five

wear processes as: abrasion, adhesion, fatigue, erosion, and corrosion. These processes will be discussed in detail in the following sections.

Finally, it was in this period, mainly in 1960s and 1970s, the subject known as *tribology* was recognised and received inevitable significance and appreciation due to economic pressures on the life, reliability and efficiency of machinery. Also, the term 'bio-tribology' was introduced by Dowson and Wright in 1973 for the first time which was to cover 'all aspects of tribology related to biological systems'. The most common subjects in this field were self-acting bearings, synovial joints, and the design and development of total joint replacements. Later on, these subjects were extended to a wider range including the abrasive characteristics of human dental tissues, fluid-transport problems ranging from the fluid mechanics of the ureter to the lubrication by plasma of red blood cells in narrow capillaries, and the wear characteristics of bone implants and replacement heart valves.

It should be noted that it was not possible to list every achievement in the history of tribology in this work, particularly during the twentieth century. Therefore, in addition to the presented section a short background of the subjects covered within the scope of this work will be presented in each relevant section.

2.4 Friction

The interactions of the surfaces within a given environment depend on various factors. One of the important factors is the coefficient of friction, especially when the main concern is energy dissipation, which determines the resistance to motion of the interacting surfaces against each other. Also, during the tribological interactions, the properties of the surfaces are continuously altering to certain extents which transform the tribological behaviours. The interacting surfaces can become rougher or smoother and change their hardness. These changes could be beneficial or detrimental based on the purpose of the process. In contrast of the general misconception that the friction is disadvantageous in many of the engineering applications, the required function is fulfilled using friction; such as nut and bolt joints, brakes, and clutches. In this section friction and effects of friction will be reviewed.

Friction is the resistance to the motion of two bodies when they slide against each other. The resisting force is parallel to the direction of the sliding. The friction force is either static or dynamic (kinetic). The static friction force is the magnitude of the tangential force

needed to initiate the sliding motion. The kinetic friction force is the magnitude of the tangential force needed to maintain the sliding motion which is normally smaller than the static friction force. The area of contact and the surface roughness (described in section 2.2) should be well-noted in consideration of friction process. In order to express friction qualitatively, two situations will be encountered [32]:

i) 'Where the resultant of the tangential forces is smaller than some force parameter specific to that particular situation, the friction force will be equal and opposite to the resultant of the applied forces and no tangential motion will occur'. According to Newton's first law when a small tangential force is applied the friction force at the contact is equal and opposite of the applied force. The sliding does therefore not occur. However, this is not completely true. Courtney-Pratt and Eisner (1957) showed that on a microscopic scale when the small tangential force is applied an initial displacement with a distance of 10^{-4} or 10^{-3} mm takes place instantaneously. The motion can carry on if one of the materials tends to creep, otherwise the motion stops.
ii) When the tangential force is sufficient to cause the tangential motion, 'the friction force always acts in a direction opposite to that of the relative velocity of the surfaces'. There are exceptions for this situation as well. If one or both of the surfaces do not have a pronounced directional properties, or they have lapping marks or scratches, the direction of the instantaneous frictional force fluctuates by some degrees. If the face of a crystal is present at the surface, the direction of the frictional force may vary due to the angle of the grain at the surface.

2.4.1 Laws of friction

Friction obeys three main laws mentioned in the previous section (2.3). These laws are quantitative and concerned with the magnitude of the frictional force. The first law states that 'the friction force is proportional to the normal load between the bodies' which defines a constant known as the coefficient of friction (μ). It should be noted that the coefficient of friction is not an intrinsic property of a material. It is very dependent on the sliding bodies and it is constant only for the given pair under given circumstances. For example, the value may vary due to changes in humidity, gas pressure, temperature, sliding speed, contact pressure, and shape of contact. If we have the normal force shown by (*W),* the frictional force (*F*) will be [42]:

$$F = \mu W \qquad (2.1).$$

If the sliding takes place over an inclined plane and the angle of the inclined plane is (ϑ), the coefficient of friction will be:

$$\mu = \tan\theta \qquad (2.2).$$

The first law is generally well obeyed with very rare exceptions. An example for the exceptions is when a surface consists of a hard surface layer and soft substrate. The proportionality of the frictional force to the normal load is consistent unless the load breaks the surface layer through. In this case the characteristics of the substrate become very important.

The second law points out that large and small objects have the same coefficient of friction and the frictional force is independent from the apparent area of contact (*A*). Similar to the first law, this law is generally obeyed with few exceptions. The adhesion occurring during sliding between the clean surfaces is one of the deviations from the second law. In this case, the frictional force become proportional to the real area of contact as the bigger area of contact increases the possibility of adhesion taking place. The adhesion process will be explained later in this section.

The third law emphasises the independence of the frictional force from the sliding velocity. The inference from this law is that, at any specified sliding velocity, the force required to maintain the sliding motion is the same as the force that initiated the sliding. Although this law is approved in many cases, it can be argued. Kato (1972) showed that there are cases of sliding systems where increasing the sliding velocity decreases the coefficient of friction. As a result squeaking and chattering in the system may happen.

2.4.2 The causes of friction and the influential factors

The cause of friction is the interactions between the opposing surfaces. The interactions include adhesion and material displacement. It is widely believed that adhesion is one the factors that has a great impact on friction. Some even believed that friction is due to adhesion. Coulomb, and later Bikerman (1933), denied this idea introducing adhesion as the resistance to normal separation of surfaces whereas friction is the resistance to parallel motion of surfaces. When contacting surfaces are separated by lubricants, the impact of

adhesion is neglected, where this can be easily argued as wetting, surface tension and viscosity are the parameters of bonding forces. Bowden and Tabor in their book [31] studied the surface interactions comprehensively with different names: metallic junctions (adhesion) and ploughing (displacement). Adhesion takes place when the two bodies are loaded together. A plastic flow starts at the tips of the asperities and it continues until the area of contact has grown sufficiently to support the load and this intimate contact may lead to a 'cold weld'. To initiate the sliding motion, the formed junctions should be sheared.

The other cause of friction is material displacement. The material displacement occurs because of either the asperity inter-locking or macro-displacement [42]. To accommodate the relative motion, the surface material should be either deformed or displaced. The relative motion between surfaces A and B, when the asperities are inter-locked (Fig 2.5 – a), cannot occur unless some of the asperities displace. In Fig 2.5 – b material A is a hard material loaded again a softer material, material B, and it is in the rest condition. In order to move material A, material B needs to be deformed. This is happening in a larger scale than the microscopic asperities and called 'macro-displacement'.

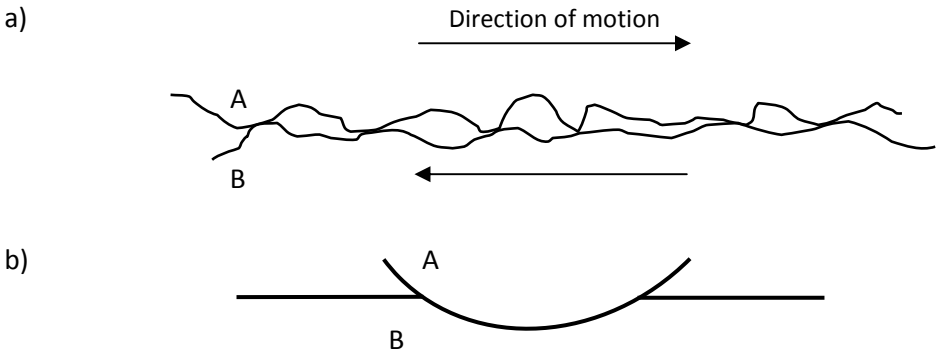

Figure 2.5 – a) Asperity interlocking, b) Macro-displacement

Bowden and Tabor [31] defined the frictional resistance as the sum of two terms, the shearing and the ploughing process. To simplify the form of the contact and separate the forces of shearing and ploughing, they used a hemisphere shape for the hard material and a plane surface for the softer material. They also assumed that the surfaces are perfectly smooth, so the real area of contact is equal to the geometrical area. The hard hemisphere

with the undertaken load (*W*) sinks into the softer material until it is supported sufficiently. If the yield pressure of the softer material (*p*) is known, then the projected area of contact (*A*) will be:

$$A = W/p \qquad (2.3)$$

The shearing force required to face the metallic junction is:

$$S = As \qquad (2.4)$$

where (*s*) is the force per unit area required to shear the junction in a tangent direction to the interface. The ploughing force (*P*) to displace the softer material is:

$$P = A'p' \qquad (2.5)$$

A' is the cross-section of the grooved track and *p'* is the mean pressure value during the displacement. Assuming the *d* is the track width and *r* is the radius of curvature of the hemisphere, equation (2.3) can be re-written as:

$$P = \frac{1}{12}\frac{d^3}{r}p' \qquad (2.6).$$

Therefore, to have the slider moving, the total frictional force (*F*) is:

$$F = S + P = As + A'p' = As + \frac{d^3}{12r}p' \qquad (2.7).$$

The advantage of this method is any type of sliders can be used for this procedure as long as the area of contact is known or calculable. In this theory, Bowden and Tabor have considered friction as a linear phenomenon. However, friction can have non-linear features, too, which should be resolved through dynamic friction such as dependence on velocity. The stick-slip motion is an important non-linear effect due to decrease of friction in higher velocities. As the static friction force is normally greater than kinetic friction force, to initiate the relative motion between the two bodies as they are in the sticking state, the applied load should steadily increase until it exceeds the static friction force. At this point, resistance instantly drops to the value of kinetic friction and acceleration occurs. This in

decrease of the applied force and deceleration until the body sticks again. The stick-slip motion can be found in relative motions such as a car brake vibration and noise [42].

As it was mentioned earlier, when the surfaces are cleaned in the atmosphere, a thin film of oxide, water vapour or other impurities with at least several layers of molecules are present on the surface layer which must be taken into consideration as even the thinnest surface films can affect the frictional behaviour. Although these contaminant films may be removed from the surface by lapping, polishing, or scraping, the most effective method to have a real clean surface is to heat the surface in vacuo [31]. This method significantly increases the possibility of adhesion. Yet it facilitates the more accurate evaluation of the coefficients of friction. Experiments have shown that no matter how small the quantity of contaminants is, it still subsequently affects the intimacy of contact and the frictional force.

During the relative motion, the material may be deformed elastically, plastically or may even be fractured. Plastic deformation is the main cause of energy dissipation. The energy dissipation in the elastic deformations in metals is very small and sometimes negligible as most of the energy is recoverable. In visco-elastic materials such as rubbers however, due to their elastic hysteresis, the energy cannot be recovered. The formation of wear debris is the sign of the occurrence of fracture. Although fracture is also a cause of the energy dissipation, the magnitude of the energy loss is much smaller than the one caused by plastic deformation. This is because the plastic deformation is happening continuously during the sliding whereas the fracture of an asperity and subsequent generation of wear debris takes place after almost a thousand contacts on average.

There are some other factors that can affect the frictional behaviour. Surface melting is one which may not happen frequently but it is possible to occur at very high rubbing speeds, especially when the thermal conductivities of the relative materials are low. In some cases the molten material may act as a lubricant. The sliding velocity can affect the frictional behaviour in different ways. For example in metals and crystalline solids, higher sliding velocities decease the frictional force. This can be because of the reduction of coefficient of friction due to surface melting process. In polymers however, the sliding velocity acts in the opposite way and the reason can be the visco-elasticity response from the materials [30]. Another factor can be the temperature. The greatest amount of energy dissipated due to friction appears in the form of heat at the interface. It is important to calculate the maximum generated heat it terms of selecting appropriate material for the interface. The

generated heat can be considered as two components: a 'bulk temperature' rise and a 'flash temperature' rise. The flash temperature is more important as it creates the 'hot spots' on the sliding surface; it is however relatively constant as the hot spots shift their location during sliding. Temperature does not have major effect on the coefficient of friction unless it is relatively high to increase the oxidation rate which reduces the sliding speed [32]. The starting rate is also important in considering the friction process as a rapid start from standstill condition can lower the coefficient of friction for a short interval. Also, there is an extremely small possible effect of unlike electrical charges. When two different materials are in contact, an electrical double layer may exist at the junctions (adhesion points). This may increase the friction force due to separation of unlike electrical charges.

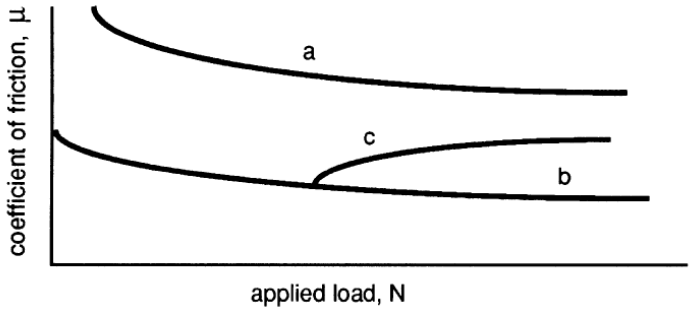

Figure 2.6 – The effects on contact pressure on friction (a) clean surface (b) Treated surfaces (c) oxide surfaces

As it has often been mentioned, the applied load or the contact pressure is a very important factor as well as the surface roughness. Figure 2.6 shows the impact of contact pressure on the coefficient of friction. The coefficient of friction can be very high for some materials especially when they have clean surfaces. Curve 'a' shows that for clean surfaces where the coefficient of friction is around 2, increasing the load in the relative motion can reduce it significantly to a value around 0.5. For the materials with an average coefficient of friction 0.5 due to surface treatment or coatings, this is shown by curve 'b', a similar story takes place though in a smaller range; unless the surface consists of a brittle oxide. The oxide can be chipped off by increasing the load. As a result the clean surface interferes with the relative motion and leads to an increase of the coefficient of friction. This situation has been shown by curve 'c' [30]. The surface roughness, too, can affect the frictional behaviour particularly in a lubricated system where the height of the asperities excesses the thickness of the lubricant films. Also, when the surface possesses larger roughnesses,

the adhesive force decreases significantly as the contact points are less [43]. There are some reports on the role of the wear rate of the sliding materials on friction which will be discussed in the next section.

Further to the factors that can influence the frictional behaviour, it is very possible to observe vibrations in a mechanical sliding system. Although most vibrations are benign, more extreme vibrations can damage the machinery or the products. Vibrations can cause variations in measured friction and the wear rate. The magnitude of vibrations and their effect on friction is difficult to predict. The frictional properties of a material are not absolute and the frictional behaviours of materials are generally examined empirically. Therefore, the results from arbitrary tests cannot lead to a general inference. Although the mechanical dynamics can be evaluated mathematically, the analysed data is highly based on the basic mechanical model chosen for the mechanical model and it is very difficult to verify a comprehensive characterised frictional behaviour in the vibration conditions. Nevertheless it is best to reduce the frictional vibrations by changing the system dynamics to an acceptable range.

2.4.3 Types of frictional contacts

Frictional contacts are classified into four categories:

i) Force transmitting components: Components that are expected to operate without interface displacements. Examples for these are drive surfaces or traction surfaces such as wheels on the roads and power belts and clamped surfaces such as bolted joining surfaces in the machines and hose clamps.

ii) Energy absorption-controlling components: Materials with intermediate coefficient of friction such as materials used for brakes and clutches to undertake large normal forces and causing low vibration.

iii) Quality control components: Materials used should be capable of undertaking constant friction. For example to produce uniform fabric in knitting and weaving of textiles, the tightness of weave should be controlled and reproducible. Another example can be sheet-metal rolling mills where to maintain the uniformity of thickness, width and surface finish, the coefficient of friction should be well-controlled.

iv) Low friction components: Materials used where the energy losses should be minimised and precision and maximum efficiency are expected such as gears in watches.

2.4.4 The measurement of friction

There are several methods to measure friction. Before considering the test methods, we should note that the data from the test are not generally constant and rarely reproducible. This is not due to the procedure or the operator's skills. The main reasons are inhomogeneity of the sliding materials, vibrations and unpredicted motions due to the mechanical dynamics of the machinery or the data collector. Although there are several kinds of standards commercially available devices to measure friction, the tested materials should meet some certain criteria and they rarely simulate the real system conditions. To have an accurate set of data, these problems should be taken into consideration. For example, in American Society of Testing and Materials (ASTM), to formulate standards for friction, several identical test devices, samples, and data collectors are sent to several groups of experts. Even though the expected results should be identical, they often differ by 25% or more. The data gets revised, agreed on, and formulated after a few meetings by the committee [30].

The basic method to measure the friction is to measure the force required to initiate the sliding. This method can be performed using a tilting plane apparatus. The normal load can be simply controlled and the friction angle (ϑ) can be measured directly leading to the static coefficient of friction. Figure 2.7 shows a schematic view of the apparatus [32]. In the tilting plane apparatus, the coefficient of friction is calculated using equation 2.2. Another basic method to measure friction is to use pulleys and weights (Figure 2.8).

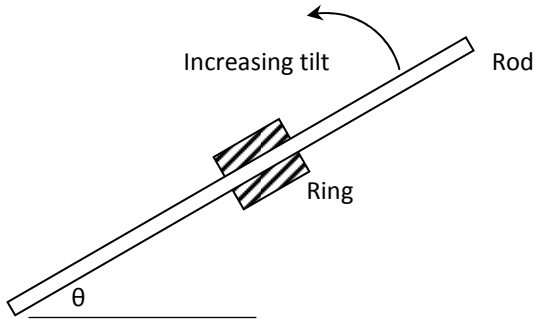

Figure 2.7 – Tilting plane schematic view

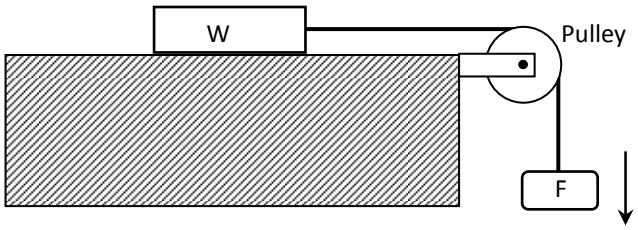

Figure 2.8 – Dead load apparatus

The dead weights are acting as the frictional force (*F*) in this method and it gets increased until the sliding of the slider (*W*) is initiated and then the static coefficient (μ_s) can be calculated.

$$\mu_s = F_s / W \qquad (2.8)$$

To calculate the kinetic coefficient of friction (μ_k), the dead weights are applied and the slider is moved manually and released. This action gets repeated until a uniform velocity is observed and then the kinetic coefficient of friction will be:

$$\mu_k = F_k / W \qquad (2.9).$$

For measuring the friction during sliding and of course the coefficient friction under dynamic conditions, using a dynamometer method is very common where a stationery body is pressed against a moving surface and the friction force is recorded continuously. These types of machines are classified by range of loads, sliding speeds and vibration characteristics. The most common procedure is to use a pin against a translating plate (disk). The pin helps to narrow the track and also the apparent and the real area of contacts are equal. There are some other forms of geometry for the contact point to be used based on the purpose and the conditions of the tests such as cylinder on cylinder, three pin on a disk, of four-ball apparatus. A simplified form of a pin on disk device is shown in figure 2.9 [30]. To obtain a set of data which reflects the reality, the tests should be done in a manner that simulates the full range of variability of the real environment including the vibration, time of standing still between uses, sliding speed and other relative parameters.

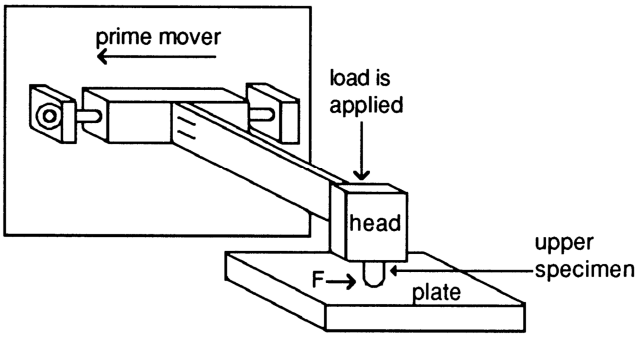

Figure 2.9 – A simplified pin-on-plate device

2.4.5 Friction of materials

When different pairs of materials are rubbed against each other, they may exhibit different types of frictional behaviour even under similar conditions. For common non-metal materials such as wood, leather, and stone against different types of materials, they show a coefficient of friction between 0.2 and 0.6. These types of materials normally do not possess a regular surface pattern and this affects their frictional behaviour. The frictional behaviour in metals and alloys are more sophisticated. To estimate the model of the frictional behaviour of metals, a number of inspections on the test conditions and the material itself should be conducted prior to the test. This includes the sliding speed, contact pressure, cleanliness of the surface, temperature, atmospheric pressure, and relative humidity. The effects of the named parameters have been discussed earlier. The metals with an oriented or single-crystal structures act crystallographically under sliding conditions. However, this is not the case in poly-crystalline engineering alloys. The wear process occurring during the sliding of two metals against each other is also an important factor in the frictional behaviour. For example, after some time of rubbing and removing the oxide layer of from the interfacial layers, the generated oxide and metallic debris may reside on the surface an affect the friction. This phenomenon will be reviewed thoroughly in the next section. Ceramic materials, oxide ceramics in particular, have been used to produce gears, bushings, face seals, slideways, rolling element bearings, tooling and dies for many applications. Therefore, a good understanding of the frictional behaviour of this type material is necessary. The important point is there are many forms and grades of ceramics which are based on the same basic components. For example in metals, when we consider

different kinds of steel, they are based on one basic alloy system (*Fe-C*), but exhibit a variety of frictional behaviours. This is very similar for ceramics, too. For instance, zirconia (ZrO_2) is the basic component of a variety of ceramics which may differ in composition, grain structure, crystal structure, and other properties. Also, the frictional behaviour of ceramics sliding on other ceramics is very sensitive to the relative humidity and the chemistry of the surrounding environment. If the coefficient of friction is ranged between 0.5 and 0.8, the possibility of wear or surface fracture is high. The continuous fracture and presence of debris enhances the friction. Moreover, the coefficient of friction is due to increase in lower humidity as the wear rate is higher. However, when the coefficients of friction of the ceramics are range between 0.1 and 0.3, the possibility of wear happening is substantially lower. It should be noted that this is not valid for a situation where ceramics are coupled with other type of materials. In consideration of frictional behaviour of glass, the data available for the coefficient of friction of glass against other materials is not very wide. Glass produces a coefficient of friction range between 0.1 and 0.7 against metals and polymers [44].

In the study of friction of polymers, they can be considered in two different levels. The first level is during the processing of such materials and their frictional behaviour against injection moulding dies, guides, spools and other components. The second level is when they are used as ready materials such as bearings, gears, seals, bushings, and gaskets, in which the frictional behaviour of the polymers defines the suitability of such materials for the named applications. The visco-elastic and hysteresis properties of polymers play an important role in their frictional behaviour. The internal friction due to weaving of yarns and fabrics in a polymer product can affect the performance of such materials. Bartenev and Lavrentev (1982) classified the friction of polymers into three categories:

i) ‘Friction in the glassy and crystalline states
ii) Friction in the rubbery state
iii) Friction in the viscous state’.

As we are looking at the friction of solid materials, only the first group is the matter of interest. They found non-linear relationships between the friction force of polymers and the normal load, contact pressure, sliding velocity, and temperature. This can be explained by visco-elastic and hysteresis properties of these materials. Thus, the test conditions to predict the frictional behaviour of a polymer should be very similar to the real application

environment. Many polymers are used in combination to control friction and one of the most common additives for this purpose is poly-tetra-fluoro-ethylene (PTFE) which exhibits a low friction coefficient in many applications [45].

The friction measurement tests and attempts to predict the behaviour of materials in applications are to enable engineers to select appropriate materials with required properties. However, sometimes it is best to develop a material to meet the requirements. Surface treatment is one of the most useful methods to do so. Surface treatment can include coatings, overlays, textured finishes, and compositionally modified surfaces. This process is done to address many problems such as friction control, but the method and the material used for treatments should be selected very carefully. For example, a low-friction coating is not a wise choice for surfaces exposed to corrosive environments. Similarly, if the primary reason to apply a coating is to control corrosion the frictional performance of the coating must also be taken into consideration. Therefore a 'balance of properties' is crucial in surface treatments. The properties of the substrate materials are very important and need to be checked before applying any treatments. For instance, two identical coatings can act quite differently under the same frictional conditions. This can be related to the properties of the substrates such as heat flow in the substrates, crystallographic mismatch-induced interfacial strains, residual stresses, and chemical compatibilities [44].

The friction is limited only to bulk bodies. Friction is an important aspect of the role of third-body particles during their flow in the interface. The friction of particle aggregates can be studied as inter-particle friction and the friction between the particles and the containing walls as a third body. In study of particles, the angle of internal friction is basically the source of measuring their static coefficient of friction. The parameters that may affect the inter-particle frictional behaviour are the moisture, internal cohesiveness, shapes and distribution and the roughness of the particles. As the friction between the particles and the containing walls during sliding leads to interfacial wearing, it is time to discuss this subject and its categories in details.

2.5 Wear

The wider definition of a wear process is the loss of material from a surface, transfer of material from one surface to another or the movement of material within a single surface.

In 1964 the Organisation for Economic Cooperation and Development (OECD) launched a programme which aimed to form a basis for reporting and comparing the results of different types of tests. This was in order to come to an agreement on the wear behaviour of different types of material combinations, through the use of various test rigs by the participants. The attempt was unsuccessful as the participants did not find similar results out of their test methods. However, the participating laboratories agreed on the type of wear mechanisms. OCED then defined wear as 'the progressive loss of substance from the operation surface of a body occurring as a result of relative motion at the surface'. The definition was refined by the American Society for Testing and Materials (ASTM) in 2001 as 'damage to a solid surface, generally involving progressive loss of material, due to relative motion between that surface and a contacting substance or substances'. This definition covers degradation by the displacement of material within the surface, surfaces sliding or rolling against one another and the effects of hard particles moving across a surface causing either abrasion or erosion in either diluted or in dry conditions. It is important to note, however, that wear phenomena is not only limited to the descriptions given by the institutions cited [3].

According to DIN 50320, similar to the coefficient of friction, wear is not an intrinsic property of the material but a system property. Hence, the wear performance of a material is based on the wear system. Typically the properties of the interactive surfaces are adjusted to control the effects of wear, but modifications do not necessarily make a surface immune to wear effects [46]. Any kind of interactive surface motion can bring about a wear process and this process can govern the lifespan and the performance of a component. The consequences of occurrence of wear are not only limited to the reactions of the surfaces. For example, the generation and circulation of wear debris in systems where the clearances are smaller to the size of the wear particles is more of a problem than the actual amount of wear. Therefore the impacts of the wear on the whole system should be well-understood [47]. The definition and nomenclature that have been used for different types of wear are fairly confusing. A lack of a good definition has made it difficult to distinguish the defined types wear clearly. The widely accepted names for different types of wear are adhesion, abrasion, fatigue, erosion and corrosion [2]. According to Eyre [47] although transitions occur between different types of wear and a number of wear mechanisms may operate together simultaneously, generally those encountered in industrial situations, 50% are abrasive, 15% are adhesive and the rest are less than 10% each. Williams [48] has also

summarised the sequence of severity in different mechanical wear processes in four different categories (See Table 2.1).

Mechanical wear processes			
Abrasion	**Erosion**	**Adhesion**	**Surface fatigue**
Two & three body	Cavitation	Adhesion	Ratchetting
Polishing	Liquid impact	Fretting	Delamination
Ploughing	Solid impact	Scuffing	Pitting
Micro-machining	Slurry erosion	Galling	

Severity

Table 2.1 – The classification of mechanical wear processes

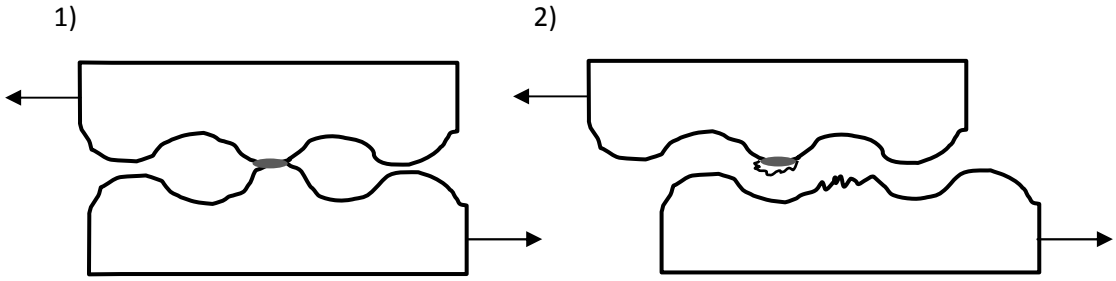

a) Adhesive wear

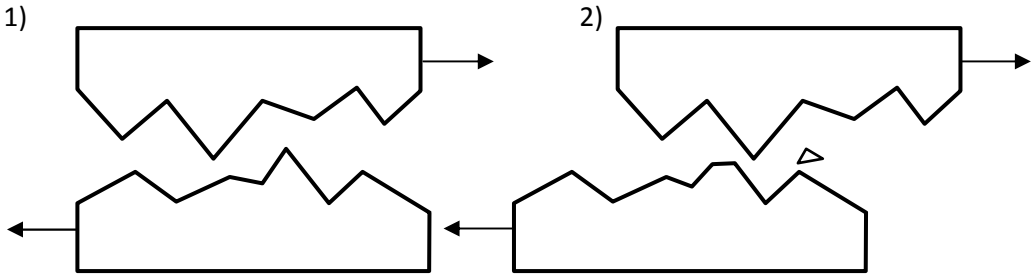

b) Two-body abrasive wear

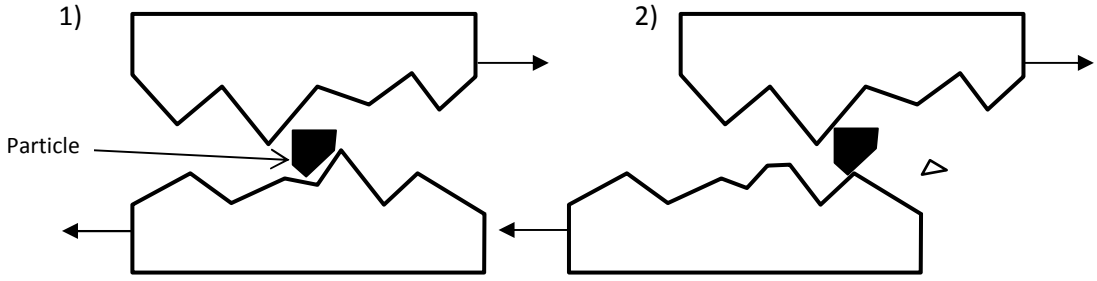

c) Three-body abrasive wear

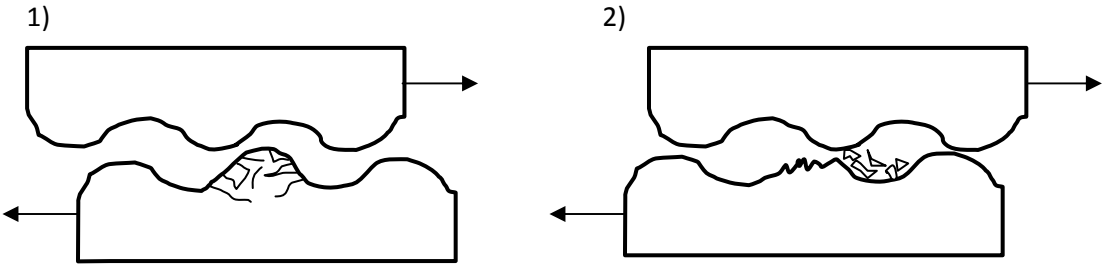

d) Fatigue wear

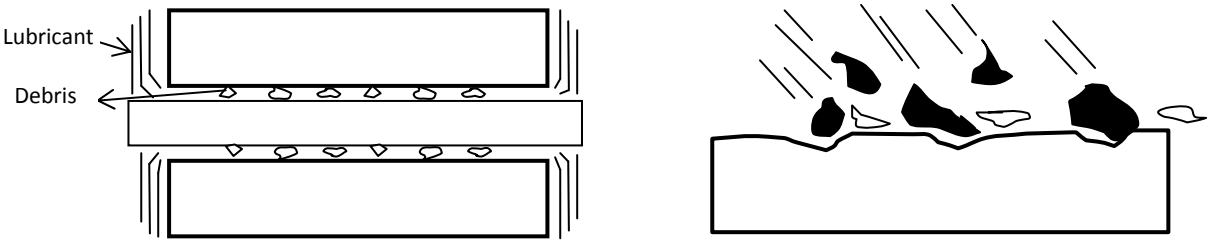

e) Fretting

f) Erosive wear

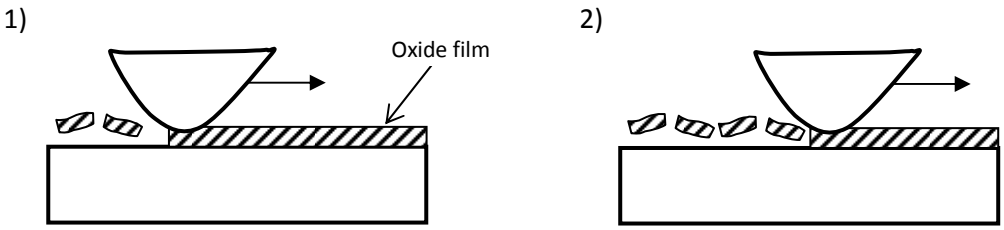

g) Corrosive wear

Figure 2.10 – Different types of sliding wear mechanisms

Three different approaches exist to classify types of wear: the appearance of the wear scars, the mechanisms of material removal and the conditions surrounding the wear situation [49]. In this section the second type of classifications of wear will be reviewed using more commonly accepted terms. Figure 2.10 presents schematic views of different wear mechanisms which are described in the following subsections.

2.5.1 Adhesive wear

As it was mentioned in the previous section, solid surfaces are never smooth on micro-scale and they are covered by asperities. Because of these asperities, when two surfaces are loaded against each other the whole of the two surfaces (the real area of contact) are very

rarely in absolute contact. In fact, the actual area of contact is the average area of an asperity contact multiplied by the number of the asperities in contact. Although this is ideal, it is not practical. When the asperities of two surfaces are loaded together, due to the contact pressure, adhesion takes place between them (see section 2.4.2). In order to move one of the surfaces sideways of the other, the adhesion (junctions) needs to break. That is when the adhesive wear occurs. By continuing the motion new junctions form and rupture continuously. Adhesive wear can be in forms of scuffing, galling, welding, wiping and smearing. Scuffing is not well-defined. It generally occurs when the temperature is heightened due to friction and one of the surfaces gets softened. In this situation severe adhesion takes place and the colour of the surface changes. It causes a change in the crystallographic structure as well as visible damage, but not in a clear pattern. Galling takes place when the relative motion of the surfaces is very slow with a high load which causes plastic deformation of the surface. Wiping and smearing are not very different from each other. When one of the interactive surfaces is significantly softer than one another, the softer material may be wiped and smeared and the frictional temperature does not necessarily need to be high. The softer surface following these phenomena looks smoother or semi-melted.

Adhesive wear does not always result in material loss. If the adhesive strength of the junction is greater than the cohesive strengths of the materials forming the asperities, the junction ruptures within the weaker asperities and results in material loss. However, if the cohesive strengths of the materials forming the asperities are greater than the adhesive strength of the junction, the rupture takes place at the point of contact, without removing any materials from either of the asperities. Typically the breaking point of the junction is very close to the original contact point, but not exactly at the original contact point. Due to the adhesive wear, there is always a possibility of having a number of atoms transferred from one of the loaded surfaces to one another. This means that after the transfer taken place, the next contact will be between two asperities with similar materials and this leads to form a greater adhesion force and of course, greater material loss as a result [2]. Using materials with high cohesive strength between their atoms for interactive surfaces can therefore decrease the material loss due to adhesive wear. Also, very similar to what was explained for ideal frictional behaviour, the inability of the pair to produce bonding (mutual solubility) can be very beneficial as fewer and weaker bonds are ideal for sliding applications. Moreover, the metals with hexagonal crystals show a better performance

under adhesive wear as shear forces in hexagonal crystals are normally smaller than the shear forces in cubic crystals. This is due to the presence of 'easy slip' planes at the surface.

2.5.2 Abrasive wear

When two surfaces are interacting it is possible that, instead of having the surface asperities deformed or adhered because of the load, the asperities on the surface cut through or even plough the other surface. This type of wear is called abrasive wear. Abrasive wear occurs due to moving surfaces or the presence of free abrasive particles or fixed abrasive particles in either surface [50]. Abrasive wear generally happens when one material is softer than one another or when one of the surfaces is experiencing a higher stress than the other. Abrasive wear is the most common type wear encountered and economically very important. The failures due to abrasive wear are not normally catastrophic which means that little attention is brought to the subject. It is very common to use abrasion resistant materials with modified chemical compositions and hardness to face this problem. However, an awareness is growing that it is necessary to study the micro-structure of the materials, especially for materials which deposition and cooling rates are involved in their manufacture [51]. If abrasive wear is to happen, it is common practice to choose one surface with a considerably softer material than the other in order to limit the damage to the component which is easier to replace. The harder material is also given a good surface finish to minimise the abrasion due to the protruding asperities [2].

The elements of an abrasive wear can be divided into six groups: first body, second body, interfacial elements, surrounding medium (environment), relative motion and the contact forces. First body is the surface that is being worn, the wear of which is of most concern. Second body is any counter-face body which is in relative motion to the first body and in direct or indirect contact, to the extent that forces can be transmitted to the first body. The second body may be referred as the counter-body. Interfacial elements or the third body can be any material present at the interface between the first and second bodies [52]. There are a number terms used to describe what we call abrasive wear here such as scoring, scratching and gouging. There is a widely accepted agreement that the abrasive wear can be classified into two main types: two-body (low stress) abrasion and three-body (high stress) abrasion. Two-body abrasion takes place when particles are transported across a surface or two surfaces are sliding against each other. In three-body wear however another body is added to the interface. This could be particles or another surface. The

volume of wear caused by abrasion usually increases linearly with load and sliding distance. This may deviate due to different reasons which include a reduction in particle size of the abrasive or clogging of the surface [47]. In addition to the conventional terms to describe the forms of abrasion, abrasive wear modes can be classified by abrasive particle dynamics at the interface as:

i) Sliding of active abrasive particles at the interface,
ii) Rolling of abrasives between the surfaces.

The sliding of the particles generally causes scratches on the antagonist surface whereas the rolling of the particles results in multiple indentations [50]. Another factor to be considered regarding the role of particles in abrasive wear is the shape of the particles. There are few suggestions to consider the impacts of the shape of the particles by measuring the particles angularity, the average tip radius of the particles and the average tip angle of the particles [53]. Particle angularity can be described by a numerical parameter called spike parameter-linear fit. In this method the particle boundaries are represented by a set of triangles and can be calculated as the fixed step size of the particle. A triangle has a start and an end point. The triangles are described by a 'spike value' which is a numerical parameter and defined as:

$$sv = \cos\left(\theta/_2\right)h \qquad (2.10)$$

where h is the perpendicular height of the triangle and ϑ is the apex angle as shown in figure 2.11.

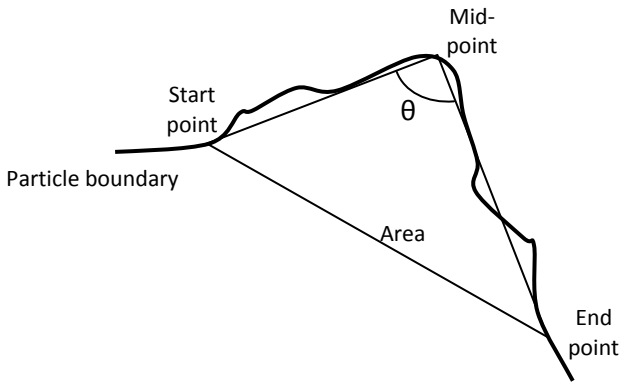

Figure 2.11 - Schematic of calculation method of spike value and constructing triangles round the boundary

To calculate the spike parameter, each 'walk' maximum spike values are normalised by their height and then averaged:

$$sv/_h = cos(\theta/_2) \qquad \rightarrow \qquad SP = \frac{\Sigma\left[\Sigma\left(sv_{max}/_{h_{max}}\right)\right]/m}{n} \qquad (2.11)$$

where h_{max} is the height at sv_{max}, m is the number of valid spike values for a given step size and n is the number of different step sizes used. This method is called Richardson's technique [54]. Although this technique seems quite accurate, it needs a lot of computation and small angles that may not come to the contact with the surface. Recently, an angularity parameter has been introduced called 'spike parameter-quadratic fit' which is more practical and considers only the boundary features that come in contact with the opposing surface [55]:

$$SPQ = sv_{average} \qquad (2.12)$$

It has been reported that there is a strong correlation between the particles angularity and the wear rate in both types of abrasive wear modes which shows that there is a linear relationship between the particles angularity and the wear rate [54]. Another related factor to the role of particles in abrasion is the angle of attack of abrasive asperities and it is reported that the most severe results take place between 80 and 120^o [47], [53]. Of course, the impact of abrasive particles on the relative surface abrasivity is closely related to the surface topography of the surface to be abraded. This was discussed in section 2.2. The reaction of relative surfaces to different types of opposing asperities can form different shapes of scars or damages. Considering the shape of the damage appearing on a surface it can be very useful to understand the nature of the abrasive wear occurring. The shape of the damage can be in the form of a set of grooves or a smooth indentation due to rolling of particles on a surface. Some researchers find it more descriptive if they define the abrasive wear by the shape of the created scar such as grooving abrasion or rolling abrasion [56]. However, it becomes difficult when two mechanisms occur simultaneously or a transition takes place during the wear process. Also, using the conventional terms does not always describe the form of the abrasive wear occurred on a surface. For example, the formation of ridges which are thin bands of unabraded material that appear in the wear scar due to inhomogeneous behaviour of the antagonist body cannot be categorised in either two-body or three-body abrasive wear modes. Ridges are generally formed at the early stages of development of the scar and typically do not alter the background profile of the wear

crater. However, it still affects the wear rate trend [57]. Stack and Mathew proposed a set of new terms to describe the abrasive wear mechanisms which is more descriptive comparing to the conventional two-body and three-body mechanisms [58]. They classified abrasive wear mechanisms into two groups: 3-2 body and 2-body-r.

3-2 body mechanisms are:

i) 2-body grooving: In this mechanism the profile of the scar is mainly formed by grooves with the possibility of formation of ridges. This is due to the adhesion of the abrasive particles to the abrading surface.
ii) 3-body rolling: This mechanism forms a sort of indentation on the surface as the abrasive particles move in non-directional manner on the surface. The roughness of the generated scar depends on the properties of the particles.
iii) Mixed: It is possible in abrasive wear for both of the former mechanisms to appear simultaneously on the worn surface or an incomplete transition may occur. This is due to the fact that, although it is expected to observe the abrasive particles moving within the contact interface, a percentage of the particles may embed in the surface leading to a groove or ridge formation.

2-body-r mechanism takes place when the ridge formation is the dominant phenomenon during the occurrence of abrasive wear. This can result in unexpected wear rates. Despite of the presence of load and abrasive particles, the wear rate may decrease due to entrainment of particles in the formed ridges or some form of protective oxide layers may form on the surface.

The entrainment takes place when the coefficient of friction of the particles and the surface are equal or very close. This can propose a model to find the critical value of diameter of a particle to be entrained or drawn into the contact. The proposed model is illustrated in figure 2.12 [59].

If we assume μ_s is the coefficient of friction between the spherical surface and the particle and μ_p is the coefficient of friction between the particle and the plane, then we have:

$$F_1 = \mu_s F'_1 \qquad (2.13)$$

$$F_2 = \mu_p F'_2 \qquad (2.14)$$

and

$$tan\alpha = \frac{\mu_s - \mu_p}{1+\mu_s\mu_p} \qquad (2.15)$$

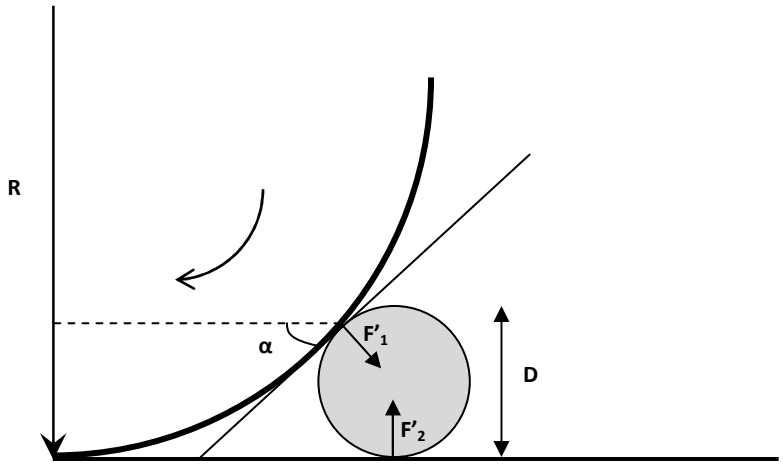

Figure 2.12 – Forces acting on a particle in an interface

If the diameter of the particle is much smaller than the diameter of the spherical surface, then:

$$tan\alpha \approx \left(\frac{2D}{R-2D}\right)^{\frac{1}{2}} \qquad (2.16)$$

Hence, the critical diameter of the particle is:

$$D_{crit} = \frac{R\left(\frac{\mu_s-\mu_p}{1+\mu_s\mu_p}\right)^2}{2(1+(\frac{\mu_s-\mu_p}{1+\mu_s\mu_p})^2)} \qquad (2.17)$$

If the diameter of the abrasive particle is above the critical value, the entrainment takes place. It is also suggested by Williams and Hyncica [10] that there is always a possibility of occurrence of transitions from two-body to three-body abrasion and vice versa due to changes in the motion of the particles in the contact region. This hypothesis assumes that these changes are due to the variation value of *D/h* where D is the particle major axis and *h* is the distance between the interacting surfaces. If the value falls under 1.74, the transition tends to be to 2-body grooving and conversely, the values above 1.74 leads to 3-body rolling. Figure 2.13 illustrates the variables of this critical value.

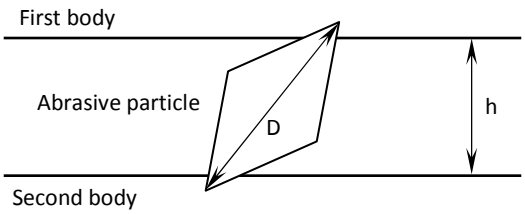

Figure 2.13 – Williams and Hyncica's hypothesis [10]

Knowing the critical values in different wear mechanisms can be very useful, especially for wear mechanism predictions and also to evaluate unexpected outcomes of wear measurement processes which will be discussed in section 2.8.

2.5.3 Gouging wear

Gouging wear typically takes place when a lump of large or heavy particles contact a surface in a matrix or with certain amount of impact. When the particles rub with enough force against the surface, they gouge out the material. Although in gouging wear the stresses at the contact point are high, the loading on the surface is fairly low. Digger blades experience this type of wear very often [2]. Gouging wear can be a subcategory of abrasive wear, but due to the importance of this type of wear in the industry it was introduced in a different section.

2.5.4 Fatigue wear

Due to repeated cycles of stress, such as repeated sliding, rolling or impacting motions, another type of wear may appear on the surface. The cycles of stress can cause cracks to form in or very close to the surface. After a certain period of time the cracks spread and link up and form discrete particles. This type of wear is known as surface fatigue. The particles formed due to surface fatigue are free to move between the contacting surfaces which enhance the wear rate by transforming a wear mechanism called three-body abrasion. The time that it takes for a surface fatigue take place is called the incubation period. it is a common feature of fatigue wear and of conventional fatigue [49]. Although surface fatigue seems to take place after many hours of operation, it happens eventually and should be noted very carefully at the design stage of the components. The life prediction of components susceptible to surface fatigue is more difficult comparing to fatigue of bulk materials, although they are very similar in many aspects. The differences are because of

firstly the variations in the life of components are much greater in surface fatigue and secondly, there is not a fatigue limit stress in the case of surface fatigue. In the case of fatigue of bulk components if the stress is below the fatigue limit stress, the fatigue life of the component is theoretically infinite [2].

In order to discover the form of the surface fatigue, it is very important to consider the nature of the stress systems occurring on the surface as the forms of the cracks are very stress dependent. The study of the stresses can be simplified if divided into macro-stress and micro-stress systems. The macro-stress system is related to geometry. The real area of contact undergoing the stress and the micro-system considers the localised geometry of the asperities. By knowing the nature of the stress systems, the fatigue wear can be encountered more accurately [49].

2.5.5 Fretting

When the interactive surfaces which are loaded against each other undergo small-amplitude oscillatory slip, a type of wear takes place called fretting. While the relative motion continues under this condition, the surfaces get damaged and pitted leading to generating loose debris. The damage keeps growing until the fatigue cracking takes place even under the minimum normal stresses. Fretting is very likely to happen in bearings, gears and splines if the design accuracy is not sufficient. Also, in sliding motions, fretting could occur when the distance of reciprocating sliding is smaller (often 1 mm) than the contact length. Fretting can be considered as a form of fatigue wear as the fretting wear causes producing cracks and then the cracks result in generating wear particles which increase the surface stresses. This is a similar mechanism to surface fatigue [2], [3].

Fretting is a form agitation in the contact which makes small displacements on the surface as a consequence of external vibrations. This consequently results in fretting fatigue due to the cyclic deformations. Fretting damage can be described as two different stages: the wear induced by the fretting and the cracking induced by fretting. The wear is due to the presence of debris at the contacting point which results in material loss. The cracks are due to the vibrations and the consequential stresses which results in the initiation and propagation of the cracks. The two stages sometimes are competing as the debris generated can eliminate small superficial cracks. Deeper cracks, on the other hand, can accommodate the debris generated and reduce the slip amplitude and debris formation.

Similar to most types wear, fretting is influenced by the nature of the loading, contacting bodies, surface coatings, environment, frequency and temperature. To predict the incubation period these factors should be taken into account precisely. After the formation of the first damage, the degradation process is very difficult to be stabilised [3].

2.5.6 Erosive wear

Another type of wear, which is quite analogous to abrasive wear, takes place when sharp particles are impinging on a surface. This type of wear is called erosive wear and there are different types of particle erosion type due to the impact of solid particles, fluid erosion due to the impact of liquid droplets, cavitation erosion due to the impact of bubbles and spark erosion due to the impact of electrical sparks. This section will focus on particle erosion.

During the process of particle erosion fine hard particles, typically with irregular shapes, collide and abrade the surface at a high speed. Each time a particle impacts the surface, a partial abrasive wear takes place. The top surface material can adhere to the surface of the particle due to the impact and can be taken away by a mechanism similar to adhesive wear. By having a continuous flow of fine particles, the severity of the erosive wear can turn it into fatigue wear when crack formation is initiated in the subsurface [3]. Similar to abrasive wear, in erosive wear particles with more angular shapes also result in a higher wear rates [54].

The main difference between abrasive and erosive wears is the altered surface roughness following these phenomena. The surface roughness produced by abrasive wear is considerably milder than the one produced by erosive wear. The impacting particles causing the erosive wear remove the material from lower points on the surface, creating a relatively severe wear mechanism. To simplify understanding erosion phenomenon, it can be considered from two different points of view:

- the amount of the material loss from the surface due to the erosive wear
- the fluid flow conditions and the properties of the impacting particles

The material loss due to erosion can result from the cutting action of the free-moving particles. One of the main factors on the performance of the surface against erosive wear is the type of the surface material. For example, in brittle materials the material removal takes place where the cracks, formed because the erosive wear, intersect. The cracks

normally radiate out from the impact point of the impingement. In ductile materials however, the material loss is because of plastic deformation. The eroding particles displace or cut the material from the surface.

The fluid flow conditions and the properties of the eroding particles can be the factors such as number, direction and velocity of the flow. These can turn this part of the tribological problem into a fluid mechanics problem. Also, shape, hardness, density and concentration are the examples of the properties of the particles which can be considered independently [2].

2.5.7 Corrosive wear

Corrosive wear which is also known as oxidational wear is a form of mild wear in which protective oxide films are formed at the real areas of contact. When the oxide film reaches a critical thickness (typically 1 to 3 μm), the oxide layer starts to break up and eventually appears as wear particles. Corrosive wear can occur at the contact area at extremely low partial pressures as in most operational environment there is sufficient oxygen to facilitate such reactions [60]. As it was mentioned in section 2.4, oxide films are readily formed on most metallic surfaces. These could be beneficial in terms of preventing inter-metallic contact and adhesion. Yet it may not be sufficient to protect or it can become deleterious as the thickness increases. Quinn (1962) proposed two mechanisms in which oxide films may grow and be removed from a surface [61]:

i) The bulk of the oxidation occurs instantly as the virgin metal is exposed. When the interactions of the surfaces begin, the shear of the oxide layer starts at the interface. Although the shear can be small at the beginning, further contacts of the asperities eventually cause growth of the shear.
ii) An equal amount of oxidation occurs at each contact. In this mechanism the growth of the oxide layer depends on the nature of the contact. If the interactions of the surfaces cause the oxide thickness to reach a critical value, then the shearing of the oxide layer begins.

Corrosive wear can often be preferential. Galvanic corrosion and parting corrosion can be examples of such processes. Further studies have shown that the material loss in corrosive wear is due to electrochemical reactions at the surface and a more accurate classification

has been suggested by Chattopadhyay (2001). Corrosive wear can take place in different ways [4], [46]:

i) General corrosion: Corrosion due to the presence of hot oxidising gases or corrosive aqueous solutions. The spontaneous corrosion which normally takes place on a surface of a metal uniformly due to the presence of a corrosive environment.

ii) Galvanic corrosion: In a conductive solution when two metals are in contact, the more anodic metal corrodes while the cathodic metal is not affected. Because the direction of the current is from anode to cathode, the metal with the more anodic potential undergoes an accelerated galvanic corrosion. The rate of the corrosion depends on the magnitude of the current. Another effective factor on corrosion rate is the relative surface contact area as a smaller anodic area leads to more severe anodic metal corrosion.

iii) Intergranular corrosion: This type of corrosion can happen during welding or heat treatment of metals when they are slowly cooled down or held in a temperature between 500 and 850^{o}C. For example in stainless steel, after the formation of chromium carbides at the grain boundaries, the chromium-depleted grain boundary regions are susceptible to Intergranular corrosion in a corrosive environment.

iv) Crevice corrosion: When two parts are mated such as gaskets or screw threaded fittings and entrapped a liquid, they confine the access of the liquid to oxygen. A liquid with a low oxygen concentration in contact with a metal surface can corrode the surface very quickly. This type of corrosion generally occurs in recesses, crevices and the enclosed area of the mated parts.

v) Parting corrosion: This type of corrosion is intentionally conducted to remove an element from an alloy by corrosion. This process is also known as selective leaching and is normally carried out in mild aqueous solutions or in buried pipes and fittings.

vi) Pitting corrosion: Localised corrosions such as pits and cavities can enhance the stress on a surface and result into the failure of the component.

vii) Stress corrosion: This type of corrosion usually occurs when the component is under a high tensile stress in a corrosive environment. This can lead to stress corrosion cracking. The cracking is normally intergranular but it can be transgranular too.

viii) High-temperature corrosion: This is a preferential type of corrosion to modify the mechanical properties of a surface or a component for special purposes such as oxidation, carburisation, nitriding, halogen erosion, sulphidation and molten-salt corrosion. The purpose of this type of corrosion can be enhancing the oxidation resistance, embrittlement, high-temperature resistance, or even destroying protective oxide layers on the surface.

2.5.8 Factors that can influence the wear mechanisms

Although there are a large number of contributing factors in a wear process, there are only general equations that can give estimated results such as Archard's equation, as it contains some of the main variables in sliding wear in relation to volume loss [5]:

$$V = \frac{\kappa NL}{H} \qquad (2.18)$$

where V is the volume loss during wear, κ represents a dimensionless constant known as wear coefficient, N is the normal load, L is the sliding distance, and H is the hardness of the material undergoing wear. This model was initially proposed for metals, but it can provide an insight into the wear of other materials, too. One of the most important outcomes of the equation above is the wear coefficient (κ) which is a valuable means of comparing the severity of wear processes. It should be noted that the wear coefficient does not describe the mechanisms occurred during the wear process [12].

There are many parameters that can influence the wear mechanisms. These include vibration, presence of loose abrasives, nature of the environment, contaminants, and damage in manufacture and assembly. The main adjustable parameters will be discussed in this work.

2.5.8.1 Hardness

Generally, increasing the surface hardness means decreasing the wear rate. For instance, in adhesive wear severe wear can be suppressed to mild by increasing the hardness to 700 VPN. For other types of wear however the wear rate reaction to increasing the hardness of the surface is not a simple relationship. Yet it can enhance the wear performance relatively [2]. This is due to the importance of considering the hardness of the particles that may be present at the interface. Richardson (1968) [62] showed that the hardness of a surface

resisting wear must be greater than half of the hardness of the particles to achieve a good resistance. There is a complex relationship between wear resistance and hardness as the hardness of the material must exceed a critical value K_T:

$$K_T = \frac{H_V \ of \ surface}{H_V \ of \ particles} \qquad (2.19)$$

where K_T must be greater than 0.5. The performance can be enhanced by reaching 1.3, but further than that is not making any considerable changes in the wear resistance. However, the thickness of the surface layer and the hardness of the substrate material can affect these assumptions. As it is costly to harden a material in bulk form, localised hardening is a more reasonable method to enhance the performance of the surface [47]. In abrasive wear increasing the hardness of the interactive surfaces will only weakly increase wear resistance. However, this resistance is normally against three-body abrasion and is much higher than two-body abrasion [63]. Hardness is an important factor regarding investigating and evaluating the severity of a contact in abrasive wear in micro-scale. Adachi and Hutchings have proposed a model to evaluate the severity of a contact in micro-abrasion [64]. Figure 2.14 represents the schematic of their model.

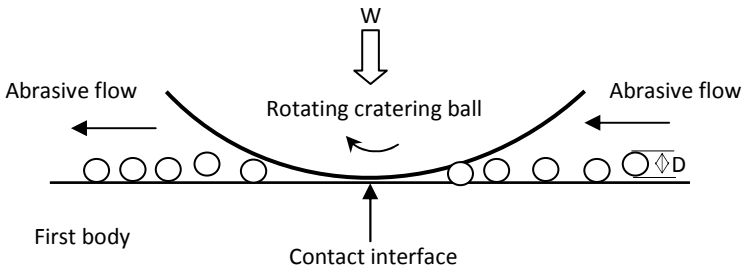

Figure 2.14 – Schematic of the severity of a contact model

Assuming there is a distance (*h*) between the first body and the counter body (rotating ball) and the diameter of a particle is *D*, then we have:

$$h = D - \frac{2P}{\pi D}\left(\frac{1}{H_b} + \frac{1}{H_s}\right) = D - \frac{2P}{\pi D H'} \qquad (2.20)$$

where

$$\frac{1}{H'} = \frac{1}{H_b} + \frac{1}{H_s} \qquad (2.21)$$

and P is the load carried by the particle, H_b is the hardness of the ball and H_s is the hardness of the surface. By having N particles in the interaction area A, hence:

$$N = \frac{Acv}{\pi D^2} \qquad (2.22)$$

where v is the volume fraction of the particles and c is a constant of proportionality. Therefore:

$$P = \frac{\pi W D^2}{Acv} \qquad (2.23) \rightarrow \qquad h = D\left(1 - \frac{2W}{AcvH'}\right) \qquad (2.24)$$

where W is the applied load at the interface. D/h is the critical value of mechanism transition (see section 2.10). This occurs at a critical value of W/AvH' and is termed as the severity of contact. It is written as:

$$S = \frac{W}{AvH'} \qquad (2.25)$$

If the value of S exceeds the arbitrary value of threshold of severity, a transition from three-body to two-body will take place. Adachi and Hutchings have also found the value of the threshold of severity through empirical findings:

$$S = \frac{W}{AvH'} \leq \alpha\left(\frac{H_S}{H_b}\right)^{\beta} \qquad (2.26)$$

as α≈0.0076 and β≈-0.49. Thus, hardness of the interface body can practically determine the expected wear mechanism in a wear system. Transition to a ridge-dominated mechanism as a function of hardness has also been reported [58].

2.5.8.2 Load

It is widely accepted that increasing load affects the tendency for wear rate to increase although transitions are not unexpected. For example in abrasive wear, ridge formation can result in decreasing the wear rate. Figure 2.15 represents the expected wear rates under applied load in different abrasive wear mechanisms [58]. The proposed plot is similar to

what Lansdown and Price suggested in 1986, although a clear explanation for the non-linear behaviour of wear rate by increasing load was not provided (Figure 2.16) [2].

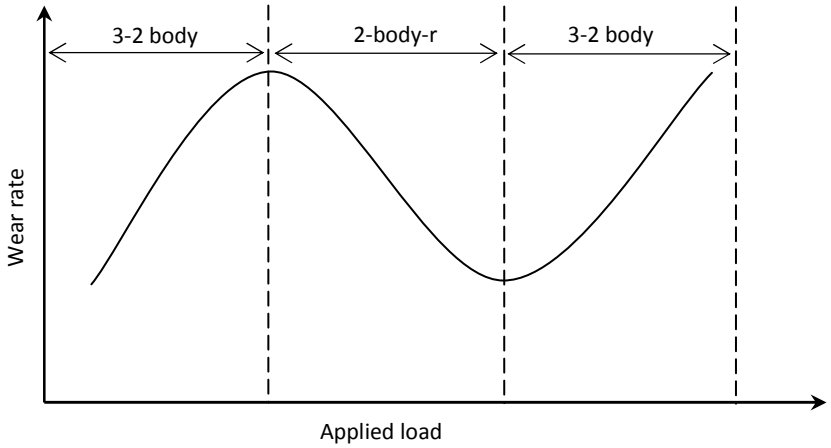

Figure 2.15 - Transitions between the wear mechanisms as a function of increasing applied load

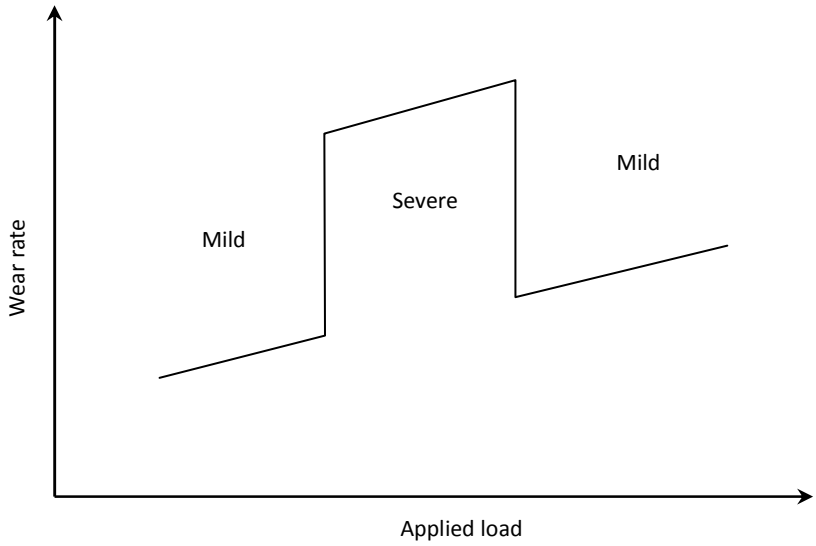

Figure 2.16 – Equilibrium wear rate against load for constant speed

2.5.8.3 Speed and sliding distance

Variations of speed can have considerable effects on the wear rate changes, but there is not a predicted relationship for the changes. For example, Lim and Ashby [65] tried to tackle this challenge by assembling wear data for steel under dry sliding condition from the literature into a wear-mechanism map (Wear-mechanism maps are explained in section 2.10). Although it was an admirable effort, irregularities in effects of speed on wear mechanisms are obvious as depicted in figure 2.17.

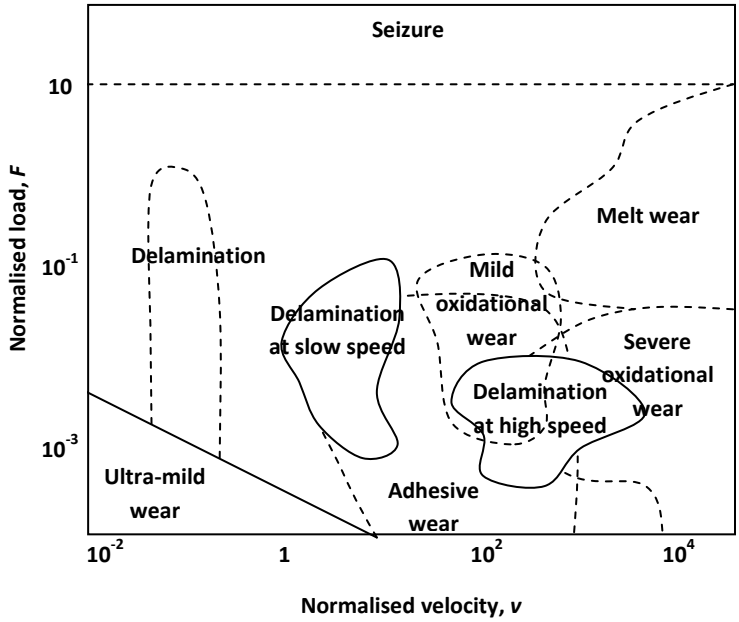

Figure 2.17 – Wear Mechanism map of steel under dry conditions

However, the generally expected behaviour of wear mechanisms affected by the combination of the load and sliding velocity in dry conditions is presented in figure 2.18 [12].

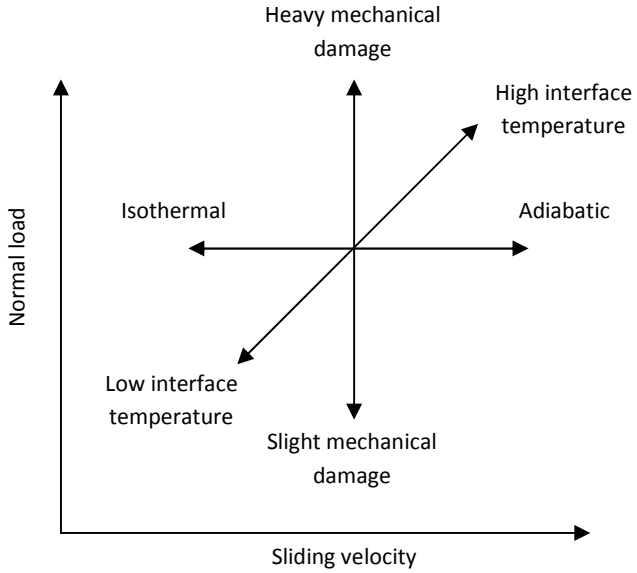

Figure 2.18 – The combined effects of load and sliding speed on sliding wear

Also, longer sliding distances may increase generated heat due to frictional forces. This heightened temperature can result in the formation of protective oxide films on the interactive surfaces can resist wear. It is one of the reasons of having deviation in wear

performance of such surfaces. Having said that it has been reported that after long sliding times, average friction coefficient, magnitude of friction fluctuations, surface roughness, depth of deformed layer and the composition and micro-structure of near surface material tend to become constant. This situation has been named as the 'steady state' [66].

According to Archard's equation, a sliding distance should have a linear relationship with volume loss [5]. It means that increasing sliding distance should increase the volume loss. Stack and Mathew [58] has pointed out that this relationship can be more complicated than a linear relationship. This contradiction is because increasing sliding distance generally leads to an increase in the real area of contact and a reduction of the applied load at the interface and on the particles present at the interface. Therefore, the slope of the linear relationship may decrease due to longer sliding distances [28].

2.5.8.4 Surface roughness

Surface roughness plays an important role in the wear performance of surfaces, particularly in abrasive and adhesive wears. Even though some surfaces are very smooth at the beginning of their operations, they can become roughened during their service time. Gradually they can reach a surface roughness equilibrium called 'run-in' roughness. For the contact between rough surfaces, the actual contact between the surfaces takes place only at localised spots (asperities). In order to consider the wear behaviour of such surfaces the contacts should be investigated on a microscopic scale. In this situation, the effects of load should be taken into account simultaneously as the increasing load can lead to merging adjacent asperities and growth of a micro-contact [67].

2.5.8.5 Temperature

Generally an increasing temperature softens the surfaces and can lead to a higher wear rate. If the temperature reaches to an adequate level, the wear process can be accompanied by creep, thermal fatigue, oxidation and even hot corrosion (molten-salt). Also, frequent and non-uniform heating and cooling of a component can develop the stress to a level where thermal fatigue cracks can be initiated and propagated [46]. However, under conditions which the surface temperatures are relatively high, due to the oxidation of the material, significant changes may apply to the wear performance. For example, as oxides reduce metal loss rates due to reducing or eliminating metal-metal contact, a

transition from severe to mild wear may appear [68]. Figure 2.19 indicates the effects of temperature on wear rate and frictional behaviour of metals [30].

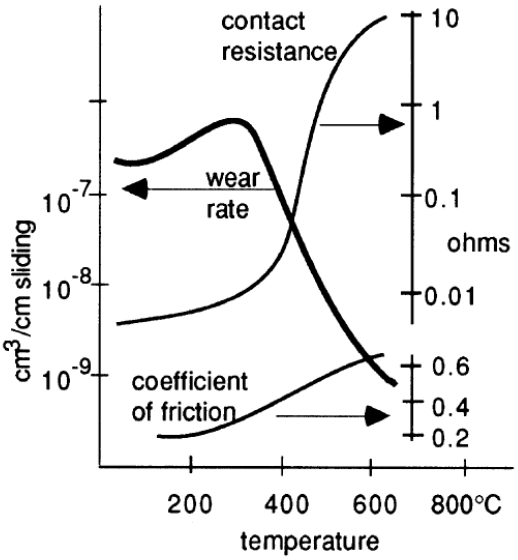

Figure 2.19 – Influences of temperature on wear rate and frictional behaviour of metals

2.5.9 The influence of surface films on a wear process

To resist wear, it is common practice to modify the properties of the surface through physical or chemical methods. Modifying surfaces through formation of adherent surface layers is widely being used due to the technological interest in preparing relatively defect-free surfaces with systematically engineered properties [29]. There are many types of films that are suitable to prevent or decrease the wear rate such as oxides, chlorides and sulphides. To have a higher protection against wear, the film should possess good adhesion, limited thickness, low shear strength and compressive strength less than or similar to that of the substrate material [2].

2.6 Bio-tribology and bio-materials

As it was mentioned in section 2.3, the term bio-tribology was introduced for the first time in 1973 by Dowson and Wright to cover ‘all aspects of tribology related to biological systems’. Jin et al. listed the typical cases of tribology applied to biology as [69]:

i) Wear of dentures
ii) Friction of skin and garments, affecting the comfort of clothes, socks and shoes, and slipperiness
iii) Tribology of contact lenses and ocular tribology
iv) Tribology at micro-levels: inside cells, vessels and capillaries such as lubrication by plasma of red blood cells in narrow capillaries
v) The wear of replacement heart valves
vi) The lubrication of the pump of the total artificial hearts
vii) The wear of screws and plates in bone fracture repair
viii) Lubrication in pericardium and pleural surfaces
ix) Tribology of natural synovial joints and artificial replacements.

Bio-materials are generally the materials used to construct artificial organs, rehabilitation devices, or implants to replace natural body tissues. The European Society for Bio-materials proposed a set of definition for bio-materials as [9], [70]:

i) 'Bio-material: A non-viable material, used in a medical device, intended to interact with biological systems.
ii) Implant: Any medical device made from one or more materials that is intentionally placed within the body, either totally or partially buried beneath an epithelial surface.
iii) Prosthesis: A device that replaces a limb, organ or tissue of the body.
iv) Artificial organ: A medical device that replaces, in part or in whole, the function of one of the organs of the body'.

A bio-material is expected to have a high grade of bio-compatibility where bio-compatibility is defined as 'the ability of a material to perform with an appropriate host response in a specific application' [70]. It is widely agreed that the surface properties of an implant influences the interaction with the biological system [71]. Williams [9] has listed the major material variables that can influence the host response which emphasises the significant role of bio-tribology in evaluating the bio-compatibility of a material (See table 2.2).

The required properties for bio-material depend on the type of the application. For example in case of implants for the replacement of bone tissue, the bio-material should be capable of undertaking high loads. For bio-materials used as contact lenses, the optical

transparency is the major criterion. Nevertheless, in most cases the key factors in selection of a bio-material are bio-compatibility, sterilisability, physical characteristics such as strength, elasticity and durability, and manufacturability [72].

Material variables
Bulk material composition, micro- (or nano)-structure, morphology
Crystallinity and crystallography
Elastic constants
Water content, hydrophobic–hydrophilic balance
Macro-, micro-, nano-porosity
Surface chemical composition, chemical gradients, surface molecular mobility
Surface topography
Surface energy
Surface electrical/electronic properties
Corrosion parameters, ion release profile, metal ion toxicity (for metallic materials)
Degradation profile, degradation product form and toxicity (for polymeric materials)
Leachables, additives, catalysts, contaminants and their toxicity (for polymeric materials)
Dissolution/degradation profile, degradation product toxicity (for ceramic materials)
Wear debris release profile

Table 2.2 – Major material variables that influence the host response

A successful application of a bio-material in the body depends on many factors including the appropriate selection of the material and design of the product. There are other influential factors which cannot be controlled by engineers such as the technique used by the surgeon, the health and condition of the patient and the activities of the patient [73]. Bio-materials can be selected from the three general categories of materials: metals, ceramics and polymers [72]. The following will examine yttria-tetragonal zirconia poly-crystalline (Y-TZP) ceramics and 316L stainless steel as the bio-materials used as denture restoration materials and cobalt and titanium and their alloys as hip joint replacement materials.

Metals have been widely used as bio-materials due to their strength, stiffness, toughness and impact resistance. These are highly desirable for load-bearing applications such as total joint replacements. Major metals used as bio-materials in medical and dental applications are commercially pure (CP) titanium and its alloys, cobalt-based alloys, stainless steel, Ni-Ti alloys, Au-based alloys and dental amalgam (Ag-Sn alloys) [74]. Table 2.3 is a list of common metals used as bio-materials [75].

Metal	Application
Cobalt-chromium alloys	Artificial heart valves, dental prosthesis, orthopaedic fixation plates, artificial joint components, vascular stents
Stainless steel	Dental prostheses, orthopaedic fixation plates, vascular stents
Titanium alloys	Artificial heart valves, dental implants, artificial joint components, orthopaedic screws, pacemaker cases, vascular stents
Gold or platinum	Dental fillings, electrodes for cochlear implants
Silver-tin-copper alloys	Dental amalgams

Table 2.3 – Common metals used for implants

Most of the metals used as bio-materials are chemically modified to:

i) Regulate cellular events and induce specific biological responses,
ii) Improve the amount and stability of bio-molecules,
iii) Obtain a suitable tissue response.

An example can be the preference of high-carbon alloys as carbide protrusions between 0.1 and 0.5 µm provide the necessary hard surface for articulation [74]. In terms of metals used as hip replacement material, experience has shown that the best performance and the optimal balance of mechanical properties with metallic components have achieved with either titanium alloys or cobalt-chromium based alloys. The only major drawback of such alloys is the rate of metal ion release [9].

Titanium is highly reactive material and absorbs water and oxygen very quickly. Typically in air, titanium is covered by a dense passive oxide layer which makes it a highly corrosion resistant and an excellent bio-compatible material [71].

In terms of bio-materials used as denture restoration materials, the good combination of metal-ceramic restorations was preferred by dental practitioners due to predictable strength and reasonable aesthetic for a long time. However, the demand for improved aesthetics by patients enforced the development of ceramics for use with inlays, onlays, crowns, fixed partial denture prosthesis (FPDPs) and implant supported restorations. Increased translucency correlated with improved aesthetic is the primary advantage of an all-ceramic restoration. The durability of a ceramic restoration depends on the material used, design, core-veneer bond strength, crown thickness, bonding techniques and the properties of the supporting material. Fracture of the ceramic material is the most frequently reported cause of failure of a ceramic restoration [76]. The major ceramics used as dental replacement materials are listed in table 2.4.

The most recent type of all-ceramic dental restorations is yttrium tetragonal zirconia poly-crystalline (Y-TZP)-based materials (also known as biomedical grade zirconia) which was initially introduced for biomedical use in orthopaedics for total hip replacement in 1969. Biomedical grade zirconia generally is stabilised by 3mol% yttria (Y_2O_3). The mechanical properties of this type of ceramics are the highest reported for any dental ceramic [77]. This material has excellent mechanical properties and bio-compatibility. Hence, this material is currently being evaluated for complete-coverage dental restorations such as all-ceramic crowns and FPDPs [78]. Y-TZP is composed of many very small particles (metastable tetragonal crystals) without any phase at the crystallite border and has a distinguished crack initiation mechanism [79]. The long-term stability is correlated with crack propagation and stress corrosion. In glass-containing systems (ceramics) the glass reacts to the presence of the water in the saliva which leads to decomposition the glass structures and propagation of the cracks formed. Since Y-TZP is a glass free material and has a poly-crystalline micro-structure, this phenomenon does not occur in Y-TZP restorations which enhances the long-term stability of such restorations [78]. Using nitric oxide synthase measurements, it has been shown that bacterial products of this type of ceramics is lower than other materials used for denture restorations including titanium [80].

Material	Available manufacturing techniques	Clinical indications
Glass ceramic		
Lithium-disilicate (SiO_2-Li_2O)	Heat pressed	Crowns, anterior FDPD, onlays, ¾ crowns, crowns, FDPD
Leucite (SiO_2-Al_2O_3-K_2O)	Heat pressed, Milled	Onlays, ¾ crowns, crowns
Feldspathic (SiO_2-Al_2O_3-Na_2O-K_2O)	Milled	Onlays, ¾ crowns, crowns, veneers, anterior crowns
Alumina		
Aluminium-oxide (Al_2O_3)	Split-cast, milled, densely sintered	Crowns, FPDP, onlays, ¾ crowns, crowns, veneers, posterior and anterior FDPD
Zirconia		
Yttrium tetragonal zirconia poly-crystals (ZrO_2 stabilised by Y_2O_3)	Green milled, milled, sintered, densely sintered	Crowns, FDPD, onlays, ¾ crowns, crowns, implant ambutments

Table 2.4 – Major ceramics used as dental replacement materials

The mechanical properties of Y-TZP are similar to those of stainless steel and it has been referred to as 'ceramic steel'. It also can tolerate cyclic stresses very well [17]. However, the mechanical properties of Y-TZP are highly dependent on its grains size where above a critical grain size the possibility of spontaneous $t \rightarrow m$ (tetragonal to monoclinic) transformation increases. Smaller grain sizes also reduce the fracture toughness of this material as the transformation becomes impossible [77]. Although most manufacturers do not recommend grinding and sandblasting of Y-TZP as it can be detrimental to the long-term performance of this material [77], Luthardt et al. showed that partially stabilised Y-TZP exhibits a much better machinability compared to densely sintered Y-TZP ceramics [79]. The main issue reported regarding this material is zirconia ageing, which is due to detrimental effects of exposure of this material to wetness for an extended period of time, but surface treatment can reduce the risk of the occurrence of ageing phenomenon [17], [81]. Although clinical studies indicate that Y-TZP restorations are both well tolerated and sufficiently resistant, further evaluations are needed as performance of Y-TZP in long time period is not yet investigated [82], [83].

Although the demand for ceramic dental restorations is growing [17], the use of stainless steel for dental crowns, retainers and implants, especially in developing countries, is very common due to economic reasons [18]. The British Society of Paediatric Dentistry (BSPD) also has recommended the use of stainless steel (pre-formed) crowns for the restoration of primary molars with multi-surface lesions, extensive caries (cavities) and those where pulpal treatment has been performed [19]. The first stainless steel used for implant fabrication was type 302 which was stronger and more corrosion resistant than vanadium steel. Due to the importance of corrosion resistance in bio-materials, a new type of stainless steel was introduced in the 1950s which contained a small percentage of molybdenum to enhance the corrosion resistance. This type of steel, later known as type 316, was later modified by reducing the carbon content from 0.08 to a maximum of 0.03% to excel the corrosion resistance. The new type became known as 316L stainless steel. The compositions of 316L stainless steel are presented in table 2.5 [73].

Element	Composition (%)
Carbon	0.03 max
Manganese	2.00 max
Phosphorus	0.03 max
Sulphur	0.03 max
Silicon	0.75 max
Chromium	17.00 – 20.00
Nickel	12.00 – 14.00
Molybdenum	2.00 – 4.00

Table 2.5 – Compositions of 316L stainless steel according to ASTM standards

The American Society of Testing and Materials has also recommended type 316L rather than 316 for implant fabrication. 316L is a type of austenitic stainless steel and contains nickel. This content stabilises the austenitic phase which leads to corrosion resistance enhancement. Also surface modifications have been used on 316L including anodisation, passivation and glow-discharge nitrogen-implementation for further improvements of corrosion, wear, and fatigue resistance of this type of steel [84]. The corrosion fatigue behaviour of 316L depends on the stability of the passive film formed on the surface reports have shown that the addition of molybdenum and nitrogen to austenitic stainless steel improves the resistance against fatigue. It also improves pitting corrosion resistance

[85]. This gives the surface a significant quality as pits can act stress raisers and preferential sites for fatigue crack initiation. Analytical studies by means of Auger electron spectroscopy and X-ray photoelectron spectroscopy show that the oxide layer on austenitic stainless steels has a duplex structure. Duplex steels aim to combine the mechanical properties of ferritic steels and the corrosion resistance of austenitic steels by using austenitic and delta-ferritic phases in equal quantities [85], [86]. The importance of corrosion is emphasised in many studies as the interactions between body fluids and the surface oxide layer may results in adverse biological reactions, because ion release can disturb cellular metabolism as well as the failure of the implant [20]. Of course, such phenomenon depends of the surrounding medium properties and the present solution, too. A study by Karimi [87] showed that in bovine serum albumin (BSA) the material loss rate of 316L under tribo-corrosive conditions is higher compared to CoCrMo and Ti-6Al-4V; however, it was due to presence of a sort of protein in the environment and cannot be generalised to oral cavity. Generally, the material loss rate of 316L due to mechanical wear under tribo-corrosive conditions is significantly higher than the corrosive wear [18].

2.7 Micro-abrasion and micro-abrasion-corrosion tests

For obvious economic reasons, and also safety in case of bio-implants, running complete mechanical assemblies with lubricants contaminated by particulate materials is not practical and the results are often difficult to interpret [10]. A variety of experimental arrangements have been used to study wear either by investigating the mechanisms by which wear occurs, or simulating the practical applications. For sliding wear, the methods are divided into two categories: symmetric and asymmetric, which the latter category is the most common. Among the employed methods to study sliding wear, only few of the methods are the subject of national standards, such as block-on-ring (ASTM G77), crossed cylinder (ASTM G83), pin-on-disc (ASTM G99), sphere-on-disc (DIN 50324) and pin-on-plate (ASTM G98) geometries [12]. Figure 2.20 shows the schematic diagrams of some of the standard methods.

Recently, abrasive wear test using cratering ball technique in micro-scale has been used to study the performance of different materials under abrasive wear. In this type of test a rotating ball is forced against the test material in the presence of an abrasive slurry. This type of tests is conducted in two main ways: either a fixed ball or a free ball [13].

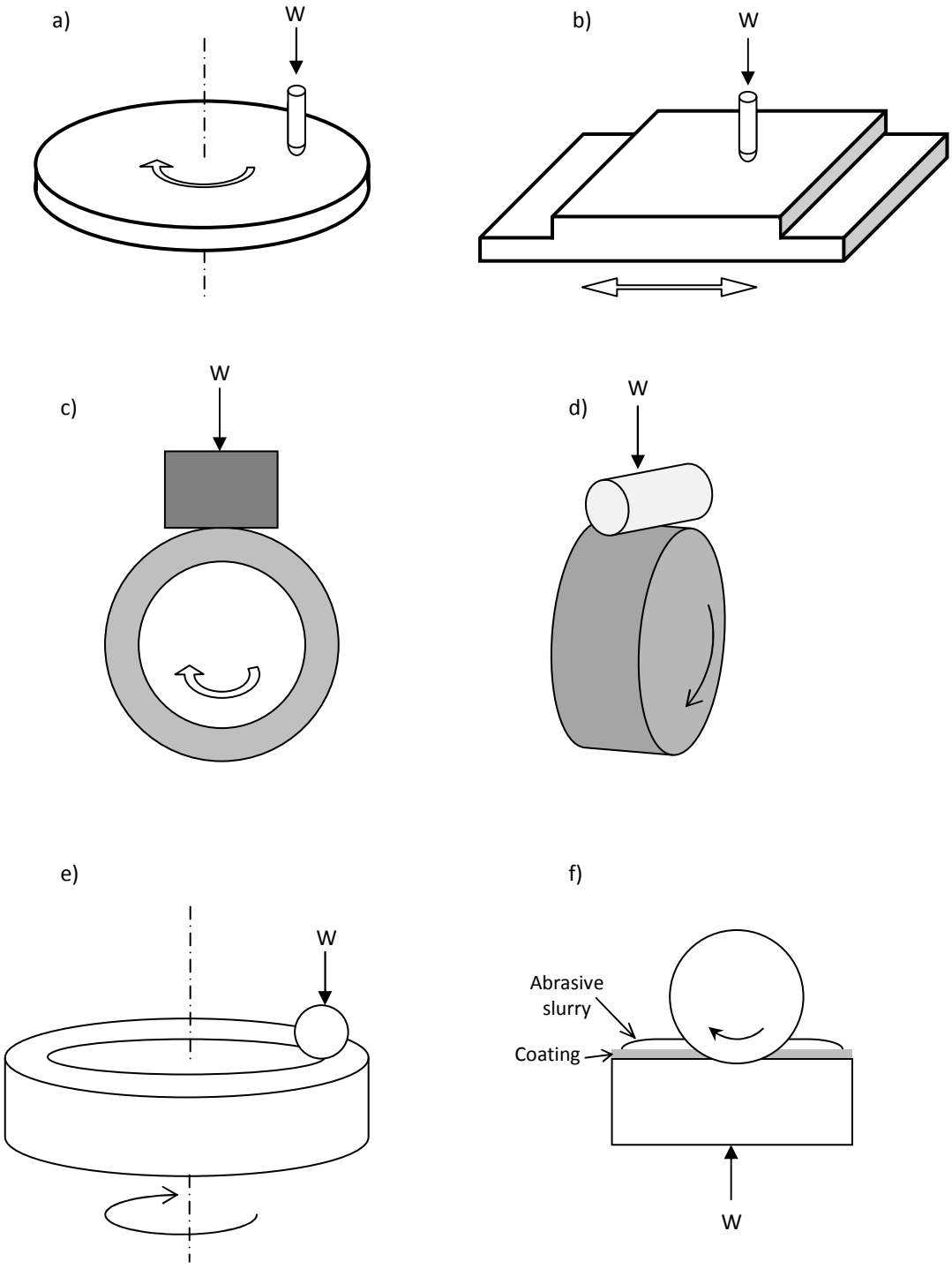

Figure 2.20 – Simple schematics of a) Pin-on-disc and b) Pin-on-plate devices c) Block-on-ring d) Crossed cylinder e) Sphere-on-disc f) Ball cratering

Bio-tribological techniques are developing constantly as long-term clinical results from various designs and materials are needed and wear testing is a critical gating item for

preclinical evaluation. Gravimetric weight loss is the standardised method to assess wear in a wide range of materials. Subsequently by dividing the mass loss with the density of the test material determines the volumetric wear which is usually calculated based on Archard's equation (See section 2.5.8). This process seems straightforward and works for genuine bulk test materials. On the other hand, this process can become very complicated especially for materials that are humid absorbent or materials with different material coating. The coating may have a different density from the substrate material. This makes the wear assessment more difficult after a delamination event or wear through of the coating [11]. However, it has been reported that thin PVD coatings can exhibit an identical form of wear to a bulk surface [59].

In micro-scale tests, the flow of the particles is normally carried out using a slurry. It should be noted that the calculation of equilibrium hydrodynamic film thickness created by water-based has shown that the film thickness of the slurries is much smaller than the size of the abrasive particles and the load carried by the film in the interface of such tests is negligible [59]. This is not valid for viscous slurries.

As it mentioned in the previous sections, friction and wear can considerably affect the sensitivity of a material to corrode. Conversely corrosion can modify the frictional and wear behaviour of a material. Synergy effects between wear and corrosion, also known as tribocorrosion, have attracted a lot of attention, although the known fundamentals of this type of wear are still limited. This type of synergism can significantly accelerate the material loss rate which can be considerably higher than abrasive wear and corrosive wear as sole present mechanisms [4], [88].

Standard test method	Description
ASTM G75	Standard test method for determination of slurry abrasivity (Miller wear test)
ASTM G38	Standard practice for making and using C-ring stress-corrosion test specimens
ASTM G39	Standard practice for preparation and use of bent-beam stress-corrosion test specimens
ASTM G49	Standard practice for preparation and use of direct tension stress-corrosion test specimens
ISO 11782	Corrosion of metal and alloys – Corrosion fatigue

Table 2.6 – Standardised dual degradation test methods

No standardised test method exists to combine more than two degradation mechanisms being applied simultaneous during lab testing. Table 2.6 exhibits examples of the standardised methods which combine two degradation methods [88].

ASTM G38/G39/G49 and ISO 11782 are standardised methods to investigate stress corrosion and fatigue corrosion. ASTM G75 is a standard test used to develop data from which either the relative abrasivity of any slurry or the response of different materials to the abrasivity of different slurries [89] It can be developed to combine abrasion and corrosion testing [88]. The main challenge in this field is how realistic the results of such tests are.

The first standardised method for computing the increased wear loss rate attributed to synergism or interaction that may occur in a system when both wear and corrosion processes coexist was ASTM G119 published in 1995 [90]. After that, techniques to investigate tribocorrosion in aqueous solutions were developed and applied on a variety of sliding contact conditions. Mischler has divided the techniques into four groups [4]:

i) Corrosion potential technique
ii) Galvanic cells
iii) Potentiostatic technique
iv) Potentiodynamic technique.

These techniques have been used in a variety of sliding conditions such as unidirectional motion, reciprocating motion, fretting and spinning contacts and the most popular technique has been potentiostatic technique.

2.8 Wear measurement in micro-scale

Many tribologists have applied Archard's equation into their experiments and attempted to complete the equation by adding new parameters. More than one hundred parameters can be found in the literature and most of them are derivatives of the Archard's equation, but they are applicable only to the specific approaches that the tribologists have followed [6]. Meng and Ludema [7] identified nearly 200 'wear equations' involving an wide range of material properties and operating conditions, but it is still believed that there is still no way of predicting tribological performances of surfaces with confidence or certainty. Cleary, the

expected wear mechanism is a function of applied load, volume fraction of abrasive in the slurry, abrasive material, materials of the surface and the counterface and the condition of the cratering surface [64]. However, measuring wear loss can be a complicated process.

For micro-abrasion tests using cratering ball, the geometry of the wear scar is typically a spherical cap. Rutherford and Hutching [59] have proposed an equation to measure such geometries and it is a derivative of Archard's equation:

$$SN = \frac{V}{\kappa} \approx \frac{1}{\kappa}\left(\frac{\pi b^4}{64R}\right) \qquad (b \ll R) \qquad (2.27)$$

where *S* is the sliding distance, *N* is the applied normal force, *V* is the wear volume, *κ* is the wear coefficient, *R* is the radius of the ball, and *b* is the diameter of the spherical cap wear scar. They have also extended this model for coated materials, where they have independent wear coefficients, as:

$$SN = \frac{V_c}{\kappa_c} + \frac{V_s}{\kappa_s} \quad (2.28)$$

where the subscripts are to refer to the coating (*c*) and the substrate (*s*). Although this is a valuable model to describe the wear, the computation for the volume loss of the coating is not very straightforward. Thus, they suggested rewriting the equation using the thickness (*t*) of the coating to simplify the calculation of the volume loss of each party:

$$SN = \frac{V_c\kappa_s + (V+V_s)\kappa_c}{\kappa_c\kappa_s} \qquad (2.29)$$

Therefore the overall volume loss and volume loss of the coating will be:

$$V = \pi\frac{b^4}{64R^2}\left(R - \frac{b^2}{8R}\right) \approx \frac{\pi b^4}{64R} \qquad (b \ll R) \quad (2.30)$$

$$V_c = \pi t\left(\frac{b^2}{4} - Rt\right) \qquad (2.31)$$

These equations were approved in another work by Trezona and Hutchings [91].

Most of tribocorrosion evaluation techniques operate without an externally imposed electrode potential. In such techniques a spontaneous potential difference is established between the metal and the surrounding solution. The potential is called corrosion potential (E_{cor}). The potential difference is affected by the surface oxidation state, solution composition, temperature, flow conditions and some other factors. Under the wear

conditions of such techniques, the passive film on the surface is locally removed and the bare metal is exposed to the solution [92]. It should be noted that although most of the predictions of mechanical wear are based on Archard's equation, this equation does not reflect the electrochemical effects.

Tribo-corrosion is not simply the sum of corrosion and wear taken separately. In fact there are interactions between chemical and mechanical factors. Stack et al. [93] have reviewed the synergistic effects of mechanical wear and corrosion by showing that the total corrosion wear loss is higher than material loss due to pure corrosion in the absence of mechanical wear and vice versa. They have stated a model as:

$$V_{cw} = V_w + V_c + \Delta V_s \qquad (2.32)$$

where V_{cw} is total corrosion wear volume loss, V_c is pure corrosion volume loss, V_w is pure mechanical wear volume loss, ΔV_s is the synergistic effects of the two mechanisms which is greater than zero. The synergistic effect can be re-written as:

$$\Delta V_s = \Delta V_w + \Delta V_c \qquad (2.33)$$

where ΔV_w is corrosion-induced wear and ΔV_c wear-induced corrosion. This model has been used and developed in further works of Stack et al. [94–96] and Wood et al. [97–99] where the mechanical wear is due to abrasion and external electrode potentials are imposed.

The synergism equations according to ASTM standard between abrasion and corrosion are:

$$Total\ wear\ (AC) = pure\ abrasion\ (PA) + pure\ corrosion\ (PC) + synergy\ (S) \qquad (2.34)$$

$$S = \Delta PC_A + \Delta PA_c \qquad (2.35)$$

where ΔPC_A is change in corrosion due to abrasion and ΔPA_C is change in abrasion due to corrosion. In the tribocorrosion rigs which are capable of *in situ* electrical measurements, the volume loss will be:

$$V_{Total} = V_{Mech} + V_{Elec} \qquad (2.36)$$

where V_{Total} is the total volume loss due to mechanical and electrochemical effects and is measured from the volume of the wear scar. V_{Elec} is the volume loss due to electrochemical effects measured from the current–time (*It*) curve obtained during abrasion–corrosion test and V_{Mech} is the volume loss due to mechanical effect [97].

The area under the current–time (*It*) curve can be converted to mass loss using Faraday's law:

$$\frac{\Delta w}{M} = \frac{It}{zF} \qquad (2.37)$$

Δw is he mass loss of the metal where *M* is the molar mass of the metal in g mol^{-1}, *t* is the time in seconds, *I* is the corrosion current in A, *F* is the Faraday constant (96,485 $Asmol^{-1}$) and *z* is the number of electrons involved in the corrosion reactions [92].

2.9 Wear regimes and wear maps

The ability to predict wear of materials is a universal challenge crucial to successful application of new materials into different technologies. There are numerous methods to describe wear data such as tabulated wear rates or elucidation of the dominant wear mechanisms using micro-graphs [100]. Wear behaviour also can be classified according to severity of the wear as three wear regimes: mild, severe and extreme. Severe wear is generally characterised by high friction coefficients, low electrical contact resistance, high rates of material transfer and loss, and rough surfaces whereas mild wear has the converse characteristics [52]. This is an appropriate approach to address a worn surface qualitatively as quantification of a wear is not always the best way to describe it. Quantitative reference points are often arbitrary. A more comprehensive method to link the wear rates and wear mechanisms in a much wider range of sliding conditions is wear-mechanism maps. Wear maps have been proposed to link mechanisms to operating parameters. Wear-mechanism maps can be an extra-ordinary informative tool for bio-materials for three main reasons [101]:

i) There is no single metric unit for wear damage
ii) There are a limited number of standardised wear testing methods and often the variables of a study is incomparable with one another
iii) Wear is strongly system dependent and the presence of a third body can massively affect the wear response

As a result, generating wear maps as an outcome of the wear data analysis has become widely accepted and in use. There are other names used for this type of diagrams such as

wear-mode maps, wear-transition maps and wear-regime maps depending on what the focus of the diagram is on. The diagrams can be either two or three-dimensional, but two-dimension maps are more common [100].

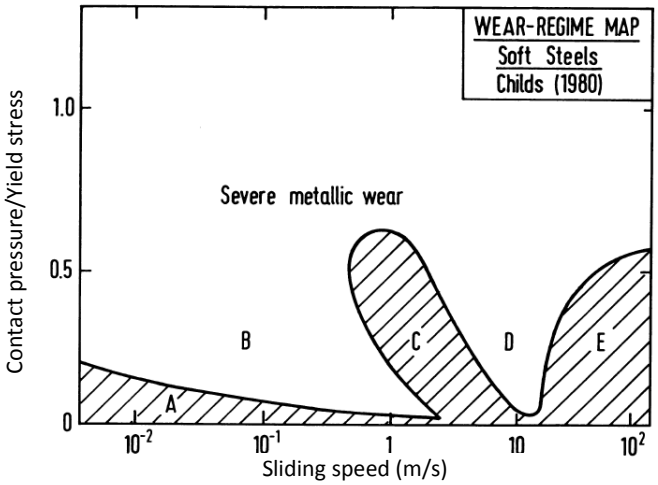

Figure 2.21 – Childs' wear map for soft steel

One of the most cited wear-mechanism set of maps from the 1980s is the Lim and Ashby's maps [48]. Reducing the time scale of the wear tests to accelerate the production of data can be hazardous as there is always the potential of moving from one mechanism to another without noticing the alterations during the transitions. Lim and Ashby plotted the severity of the normal load versus the sliding velocity for stainless steel and what is special about their maps is they have noted all the mechanisms the may happen in such conditions. Figure 2.22 shows their map. Later, wear maps for other materials such as polymers and ceramics and different types of wear such as erosion and fretting generated [33], but the milestone of wear-mechanism map generation was when Tabor remarked that wear might be the result of interacting mechanisms with no single process dominating [102]. This encouraged a lot of research groups to find the synergistic mechanisms during a wear process and generate the maps accordingly. Stack et al. [94], [103] have proposed numerous models for synergistic wear maps.

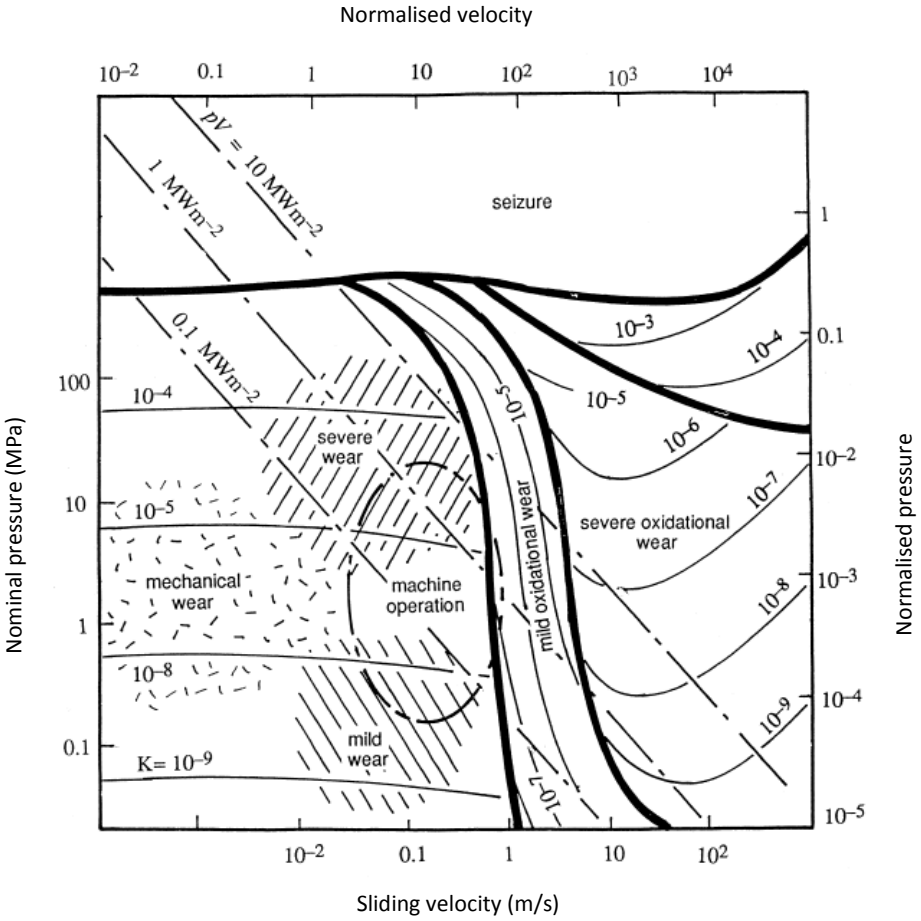

Figure 2.22 – Lim and Ashby's map for stainless steel

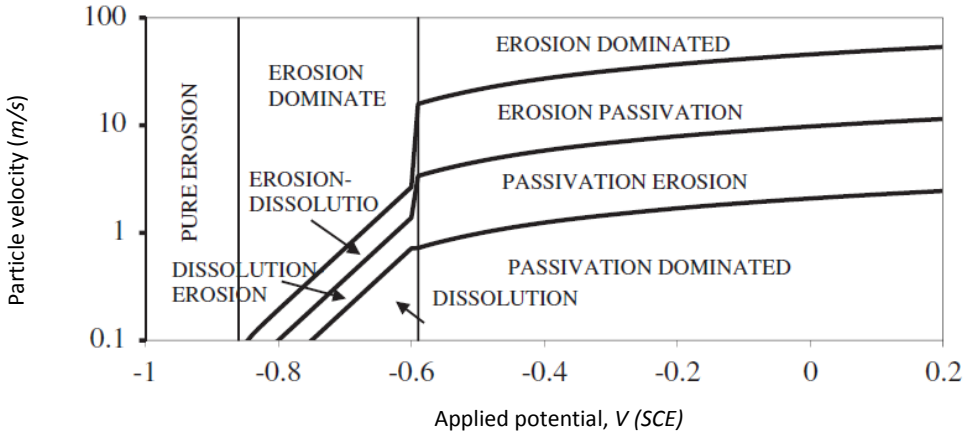

Figure 2.23 – Erosion-corrosion synergistic wear map

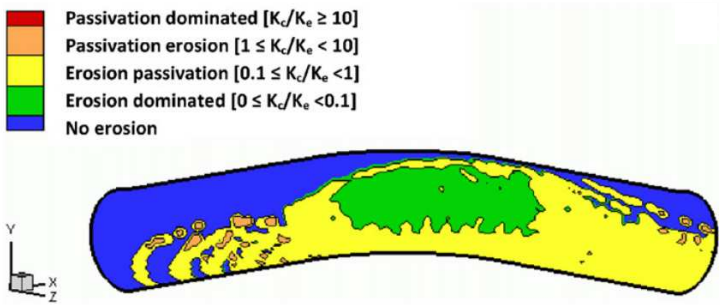

Figure 2.24 – Erosion–corrosion map for outer surface of an elbow-pipe

Figure 2.23 is an example of erosion-corrosion synergistic wear map. Wear maps have also been employed to investigate factors which can affect the wear processes such as angularity of particles and surface coatings [48]. The maps can also be illustrated on the profile of the investigated component [104]. Figure 2.24 exhibits an erosion–corrosion map for the outer surface of an elbow-pipe. More recently, Cantizano et al. [105] proposed a numerical simulation of wear-mechanism maps using finite element analysis (FEA) in a three-dimensional method and stated that this method can cover any geometry and operating condition of a mechanical system. As an idea for future work on wear-mechanism mapping, Lim [100] suggested few guidelines on how to generating more comprehensive wear-mechanism maps:

i) They should not be limited to unidirectional sliding.
ii) They should be aimed to serve the end-users.
iii) The parameters should be easily controlled in practice.
iv) Companion friction maps can be beneficial for designers.
v) Ordering the wear data in a way that enables different research groups to contribute and increase understanding the underlying wear processes.

2.10 Introduction to the present work

This study examines the wear performance of yttria-tetragonal zirconia poly-crystalline (Y-TZP) ceramics and 316L stainless steel as the bio-materials used as denture restoration materials. Also, the wear performance of DLC coated cobalt and titanium alloys as hip joint

replacement materials are investigated. Different bio-tribological techniques have been used for each set of experiments. The methodology for each technique has been explained throughout the relevant chapter. For each chapter the encountered wear mechanisms are identified and wear regime maps are generated.

3

Micro-abrasion of Y-TZP in tea

Published paper based on this chapter:

Micro-abrasion of Y-TZP in tea

Sharifi, S., Stack, M., Stephen, S., Li, W. & L. Wang

Wear, Volume 297, Issues 1-2, 15 January 2013, Pages 713-721.

Abstract of the paper:

The object of this work is to investigate the micro-abrasion of Y-TZP in tea. This material is a candidate replacement in dental restoration and to date there has been very little work carried out to investigate the wear behaviour in oral cavity conditions. Various additions such as milk and sugar, which affect the solution viscosity and pH, were assessed as part of this work and the results were compared to the performance of the material in aqueous conditions. Wear maps were generated showing the change in wear rate as a function of applied load and exposure time.

3.1 Introduction

Uneven contact between opposite teeth and chewing surfaces is a very common result of wear of teeth texture [106]. The tribological processes inside the oral cavity are categorised as: attrition (the act of wearing away of the surfaces), corrosion (mass loss due to the chemical reactions), erosion (impact of the particles in the slurries), abrasion (the process of wearing down by the friction) and abfraction (eventual fatigue and loss or cracking of the tissue) [107]. These do not happen individually. In fact, tooth-to-tooth (or tooth-to-restorative) contact (attrition), chemical reactions without involvement of bacteria (corrosion) and food movement over the enamel surfaces (erosion) may occur simultaneously along with many other chemical and physical factors including the applied force during the chewing, duration of the contact, or even the chewing behaviour in combination with neuromuscular forces. It should be noted that not only mastication, but also occlusal antagonistic contact is one of the main reasons of the gradual removal of teeth [108–110].

The main candidates as restorative dental materials to recreate the lost function and aesthetic appearance of damaged teeth are ceramic materials. This is due to their long-term clinical success, strength, toughness, relatively comparability to the natural teeth, colour, translucency and desirable processing technologies such as moulding, machining and sintering [14]. One of the most important factors is the very low thermal expansion co-efficient of ceramics comparing to the traditional restoratives such as amalgam. Another contrast between ceramics and the traditional amalgam (apart from their aesthetic properties) is that the latter material does not build an adhesion to the teeth structure and subsequently the weakened teeth will not be strengthened.

Zirconia-based ceramics exhibit more desirable properties among ceramics in this field. Advanced manufacturing technologies have also developed the ability manufacturing full-zirconia restorations with occlusal design and good aesthetic results without required subsequent veneering [109]. In biomedical grade zirconia, phase transformation toughening enhances the crack propagation resistance. Yet this involves the transformation of the metastable tetragonal grains to the monoclinics and, as a result, the volume expands at the crack tips to cause compressive stresses. This makes zirconia ceramics susceptible to ‘ageing’ in presence of water. Although it is hardly possible to prevent ageing since it is a natural return back to the monoclinic equilibrium state, the use of yttria instead of co-

precipitated powders increases the ageing resistance significantly [82]. Partially stabilised zirconia substructures provide high hardness, fracture strength, and structural reliability and show a smaller range of strength variations than porcelain [4].

Stabilising the tetragonal phase using yttria creates yttria-stabilised tetragonal zirconia poly-crystalline (Y-TZP). Y-TZP has favourable mechanical properties in load-transfer applications such as dental restoration. These included high flexural strength (900 to 1200 MPa), remarkable fracture toughness (K_{IC} 7 to 10 $MPam^{1/2}$) and Young's modulus (210 GPa) [111], [112]. Another significant ability of Y-TZP is its super-plasticity behaviour in compressive deformation which enables it to deform uniformly without fracture [113].

Y-TZP thus has a potential use as a tribological component in dental restoration. To implement a new material in a successful application however, we must anticipate the wear of the material and further characterise the wear properties of Y-TZP. The wear behaviour of such ceramics depends on the material phase, porosity, toughness, hardness and grain size along with the exposure environment [114], [115]. The object of this work is to investigate the wear mechanism of black tea on Y-TZP as a candidate dental replacement material, under micro-abrasion conditions. The consumption of tea has been considered healthier comparing to the other caffeine-based drinks because of having antioxidant properties and oral health benefits, such as a high fluoride content. Despite its beneficial effects (such as inhibitory effects on the growth of cariogenic bacteria) the consumption of tea can also be harmful and result in dental degradation [116], [117]. To date, the effect of beverages on dental enamel has been widely investigated [116–121]. Yet no study has considered the exposure of tea on candidate dental replacement materials such as Y-TZP, despite their potential application.

For this paper, in addition to the effect of normal black tea on the micro-abrasion of Y-TZP, the popular combinations of tea with sugar and tea with milk were studied. The abrasive effect of these materials in water was also assessed as a reference. Scanning electron microscopy was used to assess the wear mechanisms following exposure. Finally, wear maps were constructed for Y-TZP for application in dental restoration.

3.2 Experimental Materials and Procedure

The objective of the experiment was to determine the micro-abrasive performance of Y-TZP under various loads, sliding distances and slurry environments. In this test a ball is rotated against a specimen in the presence of a slurry of fine abrasive particles. This is known as the ball-cratering abrasive wear test [64].

3.2.1 Specimen preparation and characterisation

The samples of Y-TZP were provided by National Cheng Kung University in Taiwan and were prepared with 3 mol% yttria doped zirconia, already polished with diamond paste. The samples were machined circumferentially using a grinding machine with a coolant flow simultaneously. The crystalline state of the ceramic alters at very high temperatures (about 1300°C) and any rapid degradation takes place at 200-300°C [122]. In this case, the machining was carried out at a very low temperature at a very short period of time for each edge (less than 10 seconds) which may not affect the properties of the material. The original shape of the samples was a circular-disc. Due to the limited size of the specimen platform of the test rig however, the surface area of the samples were machined into octagon shapes to increase the available area for testing. The final size of the Y-TZP samples was 36mm in length and breadth with the thickness of 3.4mm. The mechanical properties of the samples can be found in Table 3.1.

Material Property	Y-TZP	UHMWPE	Alumina
Density (kg/m³)	6000	931-935	3800
Young's Modulus (GPa)	195-210	0.689	351
Hardness (Vickers)	1330-1470	541	2035
Fracture Toughness (MPa/m)	7-10	3.5-6	3.5

Table 3.1 – Material properties [111], [123], [124]

3.2.2 Apparatus (Test rig)

The tests were conducted using TE-66 Micro-Scale Abrasion Tester (Plint TE-66, Phoenix Tribology, Reading, UK). This rig can be used for the tests in accordance with BS EN 1071-6: 2007: Advanced technical ceramics, "Methods of test for ceramic coatings: Determination

of the abrasion resistance of coatings by a micro-abrasion wear test". The apparatus consists of an ultrahigh molecular weight polyethylene (UHMWPE) ball which is clamped between two co-axial shafts. One of the shafts is driven by a variable speed DC geared motor and the ball is driven by friction against the shaft. The other shaft, which is driven by the friction against the ball, is connected a peristaltic pump head. The pump provides the abrasive slurry feed to the contact interface through the syringe. The test sample is mounted onto a platform on a vertical pivoted arm. The arm is in balance when the sample and the ball are just in contact. The loads can be applied by hanging dead weights to a cantilever arm [18]. Figure 3.1 shows the schematic diagram of (a) apparatus and (b) details of the contact interface.

Ultra high molecular weight polyethylene (UHMWPE) ball (K-mac Plastics, Michigan, USA) has been chosen for this experiment as it is a well-known biomaterial possessing very low friction coefficient, superior mechanical toughness and excellent wear and abrasion resistance [125], [126]. UHMWPE is a crystalline homogeneous polymer with a smooth molecular profile. High wear resistance has been reported for these materials in sliding conditions with low friction coefficients (less than 0.1) when sliding against hard counterfaces [63], [127]. The counterface balls used were 25.4mm in diameter. The mechanical properties of UHMWPE have been listed in table 3.1.

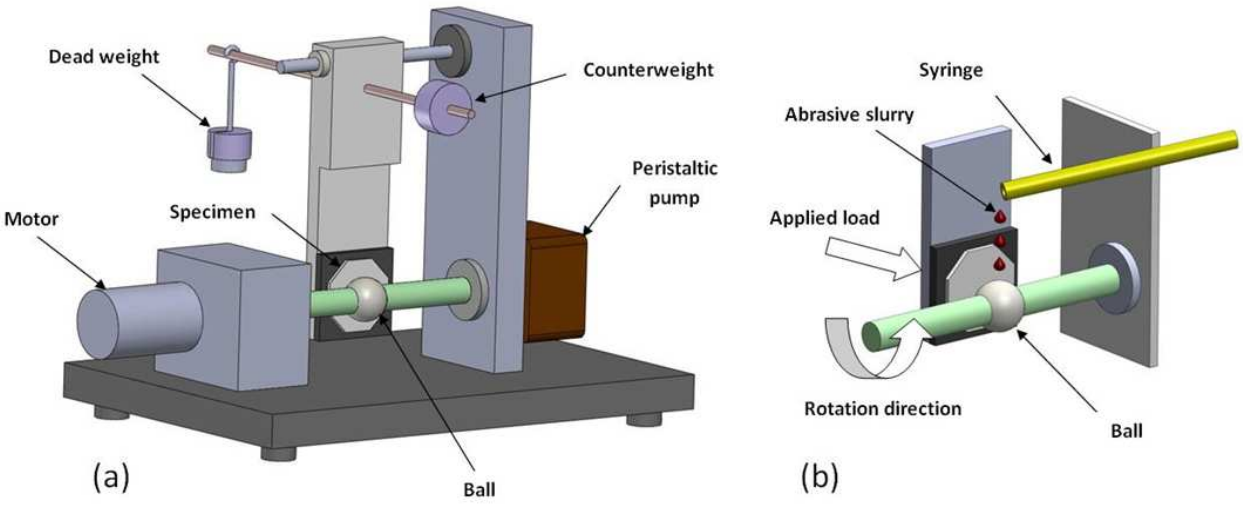

Figure 3.1 – Schematic diagram of the test rig, (a) apparatus (b) details of the contact interface

3.2.3 Slurries

Four types of slurries were used for the experiments: Tea, Tea + Sugar, Tea + Milk, and boiled water. It has been reported that during mastication movement simulating, a number of slurries can be used to simulate food bolus during mastication with a variety in hardness from 3 ($CaCO_3$) to 10 (SiC) in Moh's scale [128]. Therefore, in this study, all slurries used were mixed with $30gl^{-1}$ of the abrasive particles Calcined Aluminium Oxide Powder (Logitech, UK), with a hardness of 9 in Moh's scale, to produce abrasive slurries and simulate food bolus during mastication. This is due to the aim of this research to consider the behaviour of Y-TZP under harsh conditions. The applied particles were flat and tended to lie parallel with the contact interface and thus the applied load is more evenly spread. The size of the particles was 9 µm. It should be noted that alumina abrasive has been considered as safer as it is less friable [129]. The mechanical properties of the particles can be found in table 3.1. In order to prevent the particles from flocculating, due to the insolvent nature of the particles, the slurries were agitated by a small propeller which was situated at the bottom of the reservoir and operated at high speed. This ensured that a consistent particle mix was obtained.

To produce the tea and the mixtures, PG tips® (London, UK) tea bags were used. The Tea + Sugar slurry was made with a sugar concentration of $28.57gl^{-1}$ as this was equivalent to estimations of 2 teaspoons of sugar per serving of tea. The sugar was completely dissolved in the slurry before the testing had begun. For the Tea + Milk slurry, it was estimated that in serving of tea, up to 10% of the final liquid is milk. The slurries were replaced at maximum of 3 hours of use in order to keep a consistent mixture of the solution. They were kept in a heated reservoir which was kept at a constant temperature. The heightened temperature was in order to produce an environment as close to the operating conditions as possible. Drinking temperature of tea and the mixtures were estimated as 45 to 50 °C. Table 3.2 exhibits the properties of the slurries. It should be noted that the measurements were carried out following mixing with the abrasive particles. Due to the chemical reactions of the slurries with the abrasive particles ($Al_2O_3 + 3H_2O \rightarrow 2Al(OH)_3$) [130], the acidic state of the slurries was reduced and the pH values of the final slurries were slightly higher than the primary slurry.

Slurry	pH	Viscosity at 45°C (cP)	Temperature at sample in operation (°C)	Density at 45°C (kg/m^3)
Tea	5.3	0.726	47±2	1032
Tea + sugar	5.3	0.728	48±2	1060
Tea + milk	6.0	0.721	47±2	1033
Water	7	0.696	48±2	1012

Table 3.2 – Slurry properties

3.2.4 Procedure

The tribological properties of ceramics are mainly based on the environment (gas, liquid or vacuum), humidity, lubricants, and, of course, the material of the second element of the friction pair[131]. Recently, to assess the tribological properties of materials, smaller scales are much more in demand due to localised usage of specialist materials [59]. In this study, the micro-abrasion test was carried out in the conditions given in table 3.3. The main parameters which affect the size and the shape and subsequently the rate of the wear are the applied normal load, the sliding velocity, the sliding distance and the volume fraction of the abrasive in the slurry [132].

Test conditions	
Applied normal loads	3 – 5 N
Sliding velocity	150 rev/min (0.2 m/s)
Tests duration	1 – 3 hrs
Sliding distance	718.17 m/hr

Table 3.3 – Test conditions

Previous work using this experimental process has involved testing the effect of a wide range of loads [16], [133], [134]. In the present work, the tests were performed using the

loads of 3, 4 and 5 N, which was an appropriate choice considering a normal force on a real single tooth [135]. The ball was rotated at a constant speed of 150rev/min, which was a linear velocity of 0.2 m/s. The friction between the ball and the specimen can generate heat in the interface. The magnitude of the generated heat is very dependent on the sliding velocity. Since higher speeds result in raised frictional energies, which in turn cause higher contact area temperatures, the generated heat was calculated from equation 3.1 to avoid any serious error [131]:

$$Q = \mu P v \quad (3.1)$$

where μ is the friction coefficient, P is the normal load and v is the sliding velocity. The friction coefficient of UHMWPE is less than 0.1, and Y-TZP is 0.5 in water [136]. This means that the highest possible increasing temperature in the performed tests was 0.5°C; which comparing to the environment temperature (45°C), it was negligible.

The duration of the tests were one, two and three hours, equivalent to 718.17m, 1436.34m and 2154.51m sliding distances respectively. In the oral environment, the sliding distance per one chewing "event" is 0.5 – 1 mm and the chewing rate is 60 - 80 cycles/min which occurs 10 – 30 min/day [16], [18], [135], [137]. These numbers give us an average rate of sliding distance of 1 m/day per a tooth. Therefore, a one hour test can simulate almost two years of a tooth lifetime. With these calculated values, the early life of a Y-TZP dental implant is simulated in two, four and six years of time respectively.

3.3 Results

3.3.1 Wear scar measurement

It is thought that during the tests, an abrasive particle will effectively cut a path through the surface test material. This act of cutting (or "carving") through the test material will cause deformation from both the normal loading force and the sliding friction force. This will cause some of the test material to be removed as debris, causing wear [3], [138]. The wear scar volume can be measured from knowledge of the mass loss of the test material and the density [139]. Since the tests were conducted in aqueous conditions with the potential of Y-TZP absorbing moisture from the environment, it was necessary to dry the samples before measurement of mass loss. This class of ceramics exhibited a thermal conductivity between

2.4 – 2.8 *W/m.K* which is a relatively low thermal conductivity that even enables them to be used as thermal barriers in high temperatures [140], [141]. There was a possibility of retention of residual moisture in the samples after drying. The wear losses were calculated by measuring the residual wear scars from the abrasion test, as identified by Scanning Electron Microscope (SEM).

From inspection of the wear scars under high magnification, the wear regimes, processes and diameters could be determined. The SEM used was an S-3700N model Tungsten Filament SEM (Hitachi High- Technologies, Europe). Since the sample material was not electrically conductive, the samples were carbon coated in order to get clearer images. The high accuracy of the SEM allows the accurate reading of the wear scars geometry as it superimposes measurements on the image of the wear scar, making finding the wear volume very quick and easy. The volume of the scars where perforation of the coating does not occur (which applies to the present work), can be measured by equation 2 by assuming it is a section of a sphere [142]:

$$V = \frac{\pi b^4}{64R} \qquad (3.2)$$

for $b<<R$ where V is the volume of the wear scar, b is the scar diameter and R is the cratering ball radius. It was observed that in abrasion tests, where the samples are softer than the ball material, there was a small area around the scar that undergoes deformation. However, this is not due to abrasion. Hence, care was taken when measuring wear scar diameter to ensure this additional area was not considered [91]. To confirm the results from the SEM measurements, the surface profilometry was carried out using a stylus profilometer, which showed that the wear scars' curvature follows the ball's curvature. Also, the measured wear scar diameters from the SEM and the profilometry were compared and they were found either equal or with a negligible difference. The maximum deviation found in the final volume loss calculations from the SEM and the profilometry was 3.9%, which verifies the validity of equation 3.2.

3.3.2 Effect of applied load and exposure time

Figure 3.2 shows the wear at different loads and in the majority of cases, there is an increase in wear volume with increasing exposure time and applied normal load. However, in some cases there is a change in gradient, suggesting that wear volume does not increase

linearly as is stated in some papers [143] contradicting the predictions of the Archard's equation with a direct increase in wear rate with load.

Figure 3.2 – (a) Wear due to each slurry under 3N load

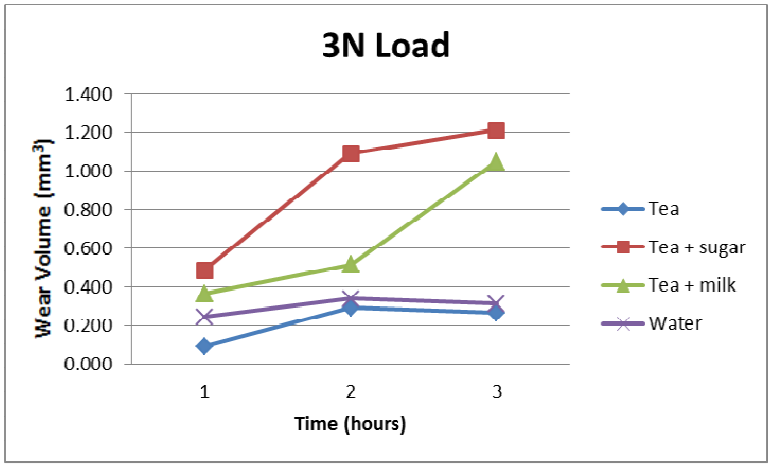

Figure 3.2 – (b) Wear due to each slurry under 4N load

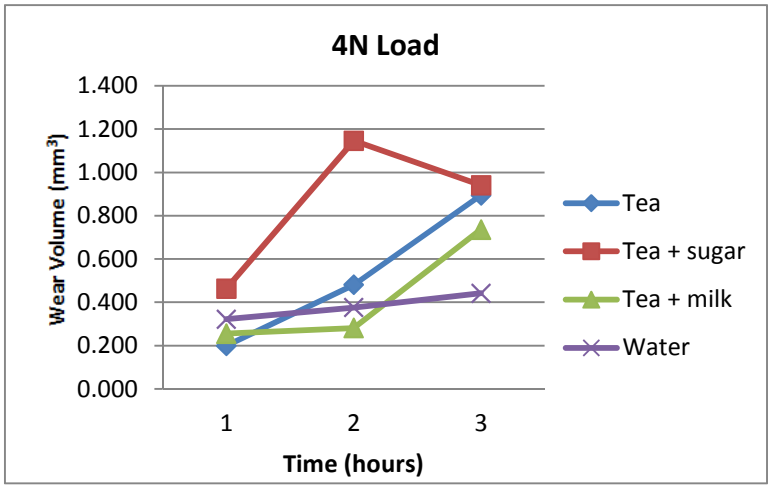

Figure 3.2 – (c) Wear due to each slurry under 5N load

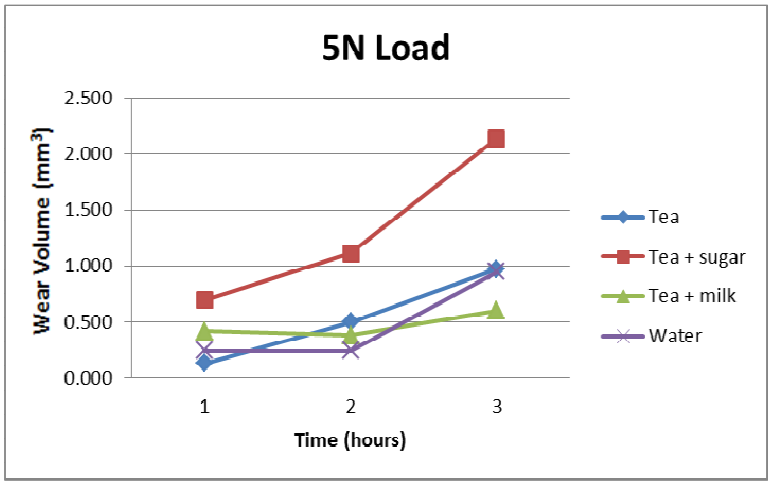

It should be noted that within the oral cavity, a range of pH between 1.2 and 10 can be experienced [107]. The results in Fig. 3.2 and the information in Table 3.2, suggest that in higher loads where the entrainment of the particles is weak, the wear rate of Y-TZP increases with increasing solution viscosity or decreasing solution pH value.

3.3.3 SEM analysis and wear regimes

The majority of the wear scars in this experiment showed evidence of 3-2-body mechanisms (explained elsewhere) [5], [12], [144], [145], and the 2-body grooving regime pre-dominated. For each slurry a new sample was used to prevent any abrasion effects from the previous slurry on the material. This helps us to discover any differences between the wear scars caused by the properties of the slurry. However, the results were very similar showing 3-2 body mechanisms. As confirmed by SEM and EDX, the presence of alumina particles embedded in the ball could be the reason dominance of 2 body grooving. Figure 3.3 shows a picture of the embedded particles on the ball's surface and the results of the EDX test after a 2 hours test. Once enough abrasive particles are entrained at the contact point, the entrance of more abrasive particles is facilitated leading to higher wear rates. Technically, this means that the ball and specimen are separated during the test. So, the ball was rotated after each test to create a fresh surface which also minimised any effects of changes in the overall shape of the ball [91]. A new ball was used for each type of the slurries.

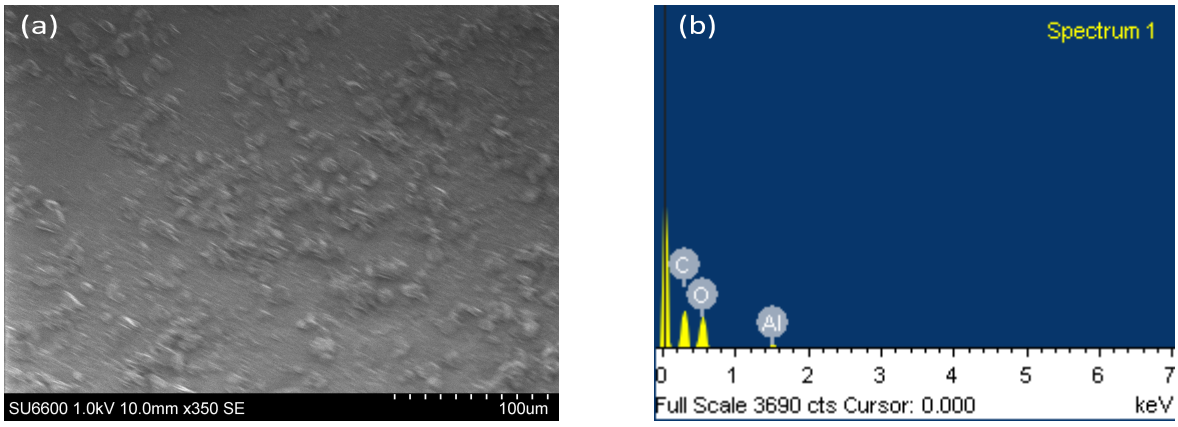

Figure 3.3 – (a) Particles embedded on the ball surface and (b) the results of the EDX test after a 2hrs test

Figure 3.4(a) shows the resulting wear scar of the test performed under 4N load, Tea and milk slurry for 3 hours. In figure 3.4(b) there is clear evidence of ploughing in the 4N test of Tea for 3 hours. In the case of ploughing, the abrasive particle displaces the material by pushing it around the path of, and into a ridge in front of the particle. Although ploughing does not result in any immediate mass loss, it can be attributed to causing greater mass loss indirectly.

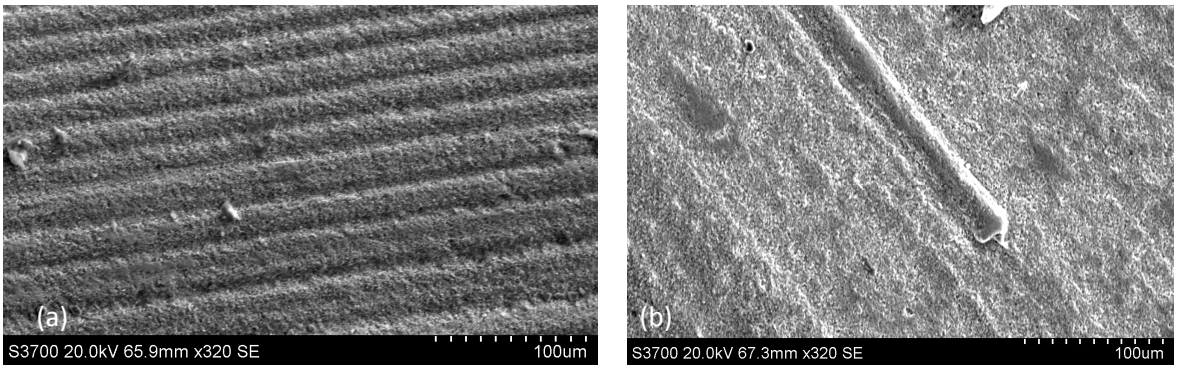

Figure 3.4 – (a) high magnification of a 2-body grooving scar (b) high magnification of scar surface showing ploughing

From further studies of the wear scars, there were other wear processes that could be identified. Figure 3.5 shows evidence that, while 2-body grooving is present, another process known as Intergranular fracture has occurred [3] during the 3N, 3 hour test of Tea and sugar. It is assumed that the surface degradation (or ageing) is caused by the tetragonal-monoclinic phase transformation due to the aqueous environment which normally leads to (a) roughening and higher wear rates as a result or (b) micro-cracking which results in grain pull-out and production of particle debris which can be clearly seen in figure 3.5. At the same time, the transformation can benefit the ceramic by creating a compressive surface layer monoclinic phase on the ceramic [82], [122].

Figures 3.6(a) is a sample of the various wear scars and their measurements to help give an idea of the range in wear scars produced. Figure 3.6(b) shows various scars with a deteriorating image quality which made it difficult to find the edges and therefore measure the volume. This problem was addressed by using the SEM settings to produce background scatter, as well as using different filters which produced clearer images.

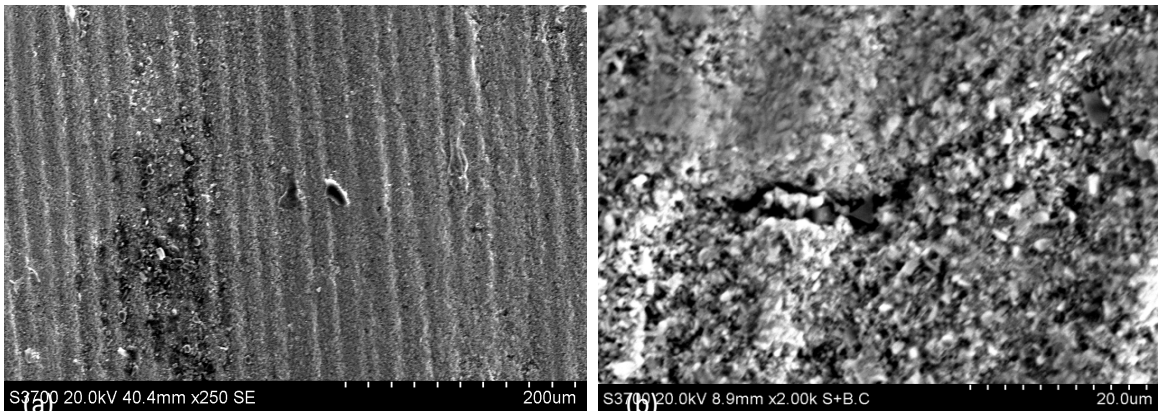

(a) (b)

Figure 3.5– (a) Surface showing evidence of lost grain (b) Evidence of cracked material

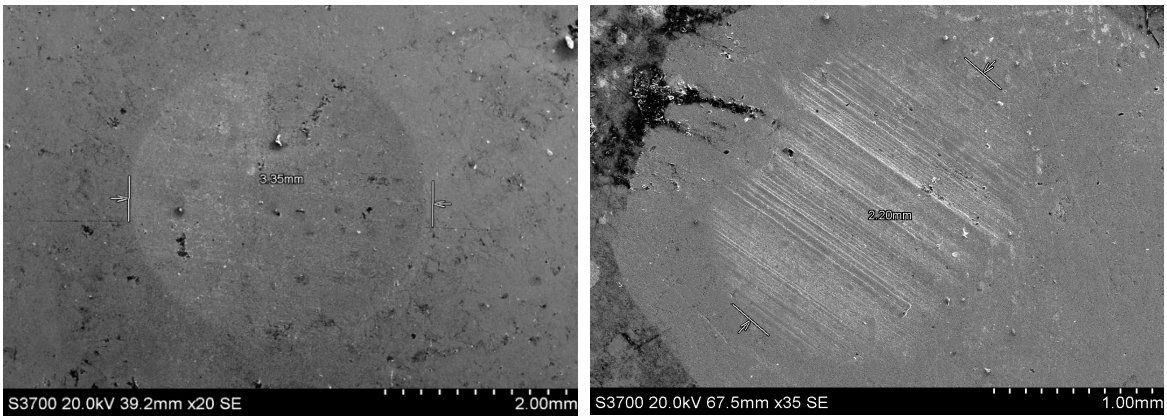

(a) (b)

Figure 3.6 – (a) 3N, 1 hour, Tea and sugar wear scar (b) 3N 1 hour applied with Tea slurry undesirable scar

3.3.4 Wear maps

In order to determine the reliability and the tribological characteristics of a material in different conditions, wear maps of the material are a useful tool to understand the wear qualitatively and quantitatively [146], [147]. In an attempt to further understand the contributing factors of the abrasive wear experienced by the material, wear maps were constructed with various parameters. The boundaries set to determine the levels of wear were as standard procedures suggest [107]:

Low: $V < 0.641mm^3$ ($V < 30\%$ of maximum) (3.3)

Medium: $0.641mm^3 < V < 1.71mm^3$ ($30\% < V < 80\%$ of maximum) (3.4)

High: $V > 1.71mm^3$ ($V > 80\%$ of maximum). (3.5)

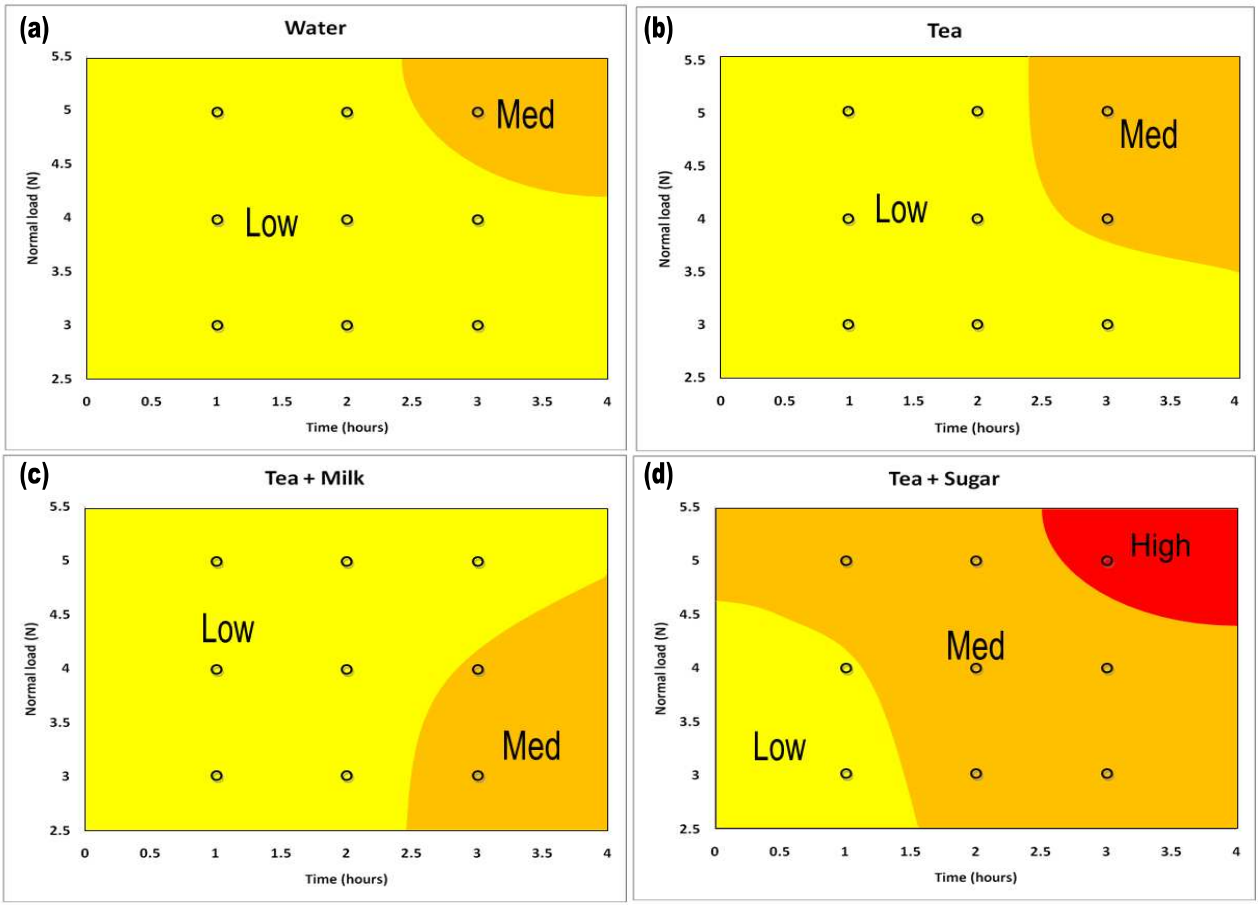

Figure 3.7 – Wear maps of Y-TZP in different slurries (Load/Time): (a) water, (b) tea, (c) tea+milk, and (d) tea+sugar.

The boundaries were created using extrapolation between the above limits for the regimes. The general trends observed from figure 3.7 indicate that with a decreasing load there is a general decrease in wear. Exposure to higher viscosities results in higher wear rates and with longer test durations, wear volume increases. Hence, at the highest values of load, exposure time, and viscosity, maximum wear occurred in the slurry of Tea + sugar for 3 hours. Figure 3.8 exhibits how viscosity affects the wear rate at the various loads.

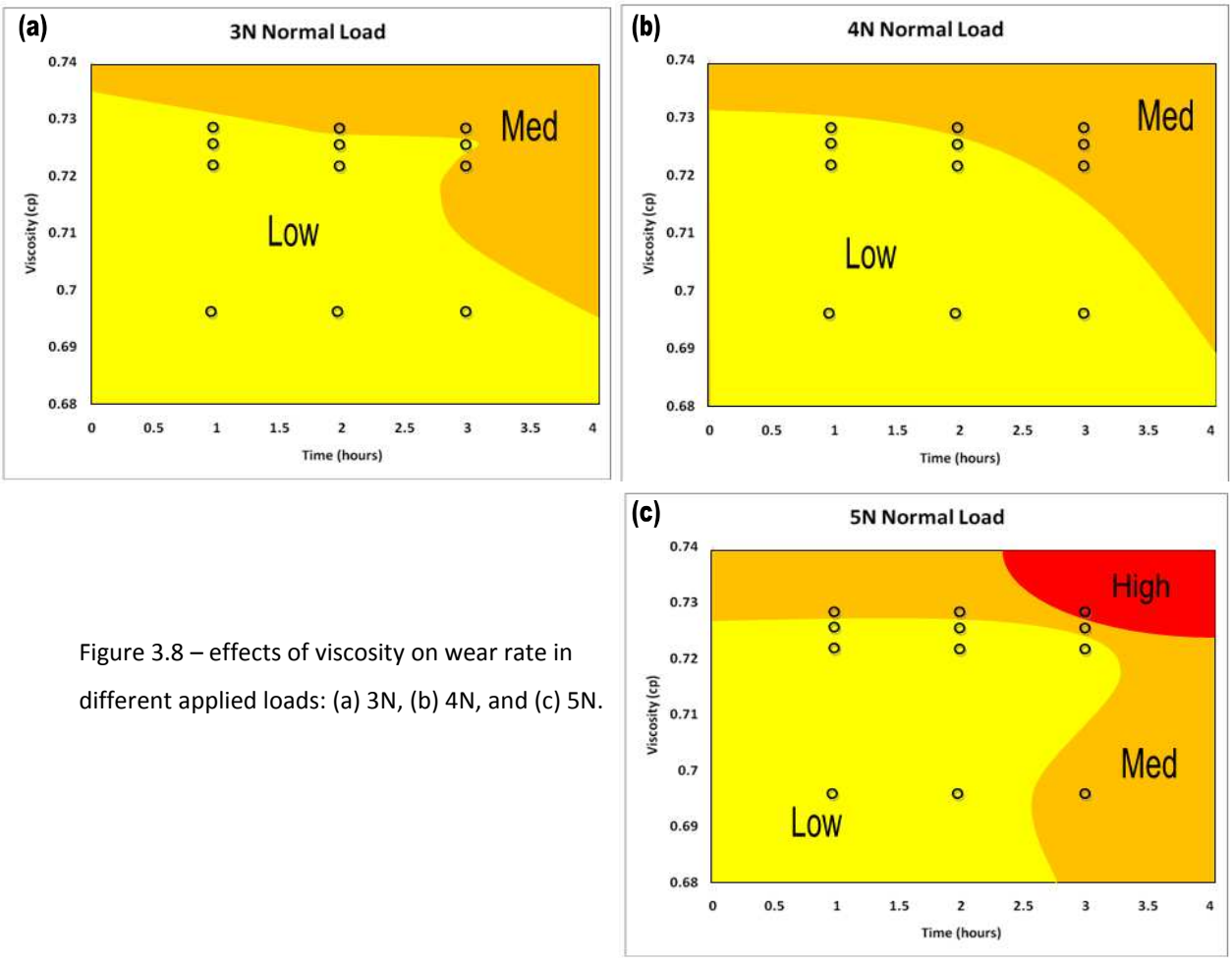

Figure 3.8 – effects of viscosity on wear rate in different applied loads: (a) 3N, (b) 4N, and (c) 5N.

3.4 Discussion

As the experiments were performed in order to evaluate the appropriateness of Y-TZP as a material to be used in dental restoration, the results indicate many important trends for the parameters considered in this study. Many of the experimental parameters were selected to represent the more extreme circumstances that the material would encounter during use, such as elevated temperature (normally tea is consumed at 50^{o}C), small particles, and high rotational speed. Taking these factors into account, the material was subjected to what was equivalent to 6 years lifetime in oral cavity conditions under these harsh conditions, however only losing a maximum of 2.138mm^{3}. The results above indicated that the incubation time to high wear of Y-TZP is expected to be significant, which is a good indicator for these materials to be used in dental restoration.

The results also indicated that the Archard's equation did not describe the wear pattern with time for these tests as it was rarely experienced that the volume increased linearly with time, Figure 3.2. It is likely that this is due to the presence of multiple wear processes, regimes and interactions as described elsewhere [5], [12], [144], [145]. In micro abrasion tests, linear relationships between the wear volume and sliding distance have been generally reported for a large range of loads and slurry concentrations [143]. Wherever the results did not follow this pattern or were not as they were expected, the test has been repeated to minimize the errors. Only 2 of the 36 experiments did not leave clear circular wear scars. Yet extra care has been taken to make a clearer view of the scar edges using different filters in the microscopy. Figure 3.6(b) shows that the scars might not show a clear edge on initial inspection. In cases where it was still hard to determine the wear edges, the samples have been carbon coated to advance the clearance. Trezona and Hutchings (1999) have studied the wear scars of the micro-scale abrasion tests; where the samples are softer than the cratering ball it is always possible to have the central spherical scar surrounded by a roughened or 'scuffed' annular region. This makes it difficult to distinguish the boundaries between the annulus and the spherical scar by optical microscopy. After conducting a large number of tests, a consistent empirical relationship between the width of the spherical part and the width of the scuffed region was reported. This suggested that it is sufficient to consider only the size of the spherical scar to determine the wear behaviour of the material. Since the ridges are quasi-stable, they have the tendency to the eventual break down and resuming the normal wear [91]. The types of tests performed in this study had never been attempted previously for this material, slurries and environments. This would be an area of further work.

The material also showed a higher tendency to increase wear rate relative to viscosity (associated with additions of sugar to the tea) rather than pH value, although the pH values tested were relatively high in comparison to those possibly found in the oral cavity. It has been reported that pH has a significant effect on wear loss in ceramics. This is where the high wear-volumes are obtained for the most acidic and alkaline environments. Yet the highest mass loss takes place in the acidic environments. It should be noted that although the environments with the pH of close to 5 are not very acidic, the wastage is much higher than neutral or low alkaline environments [107], [148].

In the current study, the results indicated that the lower pH values tended to increase the wear rate. To generate the wear maps based on pH values, a wider range of pH values is needed to study such effects on wear rates more accurately. Although it is expected to have a higher mass loss while increasing the normal loads or the exposure time, it is not always anticipated that higher loads lead to the creation of larger wear scars when the loads increase. This is due to that the higher loads result in higher pressures on the contact area thus making the entrainment of the particles more difficult [91]. For example, by rearranging the results based on the slurries in Fig. 3.9, it can be clearly seen that the wear volume for higher loads is less than for lower loads. Therefore, if the higher loads fail to create a bigger wear-volume because of weak entrainment, there may be another reason for having a high volume loss in different slurries. That would be the effects of a higher viscosity or an increased acidity.

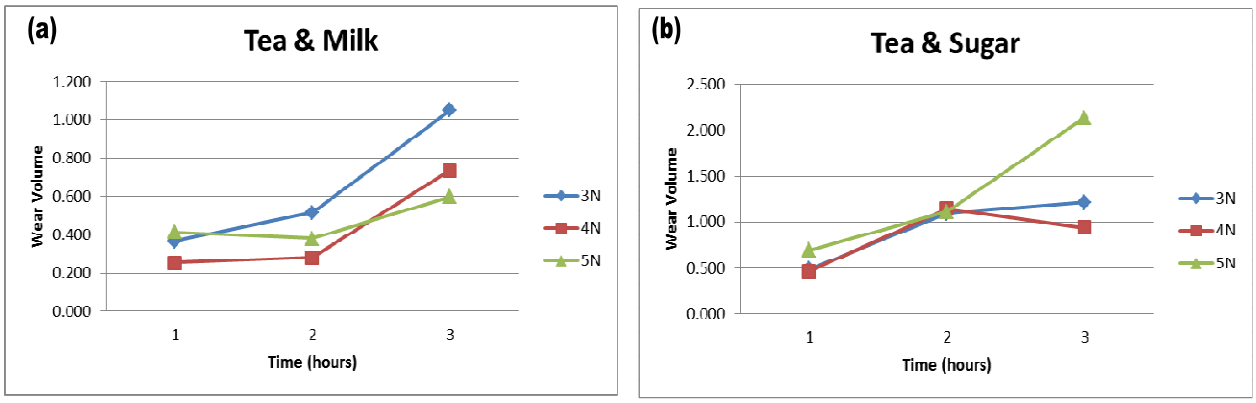

Fig 3.9 – Rearranged results for different slurries: (a) tea+milk and (b) tea+sugar

From figure 3.7, the dominant factor along with higher loads in increasing the wear rate is increased viscosity for the Y-TZP material. By generating wear maps of different loads in figure 3.8 based on this concept, a clearer picture can be drawn of how the changes in these values affect the rate at which the material is worn along with normal loads. There is a thus a necessity to construct further wear maps to investigate the contributions of load, viscosity, pH, exposure time and sliding speed in order to provide an enhanced understanding of the material performance to environments found in the oral cavity.

3.5 Conclusions

(i) The micro-abrasion of Y-TZP material was investigated in Tea with various additions to modify the pH and viscosity levels, using water as a reference solution.

(ii) The results indicated a significant change in the wear rate with load, exposure time and viscosity.

(iii) In the small pH range studied the wear rates increased with decreasing pH values. This may be attributed to an enhancement of tribo-chemical effects in such conditions.

4

A comparison of the tribological behaviour of Y-TZP in tea and coffee under micro-abrasion conditions

Published paper based on this chapter:

A comparison of the tribological behaviour of Y-TZP in tea and coffee under micro-abrasion conditions

Sharifi, S. and M.M. Stack

J. Phys. D: Appl. Phys. 46 (2013) 404008 (11pp).

Abstract of the paper:

The micro-abrasion of YTZP, a candidate dental restorative material, was investigated in a range of caffeine containing solutions which included tea and coffee. Additions of sugar and milk were used to test the effects of viscosity and pH on the wear rate. The results indicated a significant increase in wear rate in the various solutions, with some correlation between wear rate and increases in viscosity and this was linked to enhance particle entrainment in the more viscous solutions. The generally lower wear rate in tea compared to coffee was associated with a longer aging period in this solution before uniform wear was observed. Micro-abrasion maps were used to characterise the differences in performance for the material in the environments studied.

4.1 Introduction

Many people appreciate the strong bitter taste of coffee through the negative reinforcing effects of caffeine; the repeated consumption of a drink containing caffeine or glucose increases the preference for the drink [149]. However, it has been reported that the general consumption of soft drinks, excluding milk and water, damages teeth, because they typically contain sugar and have a low pH value. The acidity of these drinks erodes enamel. Also, plaque micro-organisms metabolise the sugars in the drinks to generate organic acids that cause demineralisation, leading to dental caries. The detrimental effects of consuming soft drinks on dental hard tissues, either acidogenic or cariogenic, are unavoidable as the neutralisation capabilities of saliva flow and salivary components continually decreases over time [120].

Dental defects may require the restoration or replacement of damaged tissues. A dental restorative material should have the capability to recreate the lost function or restore aesthetic appearance [14]. Due to the required biocompatibility, chemical stability, aesthetics, and processing technologies, ceramics, more specifically zirconia-based ceramics, have been widely used in dental practice for the last two decades. Zirconia ceramics were mainly used as the core material inside dental crowns, in the form of bi-layer restorations followed by the fusion of porcelain veneer shells onto them. Today, as a result of development in manufacturing technologies (CAD/CAM) and by increasing the translucency of zirconia ceramics, full contour zirconia crowns which exhibit excellent mechanical properties without any required subsequent processes (e.g. veneering) can be used. Due to their smaller range of strength variations, full-zirconia restorations have become more popular since they have solved porcelain chipping problems, which were commonly encountered in bi-layer structures [15], [109].

Recently, despite the desirable properties of zirconia ceramics, the phenomenon of zirconia ageing has caused some concerns regarding the long-term implementation of this material. Ageing takes place in tetragonal zirconia poly-crystalline (TZP) ceramics by a slow tetragonal-to-monoclinic phase transformation on the surface in contact with water or body fluid, which may lead to surface roughening, grain pull out, and micro-cracking. Initial ageing improves the mechanical properties of zirconia due to the creation a compressive surface layer of monoclinic phase on the ceramic such as bending strength and fracture toughness. However, further ageing leads to deterioration of the material. In the Lawson

review [122], it was reported that there are compositions and conditions under which ageing will not occur. There are a few steps which minimise the ageing susceptibility of these materials, including adding (or increasing the amount of) stabilisers such as yttria or ceria, the addition of a small amount of silica, and processing temperature. The use of yttria clearly increases the ageing resistance while preserving toughness and strength. It also retains the high temperature tetragonal structure of zirconia ceramics. Extra care should be taken during the sintering process to ensure it is conducted within the right temperature range (1400-1450^{o}C). Higher temperatures cause a dual cubical micro-structure, which, enriched by yttrium, leads to a lack of yttrium content in the neighbouring tetragonal grains, and subsequently increases the ageing susceptibility. Moreover, the sintering process at lower temperatures does not produce fully dense materials [82], [150].

As a result, yttria tetragonal zirconia poly-crystalline (Y-TZP), containing 3mol% yttria (Y_2O_3) as a stabiliser, usually referred as biomedical grade zirconia, has become very attractive as a wear-resistant material in dental practice. This is due to the high density, good sinterability, improved fracture toughness, and particularly its superplasticity, which is very useful in ceramic forming and joining. Figure 4.1 shows 2 implanted zirconia-ceramic restorations in between 2 natural teeth, illustrating the excellent aesthetic and machinability properties of this material [17]. However, because of the diversity of tests and the lack of absolute data of the wear behaviour and mechanisms of Y-TZP, the potential applications of this material are still limited [77], [114], [151].

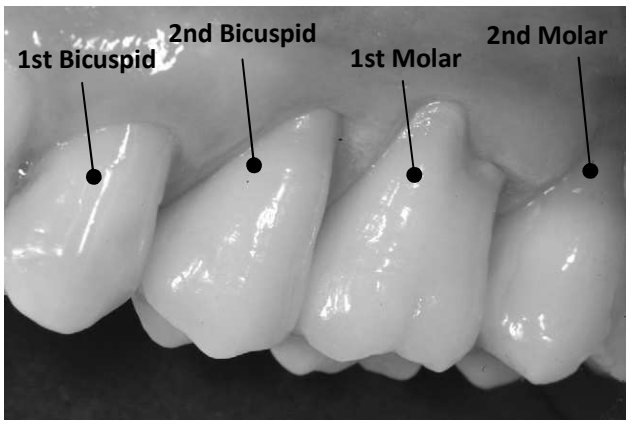

Figure 4.1 – Implanted zirconia-ceramic restorations (2nd Bicuspid and 1st Molar) [9]

The tribological behaviour of dental restorations is mainly affected by the mechanical properties and superficial microstructure of the material. It has been reported that abrasive wear is the main tribological behaviour in the oral cavity [15]. According to Antunes and Ramalho [16], the abrasive properties of dental restorations are more important than their hardness and the ball cratering technique is an appropriate test to assess these properties. The abrasive wear rate can also be influenced by the properties of the environment. In previous work, the effects of tea, a very common soft drink, on the micro abrasive behaviour of Y-TZP as a dental restorative material, were studied [152]. The aim of this work, after examining the effects of coffee on the abrasive behaviour of Y-TZP, is to compare the wear mechanisms and generate a body of data as a reference for the wear behaviour Y-TZP in popular caffeine based soft drinks.

4.2 Materials and Methods

In this study, the micro-abrasive behaviour of Y-TZP in caffeine based solutions is investigated in accordance with BS EN 1071-6: 2007: “Advanced technical ceramics, Methods of test for ceramic coatings: Determination of the abrasion resistance of coatings by a micro-abrasion wear test”, by running ball-cratering abrasive wear tests.

4.2.1 Test samples

3% yttria doped zirconia discs, provided by National Cheng Kung University, Taiwan, were used to conduct the experiments. The sample surfaces were polished with fine diamond paste (6 – 0.3 μm) and then ultrasonically cleaned in de-ionised water to remove any remaining debris. The circular samples were machined, circumferentially at a very low temperature, into regular octagons (36mm across) for improved access on the rig platform. The thickness of the samples was 3.4mm. Table 4.1 exhibits the mechanical properties of the samples.

4.2.2 Slurries

The Y-TZP samples were tested with seven different solutions: boiled water (for reference), plain tea and coffee, tea and coffee with additional sugar, and tea and coffee with additional milk. PG Tips® (London, UK) Pyramid tea bags were used to make the tea, prepared using the ‘tea brewed with freshly boiled water for 2 minutes’ instructions. As

there is no significant difference between the viscosity of spray dried coffee and freeze dried coffee [153], the coffee was made using Nescafé Original® (York, UK) (spray dried) which is a blend of Arabica and Robusta beans. The manufacturer's recommended concentration, 12 gl^{-1}, was used to prepare the coffee [154]. The solutions with added sugar were prepared with 2 teaspoons of sugar per serving, 28.57gl^{-1} in total. The solutions with added milk were prepared such that 10% of the final solution was milk. To simulate food bolus during mastication several types of abrasive particles can be used [128]. In this study, test slurries were prepared by combining the drink solutions with calcined alumina particles (9µm) (Logitech, UK), an abrasive powder commonly used in simulating oral cavity conditions. A concentration of 30gl^{-1} was used to simulate food bolus during mastication. In a lubricated abrasion process, the lubricant (tea or coffee in this case) sweeps the particles into and from the interface while creating a gap in the interface. Hence, the particles may only roll or tumble through the gap without creating any notable wear scars. The hardness of the solid surfaces plays an important role in this situation. If the hardness of the surface is relatively higher than the hardness of the abrasive particles, the particles slide on the harder surface without embedment [10]. This also degrades the abrasive particles [155], which is not the aim of this work. The hardness of calcined alumina (9 in Moh's scale) makes it an excellent abrasive particle for examining Y-TZP under severe conditions. The flatness of the alumina particles effectively spreads the load at the contact interface [129]. The mechanical properties of the particles are listed in table 4.1.

The composition of tea and coffee are both based on bioactive phytochemicals, such as amino acids, phenolic acids and polyphenols, with more acidity in coffee [156]. Table 4.2 presents the properties of the slurries. The addition of alumina particles slightly elevates the pH value of the drink solutions due to the chemical reaction ($Al_2O_3 + 3H_2O \rightarrow 2Al(OH)_3$) in the slurry. The viscosity of the slurries was measured using a CLS^2 500 Carri-Med rheometer. The viscosity of the slurries did not change significantly with increasing shear rate; therefore, the mean values have been reported. The temperature range of the drinks during consumption is estimated between 45 to 50^oC. To keep the temperature of the slurries in this range during the tests, slurry containers were kept in a reservoir with heightened temperature at all times. A small propeller, operating at 1330 rpm near the bottom of the container, was used during the tests maintain the suspension of the abrasive particles in the slurry. Each of the test slurries were used for a maximum of 3 hours to maintain a consistent viscosity.

Material Property	Y-TZP	UHMWPE	Alumina
Density(kg/m³)	6000	931-935	3800
Young's Modulus (GPa)	195-210	0.689	351
Hardness (Vickers)	1330-1470	541	2035
Fracture Toughness (MPa/m)	7-10	3.5-6	3.5

Table 4.1 – The mechanical properties of the test

Slurry	pH	Viscosity at 45°C (cP)	Temperature at sample in operation (°C)	Density at 45°C (kg/m3)
Coffee	4.6	0.781	48±2	1040.2
Coffee + sugar	4.6	0.835	48±2	1069
Coffee + milk	5.6	0.764	48±2	1043.5
Tea	5.3	0.726	47±2	1032
Tea + sugar	5.3	0.728	48±2	1060
Tea + milk	6.0	0.721	47±2	1033
Water	7	0.696	48±2	1012

Table 4.2 – The properties of the slurries

4.2.3 Test rig

The tests were conducted using a TE-66 Micro-Scale Abrasion Tester (Plint TE-66, Phoenix Tribology, Reading, UK). In this test programme, a cratering ball is rotating against the test specimen in the presence of a drip fed slurry which may contain abrasive particles. The contact pressure between the rotating ball and the specimen is adjustable using a weight hanger. Since the application of a free rotating ball confines the load range to the maximum of 0.4 N, the fixed rotating ball was chosen to have a wider range of the applied loads. By choosing a cratering ball over a cylinder, the size of the interface area is reduced. This is more suitable for small samples. The crater-depth can also be evaluated easier because of the well-defined taper angles as a result of the spherical cap geometry of the created scars. Moreover, the dimensions of the created scars can be measured directly from the

microscopy, leading to higher accuracy of the results [157]. The mechanism of the test rig is explained more elsewhere [152]. Figure 4.2 shows a schematic view of the rig.

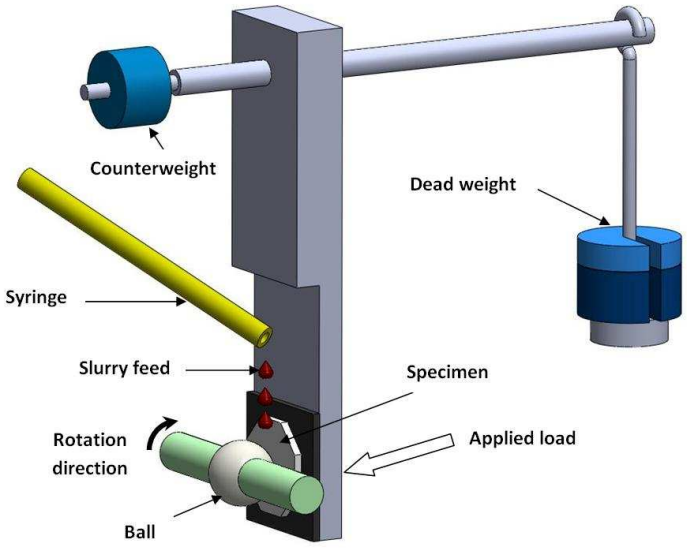

Figure 4.2 – The schematic view of the test rig

4.2.4 Methodology

The number of the mastication cycles is highly dependent on the food hardness [158]. It has been reported that the presence of fluids during the mastication does not change the physical properties of the food bolus right before deglutition, although it changes the number of chewing strokes [159].The saliva flow rate during mastication among elderly people is slightly lower than younger people. However as elderly people chew food for a longer time (more chewing strokes) it compensates the flow difference [160]. The variation of the food bolus size distribution in different individuals is also very narrow [161]. Studies show that the sliding distance per chewing cycle is 0.5 – 1 mm, with a rate of 60 – 80 cycles/min, occurs 10 – 30 min/day [15], [16], [135], [137]. This means the average sliding distance per tooth is approximately 1 m/day. Jalabert-Malbos et al. [158] attempted to define the physiological properties of food bolus by examining different types of food. They classified the hardness of the food by the force needed to penetrate the food samples (from egg white to almond) and they found a range of 0.06 to 2.59 N. Chen et al. [162] went further and examined a few more types of nuts with higher hardness which needed higher penetration forces. Assuming there is a variety of surfaces and cusps in the geometry of Y-

TZP implants (therefore, different needed penetration forces), the range of 3 – 5 N was chosen for this work.

The load, duration, properties of the slurry mixture, sliding distance and sliding velocity are the main factors that influence wear rate [163], [164]. It is also widely accepted that the chewing cycles are the main reason of wear of dental materials [165]. Therefore, the scope of this work is not to examine the antagonistic behaviour of opposite implants; it is to evaluate the performance of Y-TZP implants against the food bolus (abrasive particles) where the penetration force is provided using an antagonistic body. Figure 4.3 illustrates a schematic view of the phases in a chewing cycle: Closing phase (phase I) and opening phase (phase II) [166]. The wear sites are mainly the occlusal and the incisal surfaces [165].

Ultra-high-molecular-weight polyethylene (UHMWPE) balls, of 25.4 mm diameter, (K-mac Plastics, Michigan, USA) were used as the antagonistic body (See table 4.1). UHMWPE has a smooth molecular profile with long chain molecules sheared across each other. This gives UHMWPE excellent sliding properties at the contact interface, such as the development of films which are made of molecular chains oriented parallel to the sliding direction. This makes this material capable of having the friction coefficient of 0.1 against hard counterfaces [167]. Additionally, the slurry likely further decreases this value. The high chemical resistance of UHMWPE may result in low inter-phase bonding. However, the mechanical activation process solves this problem and also increases the wear resistance of UHMWPE to a superior level [168]. A new cratering ball was used for each type of slurry to control for differences in the slurry composition, and the ball was rotated between tests to minimise the possible influence of ball deformation.

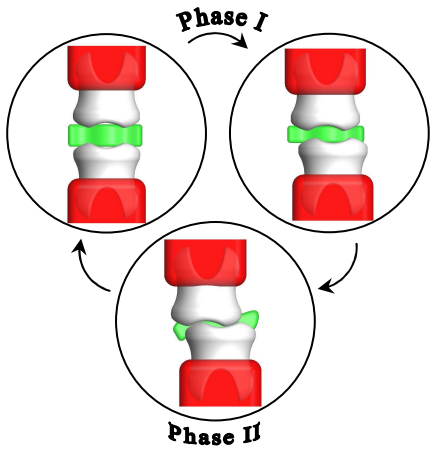

Figure 4.3 – schematic view of chewing cycles

It should be noted that it is ideal to examine a new material using *in vivo* methods. However *in vivo* methods are not suitable for particular studies of wear processes, where isolation is a necessity and specific factors (e.g. load, environment) should be continuous and under control. Moreover, *in vivo* methods cannot be accelerated and they are time-consuming and expensive [165]. Heintze et al. [169] examined 3 different kinds of dental composite ceramics (flat specimen) over a period of 12 months and found out that the range of the results from the laboratory tests and the clinical tests are very similar; although the wear behaviours might slightly differ due to the natural differences. They also suggested that 1 year is not an adequate period of time to confirm the reliability of the materials. Thus, in this study, each test applied a normal load of 3, 4, and 5 N to the sample, for 1, 2, and 3 hours; where the rotational speed of the ball was 150 rpm (0.2 m/s linear velocity). Because a 1 hour test is equivalent to 718.17 m in sliding distance, each test hour simulates 2 years of tooth wear. These experiments therefore simulate the equivalent of 6 years of wear on a Y-TZP implant. Table 4.3 shows the test conditions. It is worth noting that the previous research shows that the heat generated at the interface is negligible due to the high temperature of the slurry [152].

Test conditions	
Applied normal loads	3, 4, and 5 N
Sliding velocity	0.2 m/s (718.17 m/hr)
Tests duration	1, 2, and 3 hrs

Table 4.3 – Test conditions

4.3 Results

4.3.1 Volume loss

Y-TZP absorbs water when placed in an aqueous environment, as is the case for the slurry environment in the experimental rig or in the presence of body fluids in the oral cavity. This absorption increases the mass of the Y-TZP while the mechanical wear decreases the mass through material loss. Without accurate measures of both mass increase and decrease, the mass loss measurement method is not as accurate as a volume loss method. Wear scars were inspected using scanning electron microscopy (S-3700 N Tungsten Filament SEM,

Hitachi High-Technologies, Europe). Because the geometry of the wear scars is relatively spherical, the volume loss of each scar has been calculated using equation 4.1:

$$V = \frac{\pi b^4}{64R} \qquad (4.1)$$

for $b<<R$ where b is the diameter of the scar and R is the radius of the spherical counter-body (cratering ball) [91]. In the majority of cases, the edges of the spherical scars were quite clear (Fig 4.5(a)); however, 2 out of 63 cases showed spherical scarring with 'scuffed' annular regions instead of clear edges (Fig 4.5(b)). This phenomenon occurs particularly when the samples are softer than the spherical counter-body. However, from table 4.1 it is obvious that Y-TZP is much harder than UHMWPE; therefore, this may be evidence of ageing. Previous work has shown that annulus ridges are quasi-stable and tend to break down, eventually, to reveal a normal spherical wear scar; therefore, cases without clear edges may still be accurately evaluated [91].

The wear scars were also measured using a stylus profilometer (SJ-500, Mitutoyo, UK). The profilometry results validated the volume loss from SEM measurements with a deviation of only 3.9%. It was determined that the wear scar curvatures imitate the curvature of the spherical counter-body. Figure 4.4 presents the volume loss measurements. It is clear that coffee slurries cause a higher volume loss than tea slurries. The volume loss associated with coffee solutions consistently increases with greater applied loads and longer duration (or increased sliding distance); whereas the volume loss associated with tea solutions do not follow a consistent trend under the same conditions. This variation implies that volume loss is affected by additional factors, which are discussed below.

Figure 4.4 – Volume loss measurements

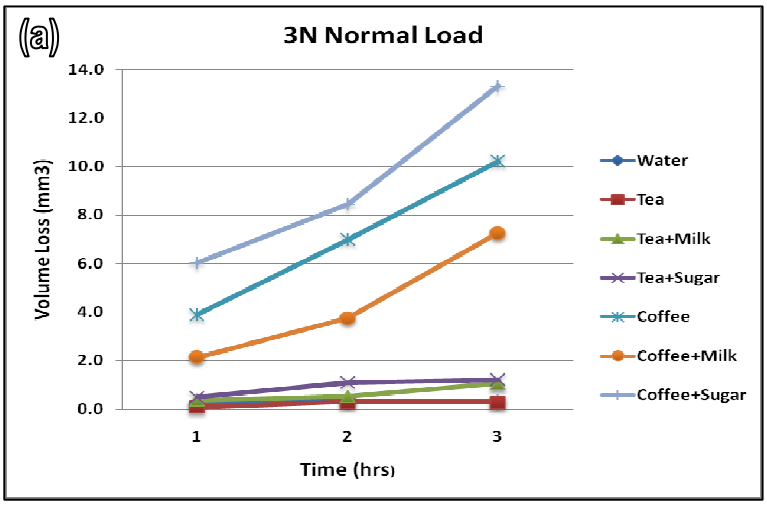

Fig 4.4 (a) - Volume loss under 3N normal

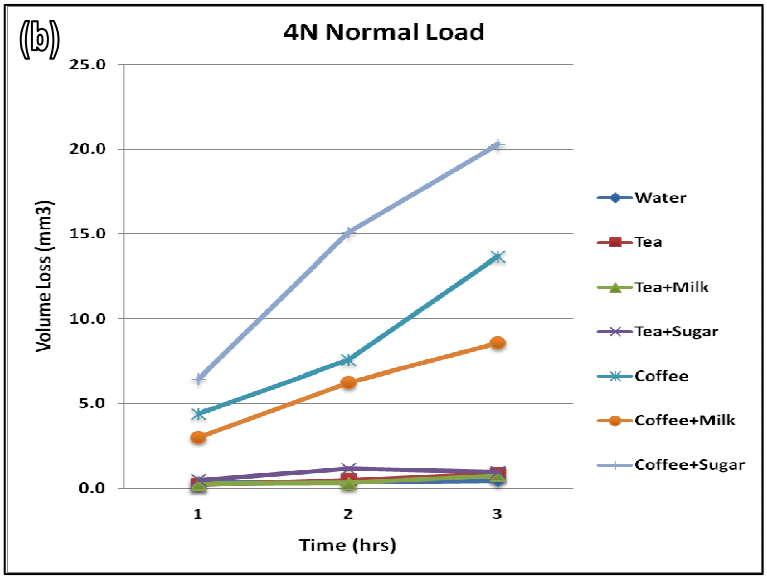

Fig 4.4 (b) - Volume loss under 4N normal

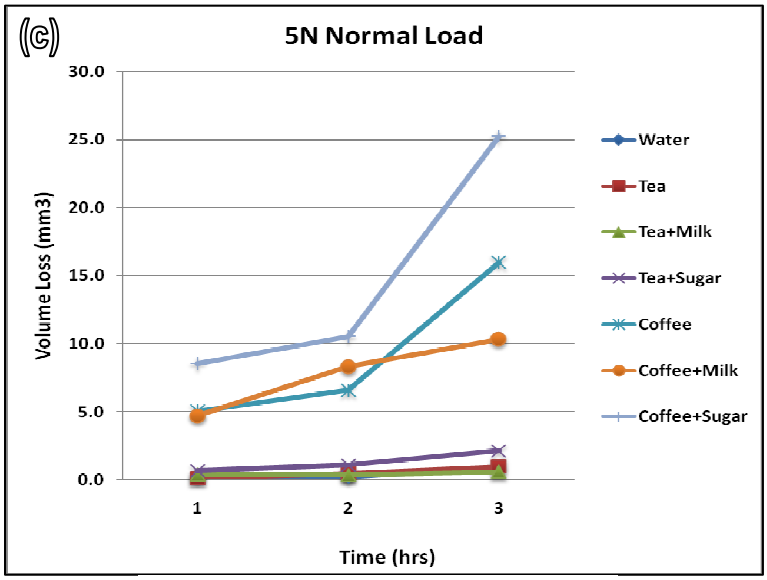

Fig 4.4 (c) - Volume loss under 5N normal

4.3.2 SEM analysis

The dominant wear regime in the wear scars was 3-2-body mechanism with predomination of 2-body grooving, regardless of the type of slurry [145]. Figure 4.6 exhibits an example the similarity of the wear scars created by tea and coffee slurries. Figure 4.6(a) is a close-up of the wear scars after a 3 hour test in tea+milk slurry under 4N normal load, and figure 4.6(b) is the wear scars after a 3 hour test in coffee+sugar slurry under 5N normal load.

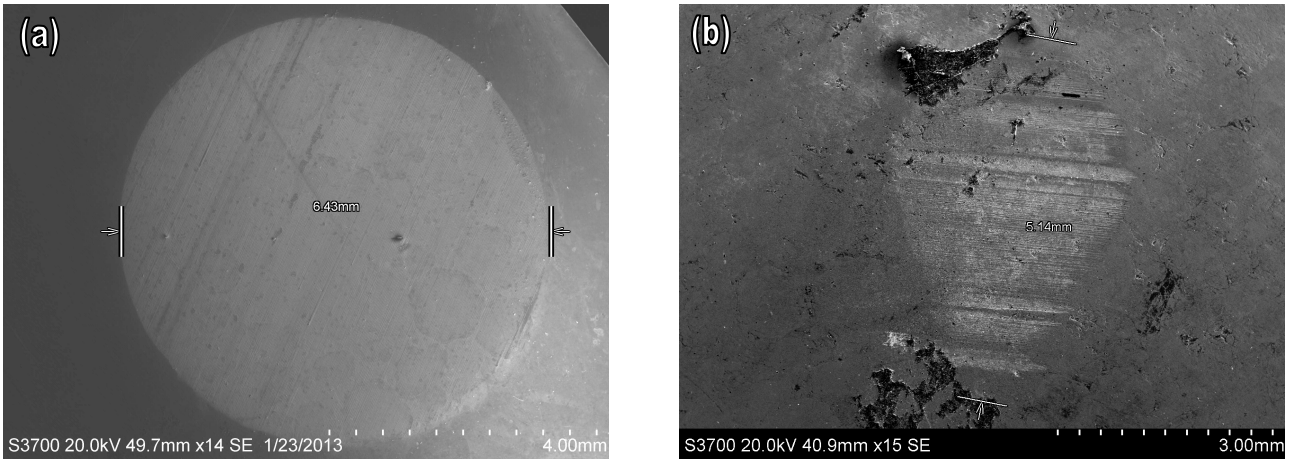

Figure 4.5 – The edges of the spherical scars (a) Coffee 5N 3hrs and (b) Tea + sugar 3N 2hrs

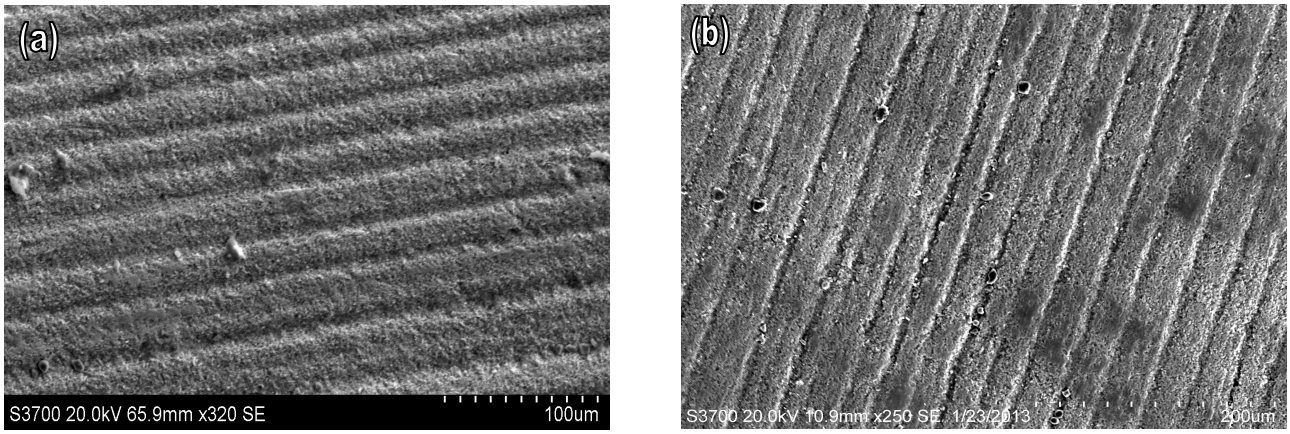

Figure 4.6 – Wear scars after 3hrs tests (a) in tea+milk under 4N load, (b) in coffee+sugar under 5N load

SEM and EDX inspection of the spherical counter-body showed that alumina particles had clearly embedded in the cratering ball surface. Following exposure, the embedded alumina particles formed up to 1.26% of the final weight and up to 2.39% of the final volume of the cratering balls. This explains the domination of the 2-body grooving wear regime [145]. This also indicates that the UHMWPE ball and the Y-TZP samples are not in direct contact during the experiments, it is technically the alumina particles that create the wear scars on the surface of the specimen [91].

Figure 4.7 shows an example of the EDX and SEM investigation of one the counterface balls after a 2 hrs test. It was observed through microscopy that, despite the deeper craters and higher volume loss, craters created in coffee slurries were more uniform than craters created in tea slurries, which showed grain pull-outs and micro cracks. These findings are discussed below. Figure 4.8 shows an example of these phenomena.

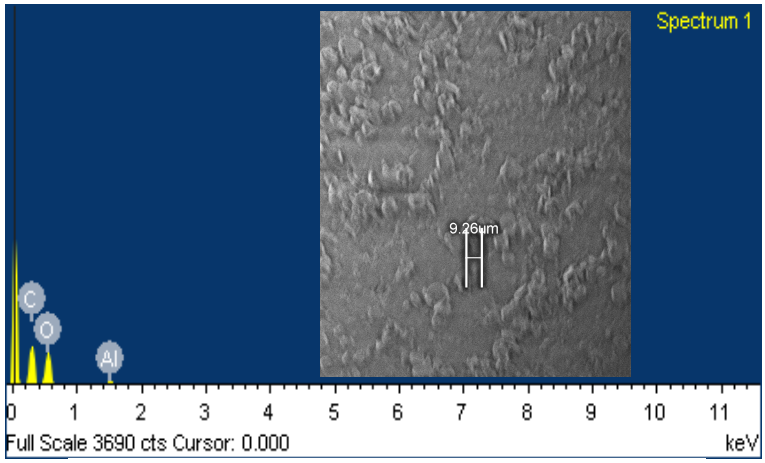

Figure 4.7 – EDX results and SEM analysis after a 2hrs test

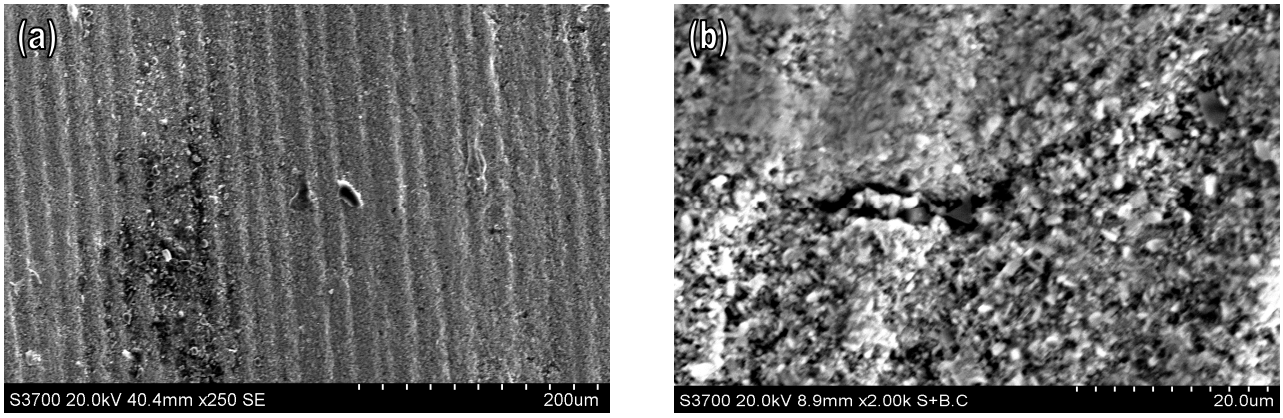

Figure 4.8 – (a) a grain pull-out incident, (b) a micro crack

4.3.3 Wear maps

Different approaches may be used to combine the available data in order to interpret the wear mechanisms that have taken place. In order to more accurately study and predict the behaviour of Y-TZP, this study presents the data as wear maps. Using table 4.4, figure 4.9 illustrates the behaviour of Y-TZP based on volume loss in three coffee solutions under different loads and exposure times (sliding distance). With a maximum volume loss of 25.247 mm^3, volume loss has been classified into 4 categories:

Very low: $V \leq 0.15 * V_{max}$ (4.2)

Low: $0.15 * V_{max} < V \leq 0.30 * V_{max}$ (4.3)

Medium: $0.30 * V_{max} < V \leq 0.60 * V_{max}$ (4.4)

High: $0.60 * V_{max} < V$ (4.5).

where V is the volume loss and V_{max} is the maximum volume loss.

Applied load (N)			3			4			5		
Test duration (hrs)			1	2	3	1	2	3	1	2	3
Slurry	**pH**	**Viscosity @ 45°c (cP)**	**Volume loss (mm^3)**								
Coffee	4.6	0.781	3.883	6.985	10.215	4.404	7.559	13.658	5.043	6.607	15.991
Coffee + sugar	4.6	0.835	6.012	8.411	13.307	6.444	15.055	20.271	8.56	10.561	25.247
Coffee + milk	5.6	0.764	2.139	3.747	7.246	3.004	6.245	8.56	4.715	8.313	10.33
Tea	5.3	0.726	0.091	0.293	0.266	0.199	0.481	0.849	0.128	0.499	0.97
Tea + sugar	5.3	0.728	0.487	1.092	1.214	0.464	1.146	0.941	0.694	1.114	2.139
Tea + milk	6.0	0.721	0.366	0.517	1.05	0.255	0.281	0.732	0.416	0.381	0.6
Water	7	0.696	0.244	0.339	0.313	0.322	0.376	0.442	0.241	0.244	0.95

Table 4.4 – Test results with regard to pH and viscosity

The data from all the wear in tea slurries falls under the 'very low' category, so tea slurry wear maps are not shown here; however, the wear mechanisms of Y-TZP in tea slurries have been specifically discussed in previous work [152]. Figure 4.9 shows that, although the adjustable parameters (normal load and exposure time) are equal for the tests conducted in different slurries, the wear rates can be extremely different. For example, in figure 4.9(b), the wear map shows that the wear rate of a coffee+milk slurry is much lower than that of a coffee+sugar slurry (figure 4.9(c)). The data in table 4.2 shows that the coffee+sugar slurry possesses a higher viscosity and lower pH than the coffee+milk slurry. This indicates that pH and viscosity, along with applied load and exposure time, can influence wear rate. Therefore, the lower viscosity and the higher pH of tea slurries, compared to that of coffee slurries, can explain why the wear rates of tea slurries fall into the 'very low' category.

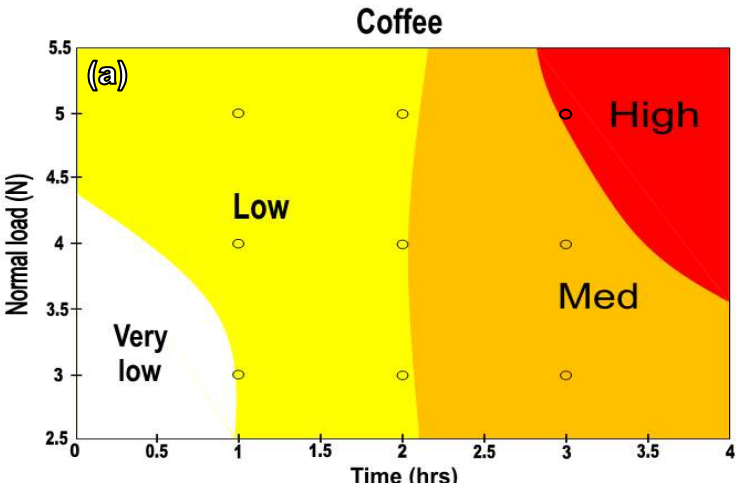

Figure 4.9(a) - Wear map of Y-TZP in Coffee slurry (load/time)

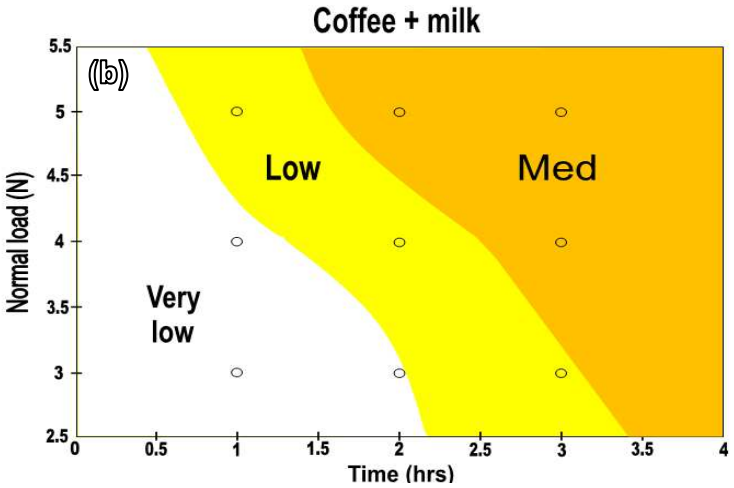

Figure 4.9(b) - Wear map of Y-TZP in Coffee+milk slurry

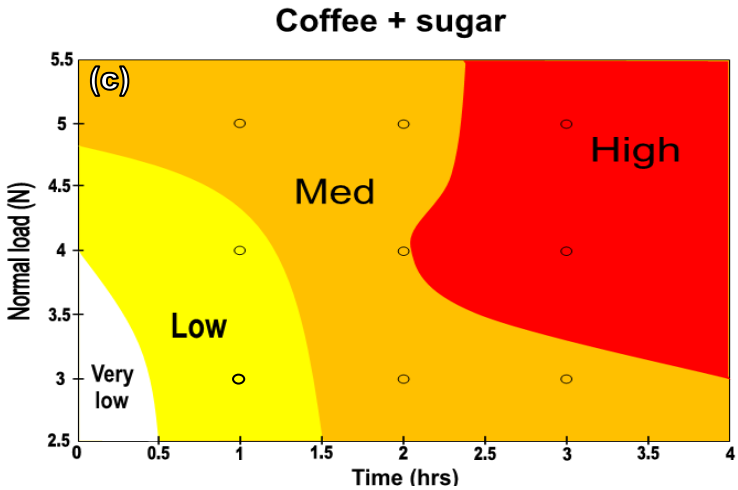

Figure 4.9(c) - Wear map of Y-TZP in coffee+sugar slurry

4.4 Discussion

The longevity of dental implants is associated with many factors, including the mobility at the start of the prosthetic phase, continuing radiolucency around the implant, and peri-implantitis with suppuration. Addressing these issues, may significantly extend this life span. Also, the early failure of the implants can be prevented by properly taking into account the width of the keratinised gingiva and the use of polyglactin sutures [170]. The destructive wear process of the dental tissue (implant) may be linked with physiological, pathological, prophylactic, or due to the finishing method [16]; however, in this study, the focus is only on the tribological behaviour of Y-TZP in two common caffeine containing solutions in a simulated oral cavity environment, assuming successful implantation.

The consumption of both coffee and tea has been recommended, as it has the potential of preventing some serious chronic diseases such as cancer and cardiovascular disorders [171]; however, these caffeine containing solutions may have detrimental effects on dental tissues (dental implants). The caffeine content of coffee and tea beverages depends on the raw material of each product, the manufacturing process, and the preparation method. The caffeine content per 100ml serving of coffee may vary between 21 and 127 mg, whereas this range for tea is between 8.5 and 25.5 mg. The phenolic and polyphenolic constituents of these solutions create an acidic environment in the oral cavity. The reported level of tea phenolics, flavan-3-ols (generally known as catechins), in black tea is between 5 and 21 mg/g. The coffee phenolics which mainly consist of chlorogenic acids for medium roast coffees are ranged from 28 to 45 mg/g [156], [172]. These numbers indicate why the pH value is lower in coffee solutions. Commonly, tea and coffee beverages are consumed along with secondary ingredients, for instance creamers (e.g. milk) and sweeteners (e.g. sugar). It should be noted that the addition of the secondary ingredients alters phenolic profiles of tea and coffee [156]; therefore these mixtures should be investigated individually. The results in section 3.1 indicate that, generally, by increasing applied load and sliding distance, higher volume loss is expected. However, bearing in mind that the experiments are conducted in similar conditions, variation of the results for different slurries shows that the properties of the abrasive slurries are as effective as increased load and sliding distance. Excluding the natural structural differences of tea and coffee, the main differences to consider may be the pH value and the viscosity of these products, which significantly affect the wear rate. Research shows that, in environments with very high or

very low pH values, wear rate increases. In other words, in very acidic and very alkaline environments, tribo-layers cannot be formed; this leads to constant wear loss during exposure time [148], [173].

Figure 4.10 plots the relationship between volume loss and viscosity; the curve indicates that generally, an increase in viscosity increases volume loss. The pH values on the curve show a similar trend. It is surprising, however, that with such a minor reduction in pH, such a large difference in wear rate is observed in both solutions and this further suggests that viscosity may play a significant role in the overall trends observed. Also the anomaly in the curve, created by coffee+milk (pH=5.6), causes a higher volume loss despite having a higher pH than the previous point. This implies that viscosity influences volume loss more than pH. The same anomaly is observed in both tea and tea+sugar slurries, which have an equal pH value of 5.3, with the tea+sugar slurry having a higher viscosity. Therefore, high viscosity could be more destructive than high acidity and this also may be linked with particle entrainment issues, with more abrasive particles being captured in the contact in the more viscous environments.

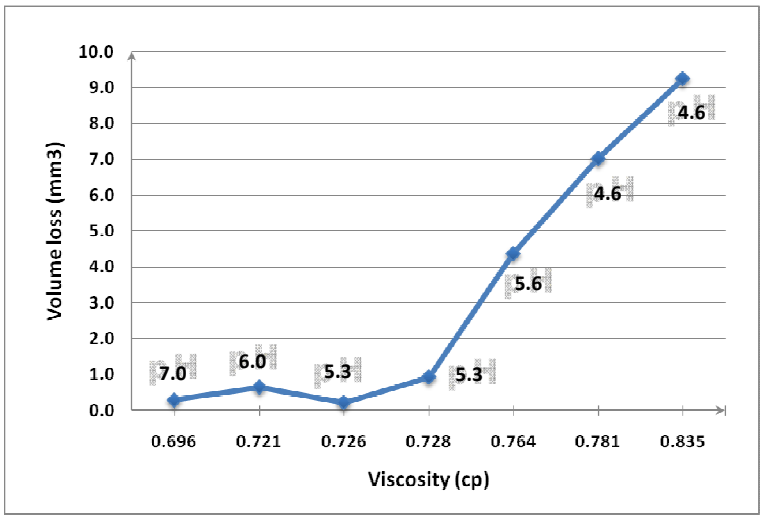

Figure 4.10 – Volume loss vs. viscosity and pH

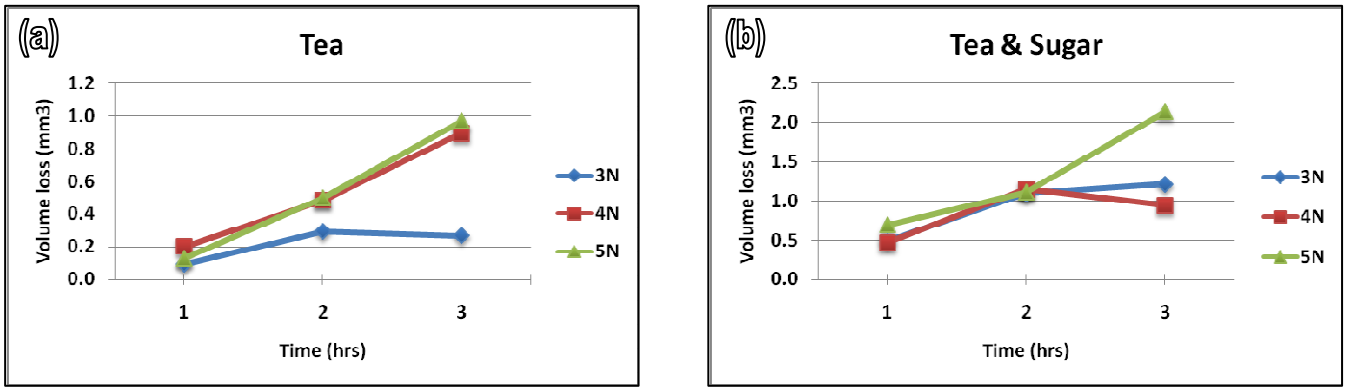

Figure 4.11 – Volume loss in (a) tea slurry and (b) tea+sugar

According to the Archard's Equation, and many similar studies, there is a linear relationship between wear rate, sliding distance, and the applied load [142], [143]; however, this is not always the case. For example, the tea and tea+sugar slurry wear rates (figure 4.11) show that higher loads and higher sliding distances do not always cause higher volume loss. This may also be due to entrainment issues associated with abrasive particles at higher loads. Higher loads produce higher pressure in the contact area, which may reduce the frequency of particle entrainment. Also, particles may take longer to entrain in specimens with higher hardness. Moreover, using a softer cratering ball does not always facilitate particle entrainment on the ball's surface [91], [174]. This indicates that the Archard's Equation does not take into account all of the factors that influence wear rates. Because this study investigates the performance of Y-TZP immediately after dental implantation, cratering balls without previously pitted and/or roughened surfaces (the two primary methods of promoting particle entrainment) are used. Particle entrainment occurs gradually during the experiment.

Initially, particle entrainment at the counter-face area occurs slowly, but as more particles become entrained further entrainment happens more quickly, resulting in higher wear rates. Examination of the microscopy images suggests that once the treated surface of the sample is fully perforated, the material wears more rapidly and the relationship between wear rate, load, and sliding distance becomes linear. SEM analysis shows evidence that ageing, including micro-cracks and grain pull-outs, occurred before full perforation was reached. After full perforation, the wear scars become deeper, smoother, more uniform, and more circular, without any evidence of ageing. Therefore, the likelihood of ageing is

highest before perforation is reached. Because perforation requires more time when using a tea slurry, the probability of ageing with tea is greater than with coffee.

Since the majority of people consume at least one of the tested caffeine containing drinks (tea or coffee) or a carbonated drink daily [175]; therefore, the severity of the mechanical conditions in the conducted tests was necessary to simulate years of mastication in mere hours. Also, it should be noted that the pre-dominant wear regime in this study was 2-body grooving. It has been reported that the wear loss of teeth due to 3-body regimes, which is very likely to happen in the oral cavity, are significantly less than 2-body wear regimes. Furthermore, the influences of the increased load are more significant under 2-body mechanisms [108]. However, the increasing common consumption of fizzy soft drinks creates an environment in the oral cavity that exceeds the acidity (with a pH of 3.0 or lower) and viscosity of the tested drink solutions [176], which has been addressed in previous work by the current authors [18], [177]. The results of these experiments suggest that there are additional factors, which are not included in the Archard's Equation and which must be considered in evaluating the performance of Y-TZP dental implants. Evidence shows that viscosity and acidity exacerbate the effects of load and exposure time. Because dental implants are exposed to aqueous environments, the probability of ageing is very high. Y-TZP manufacturing processes therefore must be carried out with greater precision, particularly in the addition of stabilisers and the sintering process temperature; because lack of yttria reduces the tetragonal-phase stability and the serviceability of such dental restorations [178]. By keeping the sintering temperature of Y-TZP below 1450 °C the ideal grain of 0.3 – 0.4 μm can be achieved. This totally prevents or at least significantly minimises the phase transformation in accelerated ageing conditions. It also maximises the ageing resistance where a long life span is aimed for [179]. Surface treatments with greater depth will also reduce wear rates [180]. It is reported that polishing and higher smoothness can significantly improve the wear performance where this type of materials has been used in monolithic restorations [15], [181]. Precise manufacturing will yield Y-TZP that is more resistant to ageing and this may be the key to production of such materials which are resistant to such environments.

Clearly the tribo-chemical environments involved in caffeine containing drinks as described above may have major effects of the longevity of ceramic restorative materials. The difference in the performance of the tribo-layer in both tea and coffee environments is a

key to the reduced wear observed in the tea solutions, with the ageing process enhanced in the latter solutions. Further work will be to investigate at the nanolayer, the reasons for such differences, thereby providing important new information on materials selection of dental restorative materials. Also, the use of tactile pressure sensors and Finite Element Analysis (FEA) are recommended to have a better understanding of the performance of new products in oral cavity where they have a specified design.

4.5 Conclusions

A study has been conducted of the micro-abrasion of Y-TZP in tea and coffee environments in which sugar and milk are added to the slurry mixtures. Within the limitations of this study, the following conclusions can be drawn:

i) The results indicated a greater dependence of wear rate on viscosity than pH.
ii) The wear rate did not increase directly with an increase in applied load, in the range studied, and this was attributed to entrainment issues associated with abrasive particles at higher loads.
iii) The reduced wear in tea is associated with a longer aging time, following exposure, to full perforation of the surface.
iv) Micro-abrasion maps were constructed showing distinct difference in the performance for the ceramic material in the various environments, with the higher wear rates associated with coffee in sugar, linked with significant surface fragmentation and particle detachment in such environments.

Acknowledgements

The authors wish to extend grateful thanks to Professor Wang-Long Li from Cheng Kung University, Taiwan, and Professor Moo-Chin Wang from Kaohsiung Medical University, Taiwan, who provided the Y-TZP samples for this study.

5

Tribo-corrosion of steel in artificial saliva: application to dental implants

Submitted paper based on this chapter:

Tribo-corrosion of steel in artificial saliva: application to dental implants

D. Holmes, S. Sharifi and M.M. Stack

Submitted to Tribology International

Abstract of the paper:

Stainless steel is widely used as dental implant. However, there has been little work on the micro-abrasion of such materials in laboratory simulated oral environments, where abrasion and sliding wear can interact simultaneously. In this study, the effects of applied load and exposure time were evaluated for a 316L stainless steel in a laboratory-simulated artificial saliva solution. Polarization curves showed an enhancement of corrosion current density with increases in applied load. Wear maps were produced showing low wear safety regimes at intermediate loads and exposure times. Possible reasons for such trends are interpreted in terms of the ability of the passive film in providing resistance against third body particle impact and the concentration of particles in contact at higher loads.

5.1 Introduction

Tribology has many applications in the field of dentistry. Assessment of the mechanism in which materials behave in the mouth, their longevity and their change in texture, colour, and shape is important and whether the material is a conventional metal or a more complex ceramic. In the mouth, mass loss in teeth is due to various tribological mechanisms and these can further interact with potential dental implants. Chemical reactions with food, interactions with particles of food and the physical process and resulting forces of chewing itself, all combine to act on teeth. So, it is important to evaluate how a dental implant material would react to these processes to ensure the longevity of the implant and to avoid adverse reactions within the mouth causing decay [152].

The corrosion resistance and mechanical properties of stainless steels make them a suitable material for use in medical implants, including dental implants and orthopaedic treatments. Corrosion resistance and ultimate tensile strength of austenitic steel in general make it appropriate for use. Typical materials include 316L grade stainless steel, using the American Iron and Steel Institute (AISI) classification system. The designation of 316L indicates a lower carbon content, less than 0.03%, compared to 316 grade which contains 0.08% carbon. 316L stainless steel is protected from grain boundary carbide precipitation, known as sensitisation and applications of 316L stainless steel include food preparation equipment, pharmaceuticals, marine and architectural applications and medical implants, including dental implants. The most common usage of 316L grade stainless steel is as a material for orthopaedic brackets. Although duplex steels are increasingly being used instead of austenitic steels, the use of austenitic steels is still widespread [86], [182], [183]. The durability and low cost of stainless steel makes it an appropriate choice for use in dental crowns, especially where the use of other materials is not economically viable. As of 2005, the British Society of Paediatric Dentistry (BSPD) recommended the use of stainless steel (pre-formed) crowns for the restoration of primary molars with multi-surface lesions, extensive caries (cavities) and those where pulpal treatment has been performed [19].The main quality of stainless steel is its resistance to corrosion, which can vary depending on the grade of stainless steel used but the formation of a passive chromium oxide film (passivation) can protect the material [18], [184].

In the oral cavity, saliva, produced by the salivary glands, acts as a lubricant and aids mastication by helping food transportation and provides the necessary lubrication required

between the hard and soft tooth tissue. Saliva reduces the amount of wear that takes place in the oral cavity, which extends the lifespan of both teeth and dental implants and reduces the need for intervention [185]. There are many components of real saliva that serve various complex biological processes, and hence it is difficult to completely produce artificial saliva that matches the composition of saliva fully. However for these purposes, the artificial saliva produced is adequate if it interacts with the metal sample in a similar way to which real saliva would [186].This solution has been used in a number of previous studies; Li et al. explored wear behaviour of human teeth in dry and artificial saliva conditions which explored the frictional behaviour of human teeth and titanium [106]. Ziskind et al. studied amalgam type, adhesive system, and storage period as influencing factors on micro-leakage of amalgam restorations [187]. Wang et al. looked at the friction and wear behaviours of dental ceramics against natural tooth enamel using Fusayama solution [15]. Other studies have examined the corrosion effects of materials in this substance [188–192], yet there appears to be few micro-abrasion-corrosion tests carried out with artificial saliva.

The purpose of this work is to address the above issues by studying the wear mechanisms of 316L grade stainless steel as an orthodontic material in artificial saliva using a micro-abrasion-corrosion apparatus. The wear mechanisms were evaluated using an abrasion-corrosion test apparatus, i.e. a micro-scale abrasion testing apparatus and corrosion interactions using potentiodynamic polarization tests. Micro-abrasion maps are generated based on the result showing region of exposure time and applied load where the wear rate is at a minimum.

5.2 Materials and methodology

Abrasion tests on the effects of applied load and exposure time were carried out. The results produced were in the form of the amount of wear that has taken place, found from the wear scar volume or mass loss. These results were represented as wear maps, showing the conditions of the highest and lowest amounts of wear occur.

5.2.1 Test samples

The composition of 316L grade stainless steel can be seen in table 5.1, below. The samples were prepared by cutting them to the desired size in order for them to fit securely into the

test rig. No surface coating was applied to the material. The mechanical properties of the test samples are shown in table 5.2.

Chemical compositions of the test samples (wt. %)									
C	**Mn**	**Si**	**P**	**S**	**Cr**	**Mo**	**Ni**	**N**	**Fe**
0.03	2	0.75	0.045	0.03	16-18	2-3	10-14	0.1	Bal.

Table 5.1 – Chemical composition of the test samples

Material Property	316L	UHMWPE	Alumina
Density(kg/m^3)	7870 – 8070	931-935	3800
Young's Modulus (GPa)	192	0.689	351
Hardness (Vickers)	170 - 220	541	2035
Fracture Toughness (MPa/m$^{1/2}$)	100	3.5-6	3.5

Table 5.2 – The mechanical properties of the test materials

5.2.2 Test slurry

The abrasive slurry was formed using artificial saliva mixed with abrasive particles. The artificial saliva was manufactured as described in previous papers using available chemicals and distilled water [15]. This solution is known as a modified Fusayama solution. This solution was selected for use in these tests because of its established use within dental material testing. The electrolytes found within this solution are considered as closely resembling natural saliva. The pH of this solution can range approximately between values of 5 and 7 [191]. The pH of the slurry used in this work was 5.7. The chemical composition of artificial saliva can be seen in table 5.3.

Artificial saliva composition (g/l)						
NaCl	**KCl**	**$CaCl_2.2H_2O$**	**$NaH_2PO_4.2H_2O$**	**$Na_2S.9H_2O$**	**Urea**	**Distilled water**
0.4	0.4	0.795	0.78	0.005	1	1000

Table 5.3 – The artificial saliva composition

Slurries containing abrasive particles can be used in order to simulate food bolus within the mouth during mastication [128], [152]. For these experiments alumina was used. The hardness value of the abrasive can affect the wear rate, with harder particles causing greater levels of wear. In the above case, the hardness of alumina is much higher than that of 316L stainless steel. This is referred to as hard abrasion and altering the hardness value of the particle slightly will have very little effect on wear rates. If the sample and abrasive particle are closer in terms of hardness value, the situation is known as soft abrasion and alterations of the hardness value of the abrasive used can significantly affect the wear rate [193]. For each experiment in this project, 1500 ml of artificial saliva was produced and this was combined with 30 gl^{-1} of Calcined Aluminium Oxide Powder (Logitech, UK) to produce the slurry. These particles had an average size of 9 µm. The mechanical properties of the particles can be found in table 5.2. The slurry supplied to the apparatus was kept agitated to avoid the particles settling.

5.2.3 Test apparatus

A ball cratering wear test was used, using the TE-66 Micro-Scale Abrasion Tester (Plint TE-66, Phoenix Tribology, Reading, UK). The test involves the rotation of a material sample against a hard ball, with the slurry fed to the sample during the test. A diagram of the test rig used is shown in figure 5.1. The counter-surface ball is held in place between two coaxial shafts by friction.

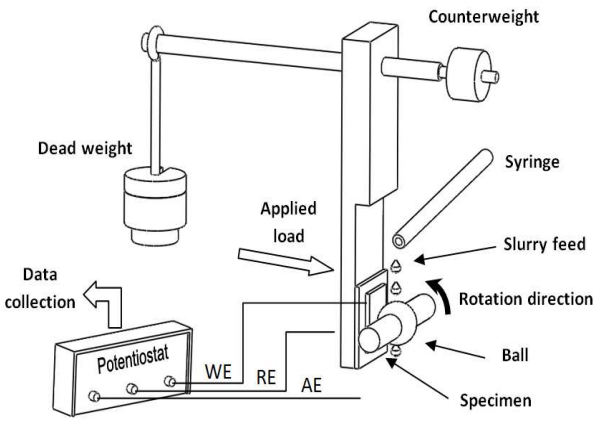

Figure 5.1 – test rig

The sample to be examined is held against the counter-surface ball by a vertical arm. The loading force to the sample is supplied using set masses.

The sample is initially held so that it is just touching the ball with no forces applied, a counterweight being used to balance the arm. From there, incremental masses can be added for the desired loading case. This loading mechanism has proved to be useful as it allows precise application of the desired force within a range of ±0.01 N. One of the co-axial shafts is driven by a variable speed DC motor, through friction the ball rotates, and in turn, rotates the second co-axial shaft which is connected to a peristaltic pump. The peristaltic pump provides the abrasive slurry to be fed on to the sample. The test can be run for varying times and motor velocities which equate to form the sliding distance for the test. The counter surface ball was made of ultrahigh molecular weight polyethylene (UHMWPE) and has a very low frictional coefficient. This results in little frictional heating, this combined with the lubrication and cooling effects of the slurry resulted in negligible heating effects [167]. The UHMWPE ball (K-mac Plastics, Michigan, USA) was used due to its ideal properties for use with ball cratering wear tests. The material is very resistant to abrasive wear as a result of its smooth molecular profile and high toughness [194]. The ball diameter used was 31.75 mm.

In order to estimate the corrosion rates a potentiostat, Gill AC (ACM Instruments, UK), was used. The working electrode was connected to the sample. The samples were isolated by a non-conductive tape apart from the interface point (A = 1 cm^2). A saturated calomel electrode (SCE) was used as the reference electrode which was in contact with the circuit using a capillary tube. Also, a platinum-titanium wire mesh was used as the auxiliary electrode. The polarisation curves were measured at a sweep rate of 50mVmin^{-1} from -1 to 0.5V. It should be noted that the experiments were conducted in a non-de-aerated condition.

5.2.4 Test method

Various parameters of the test can be altered, test duration, loading force and the sliding velocity. In this case sliding velocity was kept constant at 150 rpm. Tests were carried out with loads ranging from 0.5 N to 4 N and test durations of between 0.5 hour and 3 hours. The effects of altering these parameters on the wear mechanisms produced have been examined in previous work [144], [145]. Table 5.4 shows the list of parameters.

Test parameters	
Test duration (hrs)	0.5, 1, 2 and 3
Applied load (N)	0.5, 1, 2 and 4
Sliding velocity (m/s)	0.3 (897.75 mh^{-1})

Table 5.4 – Test parameters

5.3 Results

5.3.1 Volume loss

The mass loss can be calculated from the mass difference or using the wear scar volume equation, assuming the wear scar generated is a spherical cap. The diameter of each wear scar was measured during the SEM analysis and using this value and the diameter of the counter surface ball, the wear scar volume was calculated using equation 5.1:

$$V = \frac{\pi b^4}{64R} \qquad (5.1)$$

where V is the scar volume, b is the scar diameter and R is the cratering ball radius where $b<<R$.

Figure 5.2 shows the volume loss results for different loads over the test durations. The final magnitude of the volume loss for each load has increased comparing to the initial value, although a linear approach cannot be clearly seen.

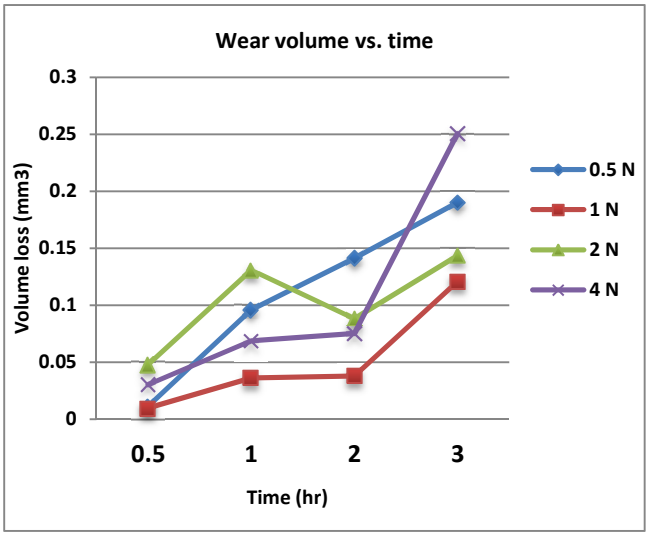

Figure 5.2 – Volume loss results

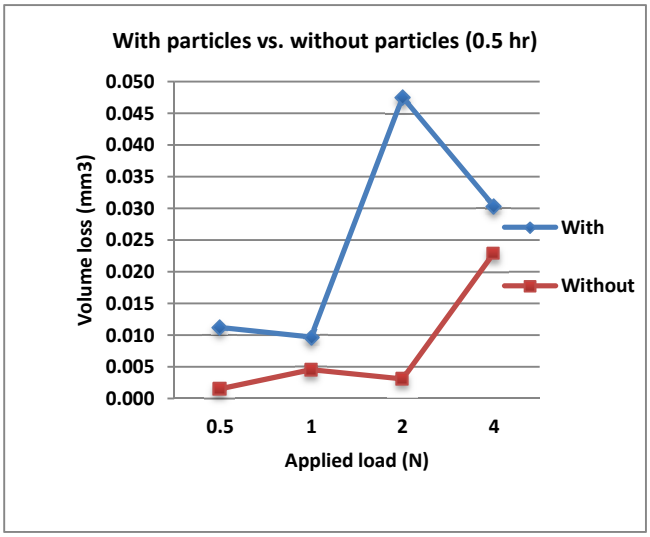

Figure 5.3 – Volume loss results for 0.5 N tests with and without particles

In order to consider the effects of the particles on the wear mechanisms, especially corrosive wear, the tests were conducted for 0.5 h for each load without particles. Figure 5.3 compares the volume loss results of 0.5 h test with particles to the tests without particles.

5.3.2 Polarisation tests

Figure 5.4 illustrates the polarisation test results. These indicate that for conditions without particles, Fig. 5.4(b), the corrosion potential was approximately similar for all applied loads.

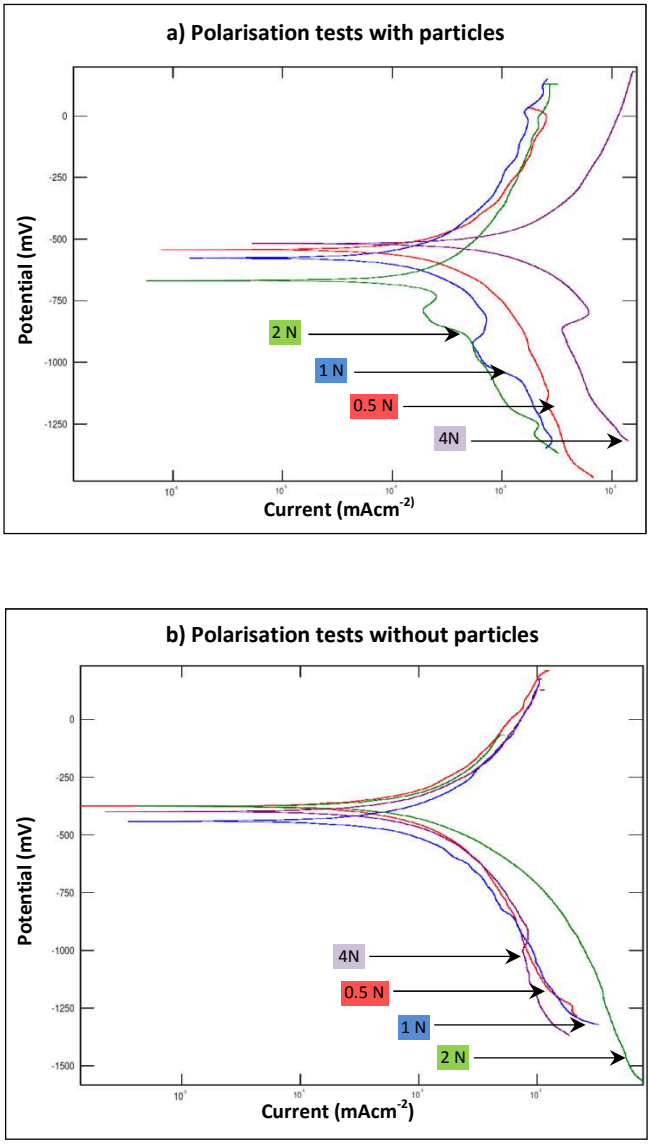

Figure 5.4 – Polarisation test results for 0.5 h tests (a) with and (b) without particles for different loads

There was little evidence of an increase in corrosion current with increasing load and passivation was achieved for all applied loads. For the test with particles, Fig. 5.4(a), there were some shifts in the corrosion potential with lower values recorded at intermediate loads i.e. 2 N, and higher values observed at the highest loads, i.e. 4N, with a difference of approximately 50 mV recorded. The passive current densities shifted significantly in the positive direction i.e. by one order of magnitude as the applied load increased from 2-4 N.

5.3.3 SEM results

It is acknowledged that, depending on the conditions of the wear, different types of abrasive wear can occur. The terminology describing these wear mechanisms will be explained using common definitions; however the main terms used (two-body and three-body wear) have been described as ambiguous and contradictory and there have been various proposals to redefine these terms [52], [144]. Despite this, the use of the terms is still widespread and the definitions described here are the generally accepted definitions. Scanning electron microscopy (SEM) is used in order to examine the wear scars. In this case an S-3700N model Tungsten Filament SEM (Hitachi High-Technologies, Europe) was used. From this, detailed pictures of the wear scars are produced showing the different wear regimes that have taken place, the size of the wear scars are also found through this method.

Figure 5.5 shows how the change in applied load can affect the type of wear that is produced and how at some intermediate load a transition must take place between two-body and three-body wear. Figure 5.5(a) is the very smooth wear scar produced after 3 hours with 0.5 N of applied load. Despite the low load, the wear volume is relatively high compared to the other 3 hour tests. This wear scar has no clear directional deformation suggesting the presence of three body wear; this is consistent with what is expected in low load situations [144]. Figure 5.5(b), shows the wear scar for the three hour, 2 N applied load test. This image gives a good indication of the type of scar produced under the influence of a mixed wear regime, with some areas of greater grooving. In figure 5.5(c), the 0.5 N wear scars are contrasted by the wear scar produced by the 3 hour, 4 N applied load test which produced a heavily deformed wear scar with clear directional grooving. This indicates that two-body wear has taken place. Figure 5.5(d) shows the wear scar for the 0.5 hour, 1N applied load test, which illustrates the clear presence of the particles at the early stages of the tests where particle embedment has taken place yet.

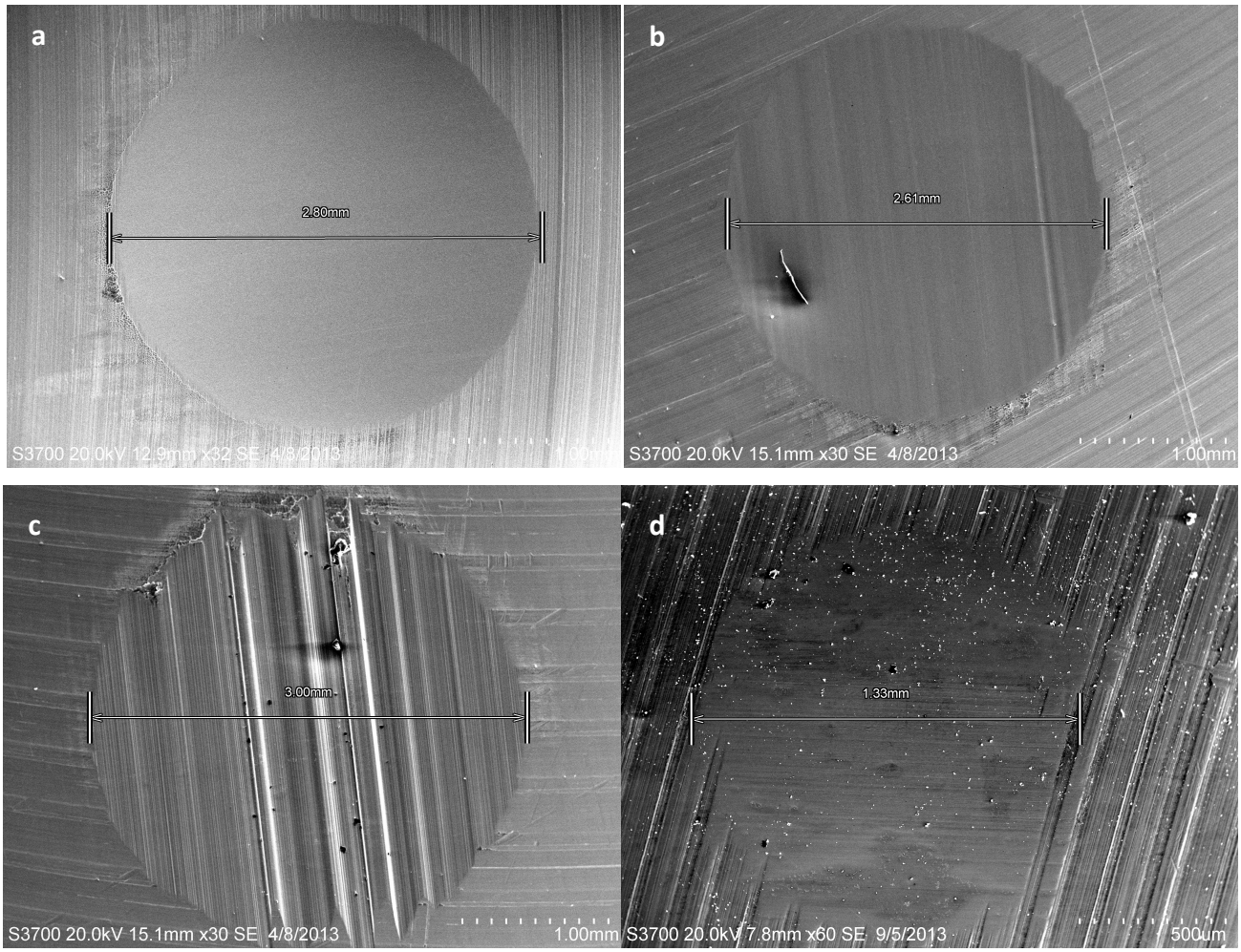

Figure 5.5 – SEM analysis results a) 3h test with 0.5N, b) 3h test with 2N, c) 3h test with 4N, d) 0.5h test with 1N

5.3.5 Wear maps

Wear maps have been constructed for dental materials and can be useful in order to compare the results in a visual manner. From the result of the wear scar measurements, wear maps were produced. Wear maps allow the amount of wear that has occurred under the various conditions to be expressed in a more qualitative manner.

In order to produce these wear maps, values for wear volume had to be defined as belong to three categories; low, medium and high wear. Based on previous work [107], the categories were defined as follows based the maximum wear volume produced (0.2505 mm^3):

- High wear≥80% of maximum wear (0.2004 mm^3) (5.2)
- 30% of maximum≤Medium wear<80%of maximum (5.3)
- Low wear> 30% of maximum (0.07515 mm^3) (5.4).

From this, boundaries were created, the results were interpolated between these points and the maps were produced as seen in figure 5.6.

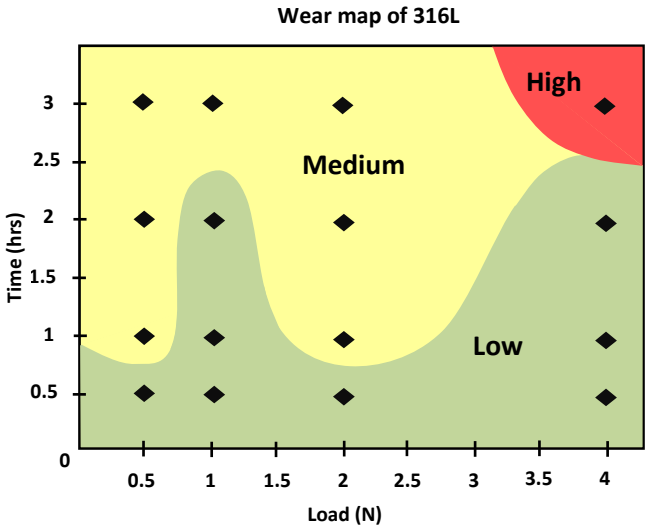

Figure 5.6 – Wear map of SS 316L in artificial saliva

5.4 Discussion

In oral environments, the average tooth sliding distance has been shown to be approximately 1 m per day based on an average amount of chewing each day and normal tooth contact [152]. Therefore, using this value and the sliding distances calculated, a one hour test corresponds to nearly two and half years of use for a dental implant, five years for the two hour test and approximately seven and half years for the three hour test. This means that the tests simulates a significant period of time in the lifetime of an implant and can give a good indication of the amount of wear that could potentially be experienced over this time. The predicted volume loss can be calculated using the Archard's equation for homogenous materials:

$$V = \frac{KWL}{H} \qquad (5.5)$$

where *W* is the total load applied, *H* is the hardness of the softest contacting surfaces, *K* is a dimensionless constant (severity of wear) and *L* is the sliding distance. According to the Archard's equation, increasing the applied load should result in a linear increase in the amount of wear produced. For steel samples, this has been shown to be true [134], up to a certain load and only under three-body conditions. Trezona et al. showed that the Archard's equation was valid for three-body rolling conditions, where wear did increase linearly with load, but for two-body grooving conditions, wear was shown to be proportional to a power of load lower than one. Also, it has been shown that when slurries with a high concentration of abrasive particles are used, wear rate is independent of applied load [144]. This is stated to be expected based on assumptions made. The abrasive particle concentration in these experiments has been kept constant. Similarly to applied load, an increase in sliding distance should be proportional to wear volume in accordance with the Archard's equation. However, this is only valid in some cases. Wear rate has been shown to increase generally with sliding distance, but in a non-linear approach [145]. It can be seen that in the case of the 0.5 N constant applied load results above (Fig. 5.2) that wear did increase linearly with time. This is due to a constant rotational speed corresponds directly to sliding distance. However for all other applied loads, the change in the amount of wear with time became increasingly non-linear with increasing applied load. This suggests the applied load has a large effect on the transitions between different types of wear, which results in different rates of wear and therefore a non-linear change in the total amount of wear produced. The 0.5 N applied load affects the wear rate the least and the 4 N applied load has the greatest effect. Comparing SEM images of the 1 N and 0.5 N tests visible grooves can be seen, unlike the very smooth 0.5 N wear scars. Higher loads are expected to produce two-body wear which results in higher wear volumes. However as wear continue to increase; particles can become trapped in ridges, causing the amount of wear to decrease. These low wear volume regions at high load can be seen in the wear map above, Fig. 5.6.

It has been established previously [145] that, with increasing load, wear can transition from 3-body abrasion at lower loads, where abrasive particles are free to move causing non-direction rolling wear, to 2-body directional grooving wear at higher loads. It has also been observed that at intermediate type of wear called 3-2 body where a mixture of the two

wear mechanisms takes place. It has been noted that wear generally begins as three-body abrasion; if there is a sufficient concentration of abrasive particles, particles can become embedded in surfaces and this can result in two-body abrasion. High loads have been noted to cause two-abrasion due to greater particle entrainment. Particles embed in a surface and produce directional, linear wear scars due to the particles causing grooving in the other surface. The instance of higher loads producing lower wear volumes suggests that ridge dominated 2-body wear has occurred.

In the above situation, the abrasive particles become entrained in the ridges that were been formed, reducing the ability for wear to take place. With continuing increases in applied load, it can be assumed that the ridges would be worn away, freeing the particles and resulting in an increase in the wear again. At lower loads, particles are free to move producing non-directional wear which is heavily deformed. The transition between two and three body abrasion has been found to occur at a critical value of applied load. Loads should be kept above or below this value if transitions are not desired. Mixed wear regimes can be produced under certain conditions at intermediate loads where there is evidence of both two-body grooving and three-body rolling. The shape of the abrasive particle and the separations of the two surfaces are important in terms of when transition occurs. It has been observed that the transition from rolling to grooving takes place at a critical value of D/h where D is the particle major axis and h is the separation of the surfaces [144], [145].

The constant, K, can be considered as a measure of the severity of wear, Fig. 5.7. The value of K for mild wear is approximately $K \approx 10^{-8}$, while for more severe wear a value of $K \approx 10^{-2}$ can be expected. The Archard's equation predicts a linear increase in wear with either load or sliding distance. However, it has been noted that this equation is not always valid, especially when there is a transition between two-body and three body wear mechanisms [144], [152]. The reduction in K with increasing load below may be due to the effects of tribo-chemical reactions at higher loads.

It is interesting that the polarization data, Fig. 5.2, only showed significant enhancement of current densities at the highest applied loads, 4N, indicating that there is a critical load below which the passive film does not rupture. In addition, the observed differences between the corrosion potentials at the various loads with and without particles indicate that the stability of the film is critically dependent on the tribological conditions in such environments.

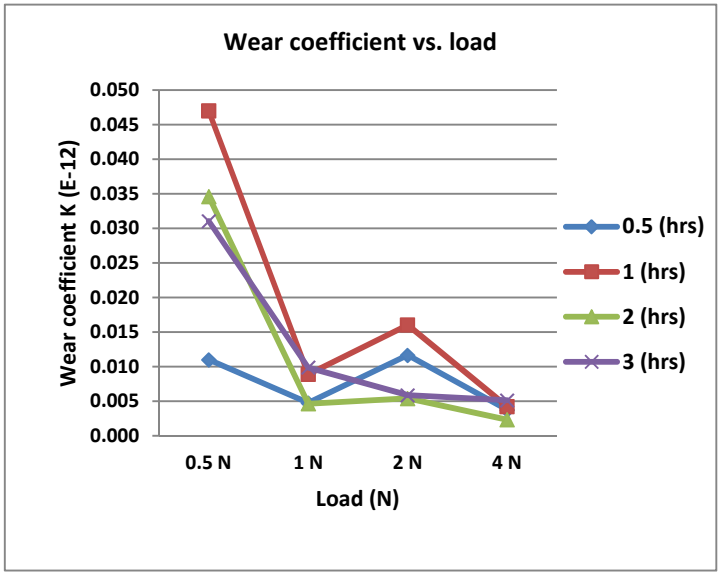

Figure 5.7 – Wear coefficient of SS 316L in artificial saliva

Based on the above analysis, it is clear that the tribological and tribo-corrosion performance suggest optimum regions based on exposure time, applied load and presence/absence of particles. Further, it is apparent that tribo-corrosion maps may be generated for dental implant materials, as functions of both tribological and corrosion variables and as have been carried out for pure metals and steels [27]. Further work will be needed to investigate the tribo-corrosion behaviour of other relevant materials to dentistry and to determine the potential of improved materials based on bio-compatibility and corrosion performance.

5.5 Conclusions

i) A study of the effect of applied load on the micro-abrasion of stainless steel in artificial saliva has been carried out.

ii) The results indicated that the corrosion current densities increased significantly in environments with particles.

iii) The micro-abrasion rate showed a peak in the wear rate with increasing load; this was not found when the tests were carried out in the absence of particles.

iv) Micro-abrasion maps have been generated based on the results showing that the severity of wear is highest in environments of high loads and exposure times, with a low wear regime identified at intermediate loads and exposure times.

6

Wear performance of DLC on common substrates for hip-joint replacements

6.1 Introduction

In the past decades significant advances have been made in the field of total joint replacements. Yet these advances have not led to a complete success. Joint implantation has been extended from elderly to younger individuals and to more active patients where the wear of the joint replacement is the main challenge. This is because the wear of a replacement is a function of use and not simply just of time [21], [22]. The main limiting factors on the life of a total joint replacement can be the periprosthetic bone desorption and the wear of the implant [21], [22]. The implant wear is a silent disease without clear clinical symptoms and in most cases is tolerated by the patients, particularly by older individuals. The debris generated can be distributed to further tissues rather than only the periprosthetic tissues, but in lower concentrations. It has not clearly demonstrated that the wear debris is the main cause of reported diseases following wear in an implant, for example in hip joint replacements, but it is potentially one of the influential factors in diseases such as necrosis, fibrosis, malignancies, sarcoma, and leukaemia [21], [195]. The factors that influence wear debris generation in an implant are the material, manufacturing process, implant design, and implant fixation. Although these factors are not independent from one another they can be studied separately to consider their impacts on this bio-tribological dilemma. Tribology research results in a higher level of efficiency, better performance, less breakdowns of implants and most importantly saving the patients from suffering [195].

The purpose of this work is to consider the tribological performance and to evaluate the wear rate of the materials which can potentially be used as total hip replacement materials. According to DIN 50320, wear is not an intrinsic property of the material but a system property. Hence, the wear performance of a material is based on the wear system and the system variables such as the operating conditions, the type of counterface and the environment [46], [195]. Any kind of interactive surface motion can bring about a wear process and this process can govern the lifespan and the performance of the components. Currently, total hip arthroplasty is performed about 200,000 and 80,000 times per year in the US and the UK respectively. These numbers are set to increase by 174% by 2030 [196]. The service life of the current implants is limited to 15 years which is not ideal when it comes to patients under 60 years of age. A longer lifetime can be expected if the wear volume of the materials used is decreased significantly [22], [23].

A hip arthroplasty can be either a total hip replacement (THR) or a resurfacing hip replacement (HRR). In the total hip replacement a femoral stem sinks into the medullary canal of the femur, connecting the stem to the head and an acetabular cup embeds in the pelvis. In the resurfacing hip replacement only the bearing couple (the acetabular cup and the femoral head) gets replaced. Figure 6.1 shows the two types of hip replacements [22].

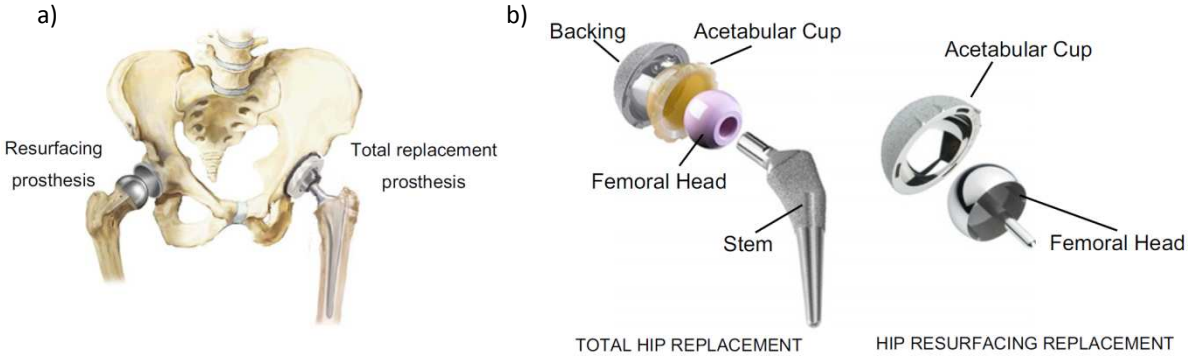

Figure 6.1 – a) Total replacement and resurfacing hip prostheses b) Main components of artificial hip joints

There are two crucial decisions to be made, during the replacement process, which relate to the fixation type and the bearing surface material. The fixation type is either cemented or cementless based on the surgeon's preference and the patient factors, e.g. age and the level of activity. Although cemented fixation was the universal preference of surgeons until 2005, its popularity declined to 36% by 2011. The reason can be the greater range of bearing surface material selection for cementless fixation as well as shorter operative time [197]. Another issue that may come up during an arthroplasty is choosing the size of the femoral head. In his original design, Sir John Charnley proposed 22 mm for the diameter of the femoral head in order to reduce the frictional torque and sliding distance. However, later research showed that the 22 mm diameter may result in creep, linear penetration, subluxation and possible dislocation if the surgical technique is not precise. Wear test results have shown that 28 mm diameter can be an optimum size [69]. Exceeding this size leads to an increase of sliding distance and frictional forces to a deteriorating level [198].

The surface bearing materials are chosen very carefully from metals, polymers or ceramics. It is very important to consider the physical and chemical properties of the implant material in accordance with the replaced tissue; as a living tissue is capable of renewing itself constantly whereas an implant material on the other hand is not. In addition to

biocompatibility of a biomaterial the durability of the material over a probable degradation or mechanical failure should be considered [72]. The most common materials used to date are stainless steel, CoCr and CoCrMo alloy, and titanium based alloys from metals, ultra-high-molecular-weight polyethylene (UHMWPE) and Polyether ether ketone (PEEK) from polymers, and alumina and zirconia from ceramics. When hip replacement operations became popular in the 1960s, head-cup material couples were originally metal-on-polymer (MoP). Then they were developed into ceramic-on-polymer (CoP), metal-on-metal (MoM) and recently ceramic-on-ceramic (CoC) couples [22]. Although these materials advanced hips revisions over this period, a minority of these implants failed mainly due to wear problems [197]. For example, in MoP and CoP couples, the worn polymer debris has generated an adverse tissue reaction. In MoM couples, the metal ions generated from wear particles are potentially cancerous and the CoC couples are brittle, expensive and require special treatments. One of the proposed solutions to reduce the implant wear is to deposit a ceramic coating on metallic and polymer bearing surfaces. This enhances the mechanical resistance of the surface with a relatively low cost [22]. The results will be more significant if both the bearing surfaces can be coated. CrN and CrCN seem to lower the wear rate of cobalt-based alloy and UHMWPE substrates substantially, as well as TiCN and TiN on stainless steel substrates [199], [200]. Relatively newly developed diamond-like carbon (DLC) coating has also shown some impressive results on different substrates [201]. Several research groups have reported excellent bio-compatibility and tribological properties of DLC as a potential candidate for coatings in orthopaedic applications such as hip replacements [24], [25]. Understanding the nature of the wear taking place in a given sensitive situation such as replacing hip joints is crucial for both the designer and the user. Having said that, being able to reduce and predict the wear rate of such a product is achievable if the nature of the wear process is known [2]. To understand the complex wear performance of hip joints a wide range of laboratory equipment and test methods has been employed. The three main forms of equipment used to date are pin-on-disc machines, pin-on-plate machines and joint simulators. Pin-on-disc and pin-on-plate have been used to evaluate the candidate pair materials under well-controlled and steady-state conditions of load, sliding velocity and the surrounding medium. Joint simulators, on the other hand, can evaluate the performance of the different designs and material combinations of the multi-dimensional loading and motion patterns experienced by hip joints [69]. Bio-materials in the human body can be exposed to simultaneous chemical/electrochemical and mechanical

stresses such as tribocorrosion. Tribocorrosion is an irreversible transformation of a material caused by simultaneous physicochemical and mechanical surface interactions occurring in a tribological contact. The evaluation of such surface degradation should be carried out as a combined mechanism of corrosion and mechanical wear [26]. Tribocorrosion tests have been previously conducted by different techniques including fretting corrosion, sliding-wear corrosion and micro-abrasion corrosion to investigate the implant materials [202]. The purpose of this work is to consider and compare the tribological behaviour of a titanium alloy (Ti-6Al-4V) and a CoCr alloy (CoCrMo), as the very common bearing materials in artificial hip joints, coated with DLC coating under micro-abrasion-corrosion conditions.

6.2 Materials and the coating

6.2.1 CoCr alloy

The two types of CoCr alloys that are widely used for implant fabrications are the castable CoCrMo alloy and the CoNiCrMo alloy which is normally wrought by forging. The test samples of this work are made of the castable CoCrMo known as surgical grade cast ASTM F-75. The chemical composition of the alloy is summarised in table 6.1. The addition of molybdenum to the alloy results in having finer grains in the material which leads to higher strength after casting. Also the presence of chromium increases the corrosion resistance of this material. The high fatigue and tensile strength of this material makes it a suitable candidate to be used in long service life products. The modulus of elasticity of CoCrMo is higher than stainless steel and it does not change due to changes in tensile strength of the material. The hardness and toughness of CoCrMo qualifies this material to be used in MoM couples showing considerably low wear [72], [73], [203]. Table 6.2 exhibits the mechanical properties of CoCrMo. The advantage of using this alloy as an implant material is particulate Cr and CoCr alloy are well tolerated by cell lines with no significant toxicity [73]. Indeed, any forms of debris from metallic implants are potentially harmful to the surrounding tissues in long term [92].

6.2.2 Ti alloy

Titanium and its alloys exhibit good bio-compatibility, high aspect ratio, low young modulus and excellent corrosion resistance. Commercially available Ti-6Al-4V alloy as a bio-material has been widely used for hip arthroplasty [26]. Titanium alloy as an allotropic material

consist of hexagonal close packed structure up to 882°C and body-centred cubic structure above that temperature. The stability of this material in different temperatures is due to the presence of aluminium and vanadium. The mechanical properties of Ti-6Al-4V are presented in Table 6.2. The resistance to corrosion of Titanium alloy is due to the formation of an oxide layer on the surface. However, when this material is used as an implant the surface will contain of a thin oxide layer, the biological fluid molecules, dissolved ions and bio-molecules. As a result of micro-motion, titanium oxide particles can be released as wear debris and form periprosthetic fluid collections and trigger the cell response around the implant and cause a stained soft tissue [73]. Therefore, surface treatment of this material prior to implanting seems necessary.

Chemical compositions of the test samples (wt. %)							
CoCrMo (F75)							
Cr	Mo	Ni	Si	Mn	Fe	C	Co
27.0 – 30.0	5.0-7.0	1.0	1.0	0.75	0.75	0.35 max	Bal.
Ti-6Al-4V							
Al	V	Fe	O	N	C	H	Ti
6.39	4.18	0.18	0.184	0.005	0.002	0.0019	Bal.

Table 6.1- Chemical composition of the test samples

Mechanical properties		
Property	**CoCrMo**	**Ti-6Al-4V**
Tensile strength (MPa)	655	860
Yield Strength (MPa)	450	170
Elongation (%)	8	10
Reduction of area (%)	8	25
Fatigue strength (MPa)	310	550
Hardness (H_V)	290 ± 8	349

Table 6.2 – Mechanical properties of the substrate materials

6.2.3 DLC coating

DLC itself is a PVD coating known for its hardness, low friction coefficients, good chemical resistance, high wear resistance and high corrosion resistance. These superior tribological properties however may vary depending on the type of PVD method used to create the film. DLC properties vary and have similarities to both ceramics and polymers; ceramic type

properties such as a high hardness with the high elasticity and low surface energy of polymers [204]. A significant wear property of DLC coatings is producing transfer layer on the partner surface. This is very beneficial when the partner surface is softer. Wear products from the DLC coatings have a graphitic nature which can be transferred to the surface of the counter-body and form a layer. When the DLC slides on the transferred layer, the transfer layer protects the counter-body surface to be worn by the harder DLC coated surface. In other words, DLC can lubricate the interface in the absence of a lubricant [24]. In the past ten years hydrogen free DLC films, also known as tetrahedral amorphous carbon (ta-C), have been more popular as they give a better wear performance that hydrogen containing (a-C:H) films. In ambient conditions the coefficients of friction of DLC films are within the 10^{-1} range, whereas in UHV or dry atmosphere this value drops to 10^{-2} range. This can be very beneficial for the applications where frictional forces can be detrimental [205]. Desirable properties of DLC films have widened the use of this type of coating from magnetic storage technology (hard disks) to razor blades, and from car and engine parts to textile industry and from miscellaneous applications to load bearing implants [24].

6.3 Tests and methodology

Wear performance of a material is not a property of the material. In fact, it is the response of the material to the wear system. In order to maintain the reproducibility of a wear test, the test conditions must be controlled very carefully so that the outcomes of the tests are sustainable and can be generalised to a wider range [64]. A proper choice of test parameters allows the test material to be evaluated in a realistic and in-service state. The bio-tribological performance of bio-implants depends of the implant inputs, such as materials, design, the test conditions such as the relative motion, applied loads and fluid environment [11]. The aim of this experiment is to consider the use of DLC, a PVD coating, as a candidate coating for hip replacements. There were two substrates used in this set of experiments. The substrates are the castable CoCrMo known as surgical grade cast ASTM F-75 and the titanium alloy Ti-6Al-4V.

6.3.1 Test samples

The test samples were supplied by University of Leeds. The size of the samples with CoCrMo substrate was 20 and 10 mm in length and breadth with the thickness of 2.5 mm.

The Ti-6Al-4V substrate samples were in circular shape with the diameter of 30 mm and a thickness of 5 mm. The chemical compositions and mechanical properties of the samples can be found in Tables 6.1 and 6.2. Prior to the tests, the samples were covered in non-conductive tape apart from the $1cm^2$ area in which the contact point is located. This was to ensure that it was insulated from its surroundings.

6.3.2 Test slurry

The slurry used was composed of Ringers solution and Silicon Carbide (SiC) particles. Ready-made ringer's solution tablets were dissolved in distilled water to create a Ringers solution of 0.25 concentrations. The composition of Ringer's solution is listed in table 6.3. The Ringers solutions replicated body fluids providing a suitable environment for the testing of an artificial hip coating.

Composition of Ringer's solution	
Component	**g/l**
NaCl	6.43
$CaCl_2$	0.27
KCl	0.19
$C_6H_{12}O_6$ (Glucose)	1.80
$C_8H_{18}N_2O_4S$ (Hepes Buffer)	2.38

Table 6.3 – Composition of Ringer's solution

Corrosive wear occurring at the replaced joint interface is due to the presence of the corrosion debris which acts as an abrasive third-body [206]. Therefore, SiC particles were added to the solution to simulate such conditions during the conducted tests. The SiC particles were purchased from UKGE Ltd with an average particle size of 3 μm. The SiC particles were F1200 black grade and were added at a concentration of 25g/l. The slurry was changed after approximately 3 experiments to ensure a constant concentration of SiC. In order to prevent the particles from flocculating, the slurry was agitated using a small propeller situated at the bottom of the reservoir.

6.3.3 Test apparatus

The test apparatus used was TE 66 Micro-Scale Abrasion Tester (Plint TE-66, Phoenix Tribology, Reading, UK). The apparatus was driven by DC geared motor which was connected to two co-axial shafts and a cratering ball in between the shafts. One of the

shafts was connected to a peristaltic pump which provided the abrasive slurry feed to the counterface through a syringe. The test sample was placed onto a platform on a vertical pivoted arm. The arm was in balance when the sample and the ball were just in contact. The loads were applied by hanging dead weights to a cantilever arm. The cratering ball used in the test was an ultrahigh molecular weight polyethylene (UHMWPE) ball. UMHWPE ball (K-mac Plastics, Michigan, USA) can act as a benign counter-body and is ideal for ball cratering abrasive tests. Due to the smooth molecular profile of the UHMWPE, it provided ideal sliding properties. It is also chemically resistant and capable of exhibiting very low coefficient of friction against hard counter-faces [207]. In order to minimise the possible influence of deformation of the ball, a new ball was used for each sample. The diameter of the ball used was 25.4 mm (1 inch).

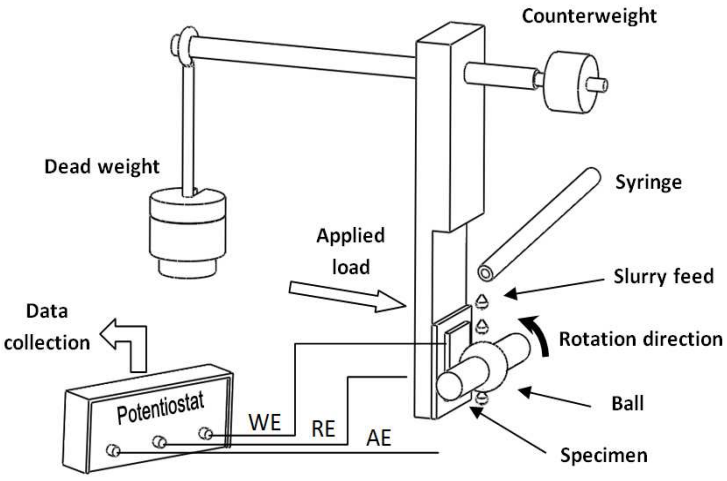

Figure 6.2 – A schematic of the test apparatus

During the experiments, in order to estimate the corrosion rate, a potentiostat was set up which created a circuit with the rig via a Working Electrode (WE) an Auxiliary Electrode (AE) and a Reference Electrode (RE). The potentiostat was provided by ACM Instruments UK and was connected to Core Running/Sequencer software on a computer allowing polarisation curves to be created. The WE was connected to the back of the sample with the RE making contact with the circuit via a capillary tube. For the AE a Platinised-Titanium (Pt-Ti) mesh was located within the non-metallic (non-conductive) slurry collection tray underneath the contact point. The platform which held the sample was also made from a non-conductive polymer to ensure that the sample was insulated away from at the point of contact. The point of contact (and therefore the wear scar) was immersed throughout the experiment as

the peristaltic pump coated the sample in the corrosive slurry which was collected underneath. The slurry itself was part of a circuit as it constantly flowed between the non-conductive collection tray and an external container via flexible tubing. Within the external container the slurry was agitated by means of a laboratory magnetic stirrer.

6.3.4 Test parameters

Each experiment lasted for 30 minutes with a ball rotation speed of 150rpm resulting in a total of 4500 revolutions and a sliding distance of 353.43m. In the first set of the experiments, in order to investigate the effects of load on the corrosion rate, the polarisation tests were carried out for different loads from 0.5 to 4 N. It should be noted that the polarisation curves were measured at a sweep rate of 50mV/min from -1 to 0.5 V.

The second set of experiments was conducted to consider the effects of applied potential on the overall wear. As such, the range of potentials applied was from -400 to +200 mV. The loads used for the second set of experiments were 0.5, 1 and 2 N. Table 6.4 represents the test parameters.

Test parameters				
Set	**Applied load (N)**	**Applied potential (mV)**	**Sliding speed (m/s)**	**Sliding distance (m)**
1	0.5, 1, 2, 3 and 4	-	0.2 (150 rpm)	353.43
2	0.5, 1 and 2	-400, -200, 0 and +200	0.2 (150 rpm)	353.43

Table 6.4 – Test parameters

6.4 Results

Gravimetric weight loss is the standardised method to assess wear in a wide range of materials. Subsequently, dividing the mass loss with the density of the test material determines the volumetric wear which is usually calculated based on Archard's equation [5]. This process can become complicated for materials with different material coatings. The coating may have a different density from the substrate material. This makes the wear assessment more difficult after a delamination event or wear through of the coating [11]. However, it has been reported that thin PVD coatings can exhibit an identical form of wear to a bulk surface [59].

6.4.1 Volume loss

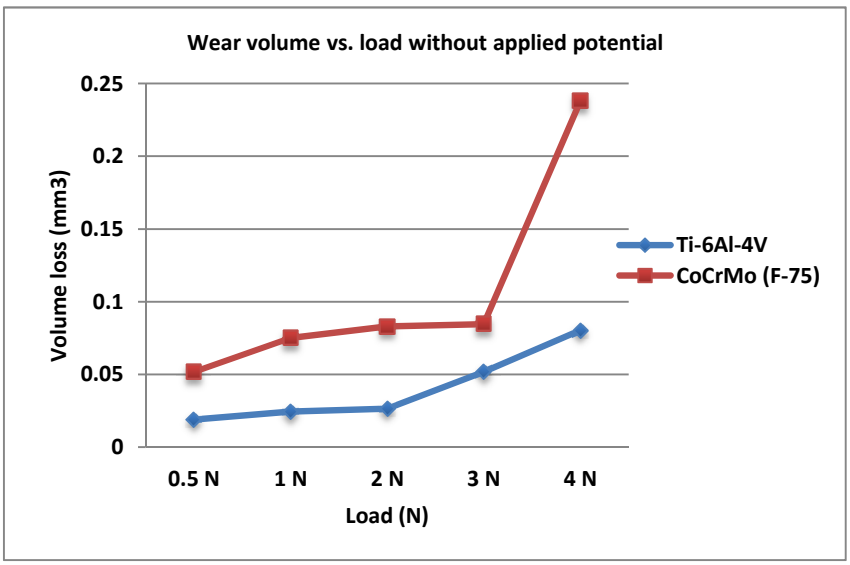

Figure 6.3 – Volume loss vs. applied load at free electrode potential

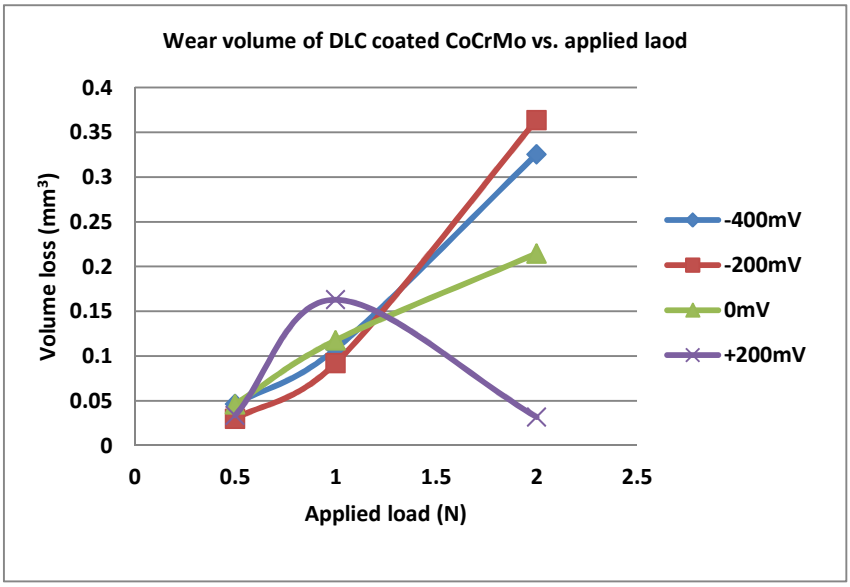

Figure 6.4 – Volume loss vs. applied load with applied potential for DLC coated CoCrMo

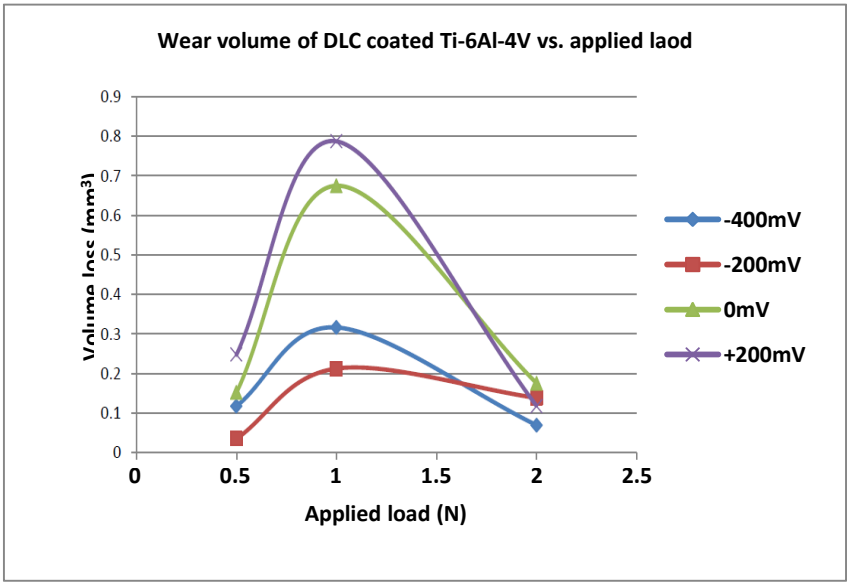

Figure 6.5 – Volume loss vs. applied load with applied potential for DLC coated Ti-6Al-4V

Volume loss during the experiments gave a good indication into the wear each sample area underwent. Since the wear scars due to the micro-abrasion-corrosion test are in shape of hemisphere cap, the volume loss for each configuration of the equipment is calculated via equation 6.1 [64]:

$$V = \frac{\pi b^4}{64R} \qquad (6.1)$$

where *V* is the scar volume, *b* is the scar diameter and *R* is the cratering ball radius where *b<<R.* Not only can this data be used in the creation of wear maps, but also be used to directly compare how the potentials and loads applied directly affect the volume loss caused by the interaction with the UHMWPE ball.

In the first set of experiments, the volume loss results surprisingly show that CoCrMo samples with the DLC coating lost more material due to the micro-abrasion-corrosion (Figure 6.3). However, after analysing the results through SEM analysis (see section 4.3), it was found that the DLC on CoCrMo showed more adhesion to the surface and that the wear scars on the surface did not cause any material removal. In fact, some forms of deformation has happened which has changed the colour of the scar. This may be due to the substrate deformation or the smeared coating. However, the wear scars on the Ti-6Al-4V substrates with the DLC coating clearly exhibited evidence of the volume (material) loss. Smearing is a subcategory of adhesive wear [2] and normally leads to material removal from the surface. In this case, it seems that the coating has prevented the material removal and that only the substrate has been deformed. The results from figure 6.3 could be explained by referring to the hardness of the substrates which CoCrMo shows a lower value (See Table 6.2). It is also interesting that the wear rate of the test samples are increasing fairly linearly by increasing the load, in accordance with Archard's equation.

The volume loss graphs of the second set of the experiments (Figures 6.4 and 6.5) indicate that for the samples with Ti-6Al-4V substrate the volume loss for each potential behaved similarly. The 1N loading creates the largest wear scar compared to the higher loading of 2N. This could be due to the varying wear regimes occurring during the contact period of half an hour experiment [58]. This is unlike the behaviour of the CoCrMo substrate, where the wear scar generally increases as the load applied increases. However, under further examination, Figure 6.5, the y-axis values in Ti-6Al-4V are far higher than those in CoCrMo. Although in most cases the volume loss of CoCrMo samples increases linearly with

increasing load, the amount of the material loss for such samples are considerably lower than Ti-6Al-4V samples. This therefore indicates that the CoCrMo substrate is more corrosion resistant as the volume loss directly corresponds to the wear rate of the material.

6.4.2 Polarisation tests

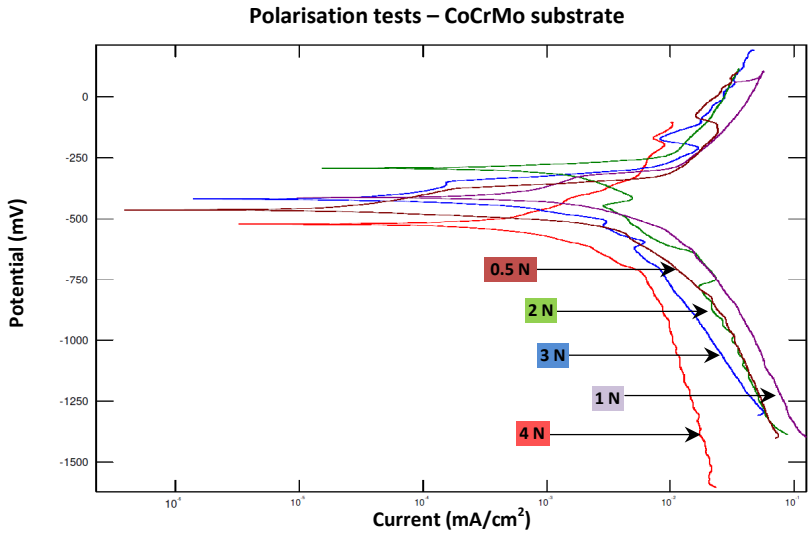

Figure 6.6 – Polarisation test results for DLC coated CoCrMo without applied potential

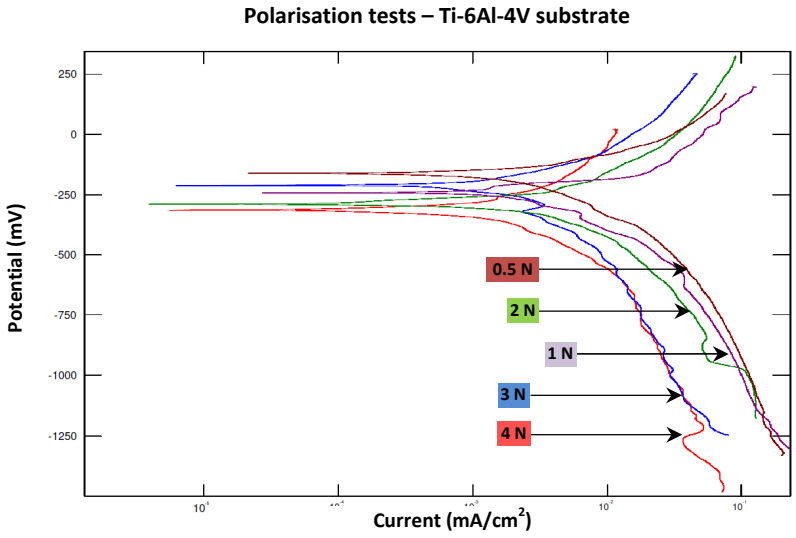

Figure 6.7 – Polarisation test results for DLC coated Ti-6Al-4V without applied potential

Figures 6.6 and 6.7 show the results of the polarisation tests for different loads without applying potentials. Although there are some irregularities in the results, higher loads seem to cause earlier depassivation compared to the other loads for both types of the substrate materials. The results of the corrosion rates for different loads also show an opposite

approach comparing to the wear volume results (see figure 6.8). In other words, by increasing the load, the corrosion rate reacts inversely for the tested loads. It also demonstrates that the corrosion rate for CoCrMo is considerably lower than the Ti-6Al-4V. Although due to the properties of CoCrMo, this type of results was expected, after conducting the polarisation tests it was noted that the corrosion potential of CoCrMo is lower than the samples with Ti-6Al-4V.

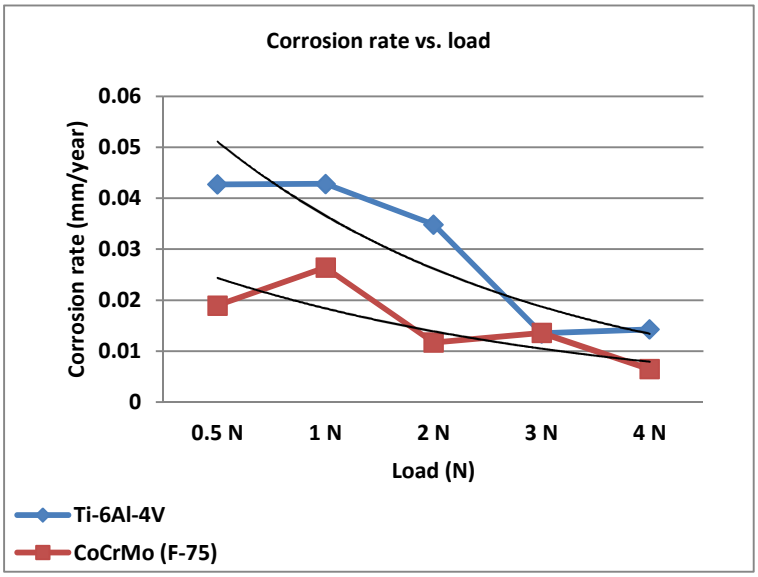

Figure 6.8 – Corrosion rate vs. applied load without applied potentials

6.4.3 SEM images

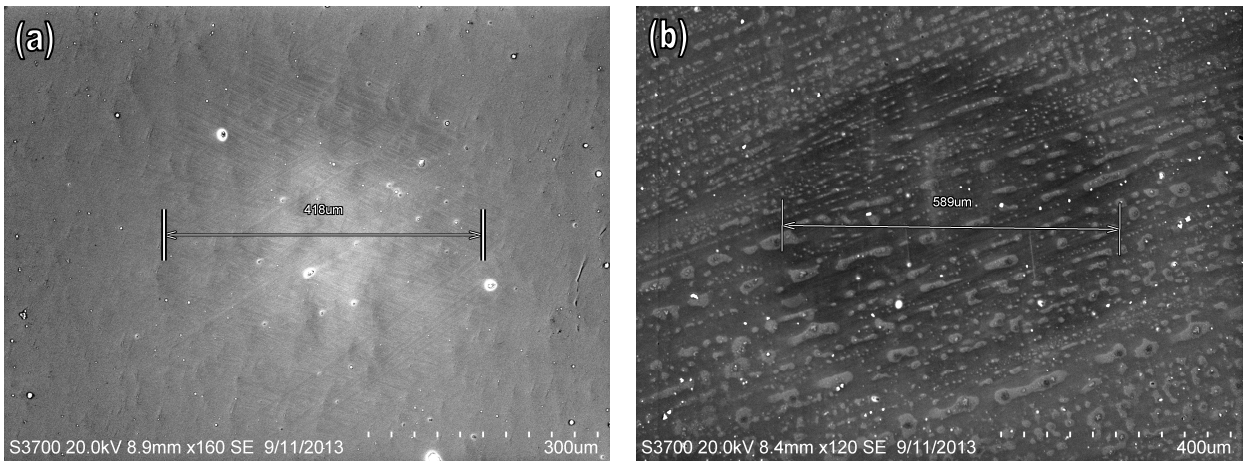

Figure 6.9 – a) DLC coated Ti-6Al-4V under 0.5N load without applied potential b) DLC coated CoCrMo under 1N load without applied potential

In order to measure the wear scar diameters and investigating the wear mechanisms occurred at the interfaces, scanning electron microscopy (SEM) was performed using S-

3700N model Tungsten Filament SEM (Hitachi High-Technologies, Europe). The SEM analysis was carried out following the tests and the presence of the adhered slurry to the surface is still clear. Figure 6.9 demonstrates that there was no evidence of material removal for the CoCrMo samples. The wear mechanism identified in this case was smearing. It is possible that the substrate has been deformed and that this caused a slight indentation of the surface. However, for Ti-6Al-4V grooves on the scars were observed which shows a form of transition from 3-body rolling to 2-body grooving mechanisms [58]. No transitions were identified for CoCrMo samples.

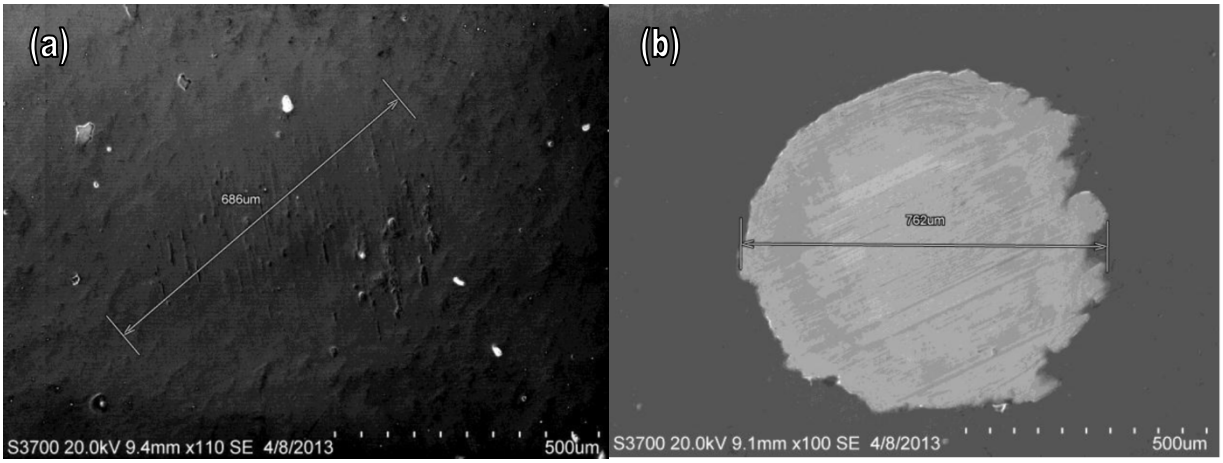

Figure 6.10 – a) DLC coated Ti-6Al-4V under 1N applied load and 0mV applied potential b) DLC coated Ti-6Al-4V under 2N applied load and 0mV applied potential

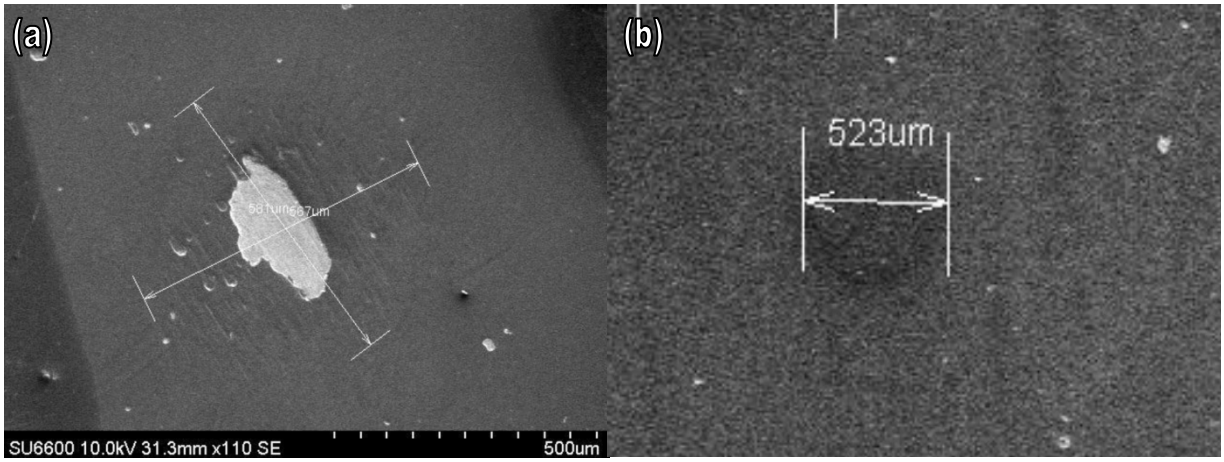

Figure 6.11 – a) DLC coated CoCrMo under 2N applied load and -400mV applied potential b) DLC coated CoCrMo under 0.5N applied load and 0mV applied potential

Figure 6.10 demonstrates results from experiments carried out on the Ti-6Al-4V substrate. Figure 6.10(a) shows the initiation of a wear scar forming and figure 6.10(b) shows that the

complete DLC has been broken through to reveal the substrate underneath; this also occurred under other configuration of +200mV, 1N and 0mV, 0.5N. This complete breakthrough in the DLC coating indicates a high level of wear under these conditions with the Ti-6Al-4V substrate. Overall the images of the scars for the CoCrMo samples were more difficult to identify, indicating that they did not have as much volume loss compared to the Ti-6Al-4V substrate. In some situations, as shown in figure 6.11(a), the coating does begin to break through however not to the same extent as those found with the Ti-6Al-4V. No wear scar imaged for the CoCrMo was found to have completely removed the coating over the whole area of contact. The CoCrMo in particular can be difficult to decipher the wear patterns as seen in Figure 6.11(b) which indicate a low level of wear; the SEM could not be directly zoomed into a possible area of wear as the outline of the wear scar was lost.

6.5 Discussion

The factors affecting the tribological performance of a metal on metal hip replacement are the radius, the bearing surface quality, applied load, type of the motion, viscosity and boundary lubricating properties of the proteins; although radius and the bearing surface quality can be dealt with in the design stage of the implant [208]. Corrosion disintegrates and weakens the implant and the corrosion products harms the surrounding tissues [73]. It has also been reported that the corrosion resistance of CoCrMo alloy is reduced when introduced to the body environment, where the pH value is approximately 7.4 and wear debris and metal ions may be released [202]. Metal ions are released due to the removal of the passive films which are already formed on the surface of the alloys and are used for the implants. The performance of the passive films, and ion transport as a result, depends on the chemical composition, structure, thickness, stability and defects of the films. The stability of biomedical metal itself depends on the surrounding medium such as the composition of the electrolyte, the redox conditions, the exposure time and temperature [72].

In the current work, the performance of DLC coating on two different substrates was investigated through two sets of experiments. The volume loss results for the first set of the experiments showed that CoCrMo samples with the DLC coating have lost more material due to the micro-abrasion-corrosion. This found to be in contrast with the results of the

SEM analysis. There was no evidence material removal from the surface of the DLC coated CoCrMo samples. However, it was clear that some forms of sliding have taken place which had made decolouration of the surfaces and a slight dent on the surface. This is thought to be due to the deformation of the substrate which was relatively softer than Ti-6Al-4V substrates. Also, this shows that the existence of great adhesion in between CoCrMo and the DLC coating protected the surface from any surface material removal. The wear mechanism which occurred at the interface of the DLC coated CoCrMo and the counterface ball was identified as thee-body rolling as there was no evidence of grooving observed. This was not unexpected as the average diameter of the abrasive particles was 3 μm despite their high hardness. Therefore, it was unlikely for the particles to reach a critical value in order for wear mechanism transitions to occur [10]. However, the additional wear mechanism identified following SEM analysis was smearing. This is a form of adhesive wear and is thought to have happened between the DLC coating and the substrate due to the force form the counter-face body. Looking into the wear scars on the Ti-6Al-4V substrates with the DLC coating, they clearly exhibited evidence of volume (material) loss in the SEM analysis although they showed lower volume loss for the first set of experiments comparing to CoCrMo substrates. The wear mechanism observed in the SEM images showed evidence of three-body rolling, with the tendency to transition to two-body grooving. It should be noted that the volume losses from the first set of experiments (at free electrode potential) were considerably lower than the results of the second set of experiments.

Although DLC coatings exhibit excellent frictional properties, it should be noted that low friction is not synonymous with low wear. For example, the coefficient of friction for clean materials and dry contact in the presence of air between PTFE and steel is 0.04 – 0.2, while the corresponding wear coefficient is 10^{-4} – 10^{-5}, whereas the coefficient of friction in similar conditions between polyethylene and steel is 0.3 while the corresponding wear coefficient is 10^{-7} – 10^{-8} [69]. Also, according to Haque et al. [25] third-body (particle) entrainment is the main cause of wear of DLC coatings. Smaller particles entrain more effectively and they cause higher coating wear rate than larger particles (Range tested: 10 – 600 μm). Also, decreasing the particle size increases the coefficient of friction at the interface. Despite having very fine abrasive particles for the current work, no evidence of entrainment was found for the first set of experiments.

In the polarisation tests interesting results were found. The samples with CoCrMo substrate showed the signs of depassivation at an earlier stage comparing to the samples with the Ti-6Al-4V substrate. However, further analysis showed that the corrosion rate for the CoCrMo is considerably lower than Ti-6Al-4V. This can be related to the rate of passivation/depassivation/depassivation process for each material. Also, it was noted that corrosion rate had a converse relationship with the increasing load. This can be due to the fact that as by increasing the load, the entrance of the abrasive particles to the interface can become more difficult. This also can be related to the transfer layer properties of DLC coatings which act as a lubricant at the interface and protect both of the counter-bodies at higher loads.

In the second set of experiments with applied potentials, penetration of the coating was identified for some cases. As the range of the applied load for the second set of experiments was smaller and lower than the one for the first set, it was surprising how the presence of the applied potentials can change the reactions of the coating. It seems in most cases for Ti-6Al-4V and some cases for CoCrMo, the applied potential prevents the repassivation process after the depassivation process takes place. As depassivation (removal of the oxide layer) occurs more wear damage (and therefore a greater volume loss) can occur on the sample. Also, the quicker the material repassivates the more protection it has against corrosion. The wear mechanisms which appeared on the surfaces for the second set of experiments were not very different from the first set, except for cases where the coating was penetrated. Another reason for the better performance of the samples with the CoCrMo substrate in the second set of the experiments can be the good adhesion between the coating and the substrate.

For further investigation, wear maps can be generated for the second set of experiments. Wear maps have been proposed to link wear mechanisms to operating parameters [101]. The wear maps were created from percentage calculation of the largest volume loss; in this case was 0.785mm^3 under a 1N load, 0mV potential using the Ti-6Al-4V substrate:

- High wear$\geq$80% of maximum wear (0.6278 mm^3) (6.2)
- 30% of maximum$\leq$Medium wear<80%of maximum (6.3)
- Low wear> 30% of maximum (0.2354 mm^3) (6.4).

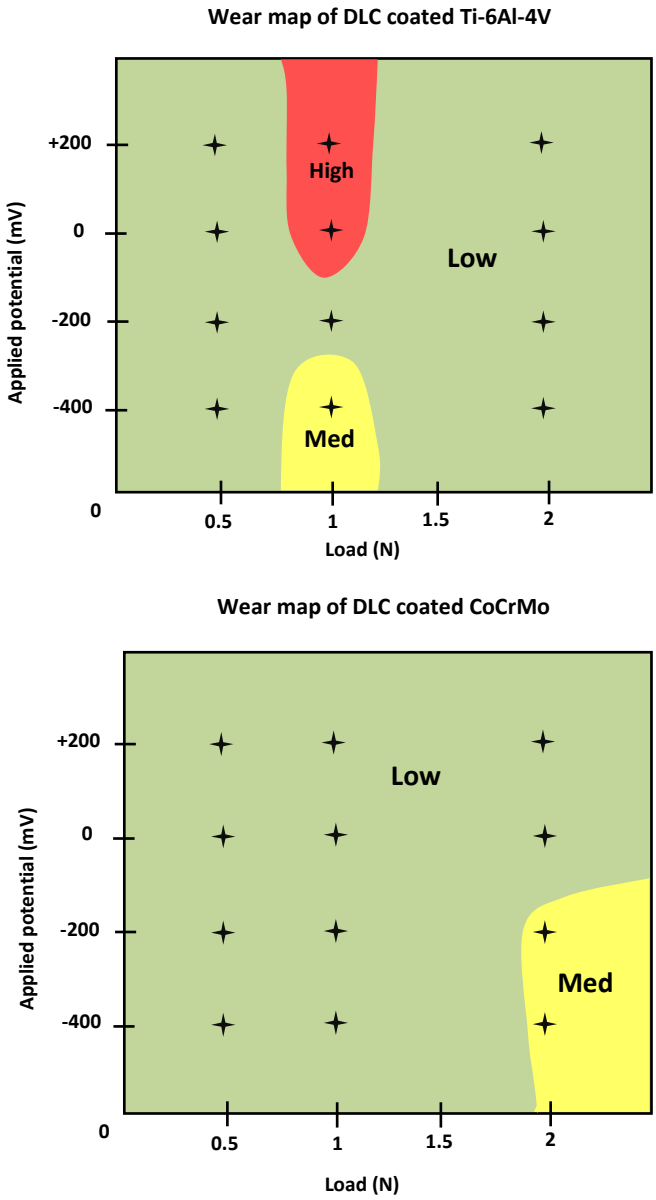

Figure 6.12 – Wear mechanism maps of the samples

Considering the differences in the wear maps demonstrates that the combination of CoCrMo substrate with DLC coating provides a better wear resistant material. Although the results of the first set of the experiments are not included in the map, despite undergoing higher loads, they all can be categorised in the low wear section. As the maps indicate, the medium and high wear rates have only occurred at the presence of applied potentials. This brings the importance of synergism between the present wear mechanisms at an interface to our attention. As there is always the possibility of presence of electrostatic potential at the interface of an implanted hip joint, the reactivity of the materials used should be

comprehensively considered. As synergism exacerbates the wear damage at the interface, it emphasises the importance of tribocorrosion studies of surfaces.

The wear maps also approve the results from other works that the wear resistance of Ti-6Al-4V is not as high as CoCrMo [26]. This also can be due to the rate of passivation/depassivation/repassivation of the substrates at different electrode potentials. The good adhesion between CoCrMo and DLC coating can be another reason for such results.

Following an analysis and comparison of the two substrate materials Ti-6Al-4V and CoCrMo, both coated with Diamond-like Carbon and candidates for replacement hip joint materials, it was found that over the variety of applied loads and potentials the CoCrMo coated substrate did not corrode or wear to the same level as the Ti substrate. This can be due to the passivation and repassivation of the DLC coating which occurred at different stages in the experiment; CoCrMo substrate may also have a better adhesion with the DLC coating.

A revision on the earlier designs of metal-on-metal components has shown that the failures often happened due to irregular geometry, poor surface finish and the high frictional torque of the produced devices; not because of the metal-on-metal combination per se [74]. It means that the appropriate selection of materials and manufacturing processes can have a high impact on the performance of replacing joint implants. Watters et al. [209] examined the wear of artificial hip joints and found that debris produced from periprosthetic tissue is typically due to lack of fluid lubrication in hip replacements. Hence, reviewing the lubricating process of the implant at the design stage seems vital. Also, electrochemical measurements are necessary to appraise the synergistic role of corrosion in the overall wear process. Thus, further research should be carried out to find the best match of bio-materials to be employed for total hip joint replacements. From the test results above, DLC shows a good performance as a candidate coating for artificial hip components especially on CoCrMo. For the future work it can be beneficial to look into a wider range of applied loads, applied potentials, and different combination of counterface-bodies.

6.6 Conclusions

In conclusion:

i) The performance of DLC coating on two common metals used in THR, CoCrMo and Ti-6Al-4V was investigated under micro-abrasion-corrosion condition with a range of applied loads and potentials.

ii) The DLC coating showed better adhesive properties towards CoCrMo substrates.

iii) The combination of the DLC coating and CoCrMo exhibited higher corrosion resistance and abrasive resistance under different applied loads and potentials.

7

General conclusions and future research

7.1 Introduction

Wear on the surface of a component as a result of its motion relative to the adjacent working parts, has far reaching economic consequences which involve not only the costs of replacement but also the expense involved in machine downtime and lost production [48]. In practice, mild wear might well be considered as acceptable by engineers, whereas the transition to severe conditions generally results in commercially unacceptable values. It is necessary for an engineer to estimate the wear rate for a given material pair in a particular set of operating conditions to prevent a catastrophe in terms of the operating conditions. For this purpose, further research on different types of wear and materials should be carried out generate a body of data to be used as a reference to predict wear. This study examined the wear performance of yttria-tetragonal zirconia poly-crystalline (Y-TZP) ceramics and 316L stainless steel as the bio-materials used as denture restoration materials. DLC coated cobalt and titanium alloys as hip joint replacement materials were also investigated.

7.2 General conclusions

The results of the tests on Y-TZP led to interesting findings. According to Archard's equation [5], by increasing applied load and sliding distance, higher volume loss was expected. However, bearing in mind that the experiments were conducted in similar conditions, variation of the results for different slurries showed that the properties of the abrasive slurries were as effective as an increased load and sliding distance. The main differences to consider may be the pH value and the viscosity of these products. Both of which significantly affected the wear rate. Research shows that, in environments of very high or very low pH values, wear rate increases. In other words, in very acidic and very alkaline environments tribo-layers cannot be formed. This leads to constant wear loss during exposure time [148], [173].

Another factor found in contrast with Archard's equation was due to particle entrainment which is not considered in the equation. It was noted that higher loads and higher sliding distances do not always cause a higher volume loss. This may be due to entrainment issues associated with abrasive particles at higher loads. Higher loads produce higher pressure in the contact area, which may reduce the frequency of particle entrainment. This found to occur in the tests on 316L stainless steel with slight differences. As wear continued to increase, particles became trapped in ridges causing the amount of wear to decrease. This may result in unexpected wear rates. Thus, regardless of the type of the surface material and despite of the presence of load and abrasive particles, the wear rate may decrease due to entrainment of particles for a period of time. Also, transitions between the wear mechanisms in higher loads are very likely to happen. This should be taken into account in predicting wear performance of a material as this suggests that the relation between the material loss and applied load is more complicated than a linear relationship.

The linearity of the relationship was investigated in more in detail using the test results of the 316L stainless steel. The findings of the experiments suggested that the wear rate depends on the wear mechanisms at the interface of the relative surfaces. The volume loss results showed the linear relationship to be true, but as with the findings of other researchers [134] it was found that this was up to a certain load and only under three-body conditions. Also, as shown by others [144], the results indicated that Archard's equation was valid for three-body rolling conditions, where wear did increase linearly with load, but for two-body grooving conditions wear was shown to be proportional to a power of load

lower than 1N. This was confirmed by all other applied loads which reached or exceeded 1N and where the change in the amount of wear overtime became increasingly non-linear.

Also, wear rate has been shown to increase generally with sliding distance, but in a non-linear approach. This was found to be in accordance with the earlier findings of the current research group [58]; an increasing sliding distance generally leads to an increase in the real area of contact and a reduction of the applied load at the interface and on the particles present at the interface. Therefore, the slope of the linear relationship may decrease due to longer sliding distances [28]. This may also be related to passivation/depassivation/repassivation processes on the metal surface and the formation of protective oxide films on the interactive surfaces which can resist wear.

Although Archard's equation is not a complete model in predicting wear, wear coefficient (a derivative of this equation) can be very useful to evaluate the wear rate of materials. The reduction found in wear coefficients of 316L stainless steel at higher loads can indicate that with an increasing load the effects of tribo-chemical reactions increase. This was found to be consistent for other types of alloys (CoCrMo and Ti-6Al-4V) tested in this work. The results of the corrosion rates for different loads showed an opposite approach compared to the wear volume results. In other words, by increasing the load, the corrosion rate reacts inversely. This can be due to the reduced rate of penetration of abrasive particles to the interface or entrainment of the particles. This was found to be consistent for all mechanisms reported in this work as the applied load increases the effects of particles are reduced. This can also reduce the aggressivity of the environment. As a result, the tribo-films can last for longer which reduces the wear rate over time. This can be a general trend for the metallic bio-materials; however at different rates. The corrosion rates for CoCrMo samples for instance were found considerably lower than the Ti-6Al-4V samples. In addition, the observed differences between the corrosion potentials at the various loads with and without particles indicate that the stability of the film is critically dependent on the tribological conditions in such environments.

As none of the wear prediction models is complete, the importance of wear mechanism maps becomes more significant. The results of this work show that wear mechanism maps can be a very useful tool to provide a reference for wear predictions. This is an appropriate approach to address a worn surface qualitatively, as quantification of a wear is not always the best way to describe it. Quantitative reference points are also often arbitrary. The

significant advantage of wear mechanism maps is that there are no limits for combining different influential factors on wear mechanisms and it can be generated regardless of the units of the factors. Also, they can accommodate more data than formulas as they can be multi- dimensional. Qualitative description of wear mechanisms simplifies the comparison of wear processes occurred in an interface. For example, the maps generated for the tests conducted on DLC coated samples indicate the medium and high wear rates have only occurred at the presence of applied potentials. This brings the importance of synergism between the present wear mechanisms at an interface to our attention. One of the most important factors on the behaviour of a wear system is synergism of wear mechanisms. For example in tribocorrosion of bio-implants it was found that the combination of micro-abrasion and corrosion could be far more detrimental to the bio-material than having them occurring separately. This is where the wear maps become very useful as it can be reflected well in synergistic wear maps whereas it may be found difficult to perform a numerical evaluation for such conditions. Also, a review of the literature shows that adding different parameters to formulas provides limited extension to applications of such models and only for specific purposes. However, an attempt to combine the existed wear maps for wider applications can be of great assistance to designers of components with interactive surfaces.

It was observed that the best solution to resist wear is not always choosing the best wear resistant materials. It is very common to observe excessive wear due to a supply of wrong materials, unsuitable heat treatments, inaccurate manufacturing processes, and incorrect changes in the operation environments. Even a change of material supplier may cause problems. For instance, a supplier provides the same product, the concentration of an element in the product, i.e. vanadium, which is required with a low maximum concentration. A change in trace amount can significantly alter the hardness of the material, even though it has not reached the maximum value [2].

An example of the importance of selecting appropriate manufacturing process in this work was the occurrence of ageing phenomenon which can govern the durability of Y-TZP dental restorations. Examination of the microscopy images suggested that once the treated surface of the sample was fully perforated due to ageing, the wear of the material increased more rapidly and the relationship between wear rate, load, and sliding distance became linear. Thus, prevention of occurrence of ageing can increase the duration of the

service life of a Y-TZP dental restoration. Y-TZP manufacturing processes therefore must be carried out with greater precision, particularly in the addition of stabilisers and the sintering process temperature. This is because a lack of yttria reduces the tetragonal-phase stability and the serviceability of such dental restorations [178]. Deeper surface treatments are also recommended as they can lead to reduced wear rates [180]. As a result, generating a universal standard for surface manufacturing processes bases on the generated data for each field may reduce the risk of failures due to surface damages. Yet, laboratory research should be carried on to enhance those standards continuously.

In addition to selecting suitable manufacturing processes for a tribo-material, choosing appropriate set of materials for the conditions as defined by tribo-corrosion maps was found to have a high impact on the wear performance of such materials. For example, after analysing the results of the tests on DLC coated CoCrMo, it was found that the DLC on CoCrMo showed more adhesion to the surface and that the wear scars on the surface did not cause material displacement. This was due to the good adhesion between DLC coating and CoCrMo substrate which could prevent material removal from the surface.

Also, in this work the tribocorrosion of some alloys were examined using micro-abrasion-corrosion techniques; however, the possibility of occurring synergisms, which consist of more than two wear mechanisms on tribo-surfaces, are high. Yet no standardised test method exists to combine more than two simultaneous degradation mechanisms during lab testing [4]. It would simulate more realistic conditions if a test apparatus could provide more than two degradation mechanisms. A potential avenue for further research would be to investigate this issue, through experimenting with either realistic models or virtual models through the use of computer software.

Finally, although numerous studies have been carried out to characterise micro abrasive wear, the terminology describing these wear mechanisms is not unified. The current terminologies are also too comprehensive and further detailed characterisation of abrasion should be more descriptive while attempting to identify the mechanisms. For example, by using common definitions the presence of abrasive particles as a third-body in the interface may induce a wrong expectation; that the particles are always rolling within the amplitude of the interface and that three-body rolling should be the outcome of such wear system. This study found this not to be true in many cases.

In conclusion, a number of mechanistic maps and diagrams can be proposed based on the results of this work.

Based on the information in section 4.2.4, the combined results from all tea and coffee slurries have been super-imposed into one wear map, figure 7.1. This provides an overview of the performance of Y-TZP when a 'very low' wear rate is maintained in the caffeine containing environments (included in this study) during mastication over time. This suggests that the tea environment is less detrimental to Y-TZP implants than that of coffee. It also suggests that Y-TZP implants will last up to twice as long when drinking coffee with milk compared to plain coffee, and up to four times as long compared to coffee with sugar.

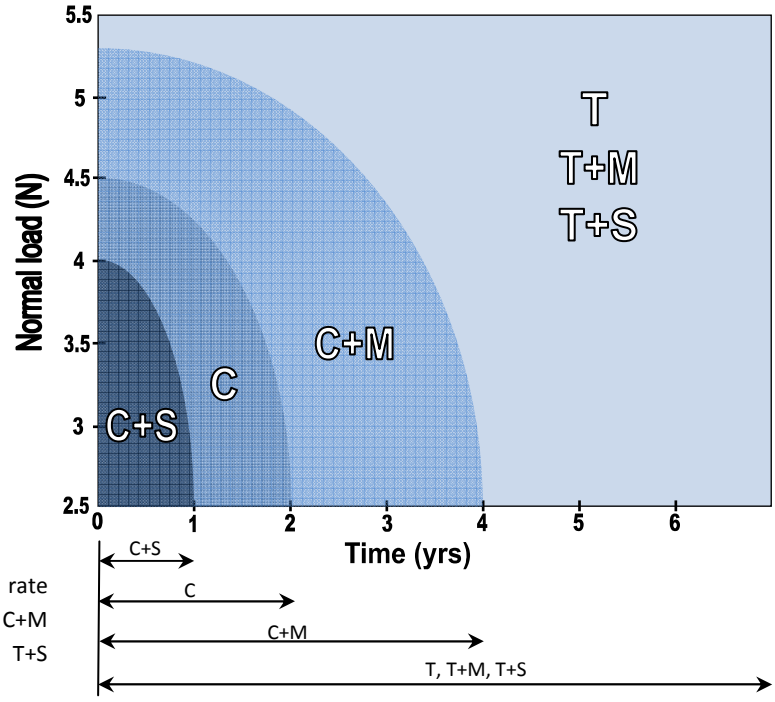

Figure 7.1 – Super-imposed very low wear rate map, C+S (Coffee+Sugar), C (Coffee), C+M (Coffee+Milk), T (Tea), T+M (Tea+Milk), T+S (Tea+Sugar)

Also, from the results of the experiments on two different types of DLC coated substrates, a super-imposed wear mechanism map can be generated to show the suitability of the tested bio-materials for different conditions where the overall wear loss of the potential hip replacement material is maintained 'low' (Figure 7.2). Although this map indicates that CoCrMo can exhibit more desirable features for such conditions, Ti-6Al-4V can still be an

appropriate candidate for this purpose by applying further treatments or using another type of coating.

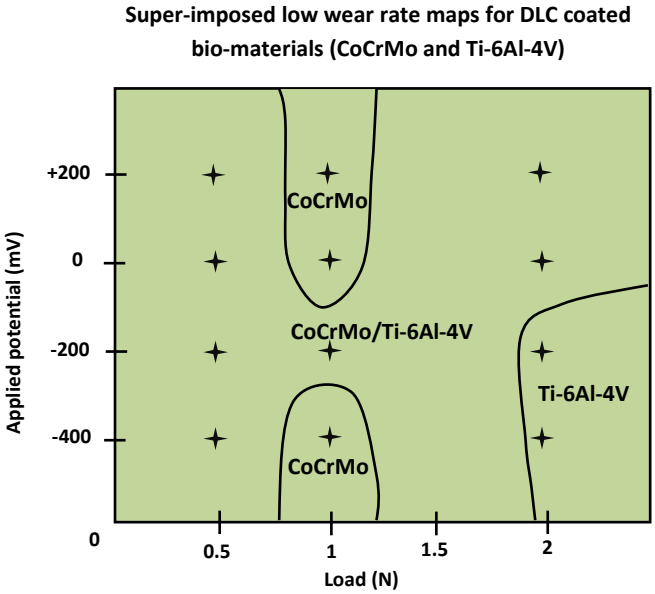

Figure 7.2 – Super-imposed low wear rate maps for DLC coated bio-materials (CoCrMo and Ti-6Al-4V)

Figure 7.3 presents a graph of the relationships between different parameters and factors found in this work which can affect the wear performance of different types of bio-implants. However, it should be noted that the factors influencing the wear performance of different bio-implants are not limited to the factors encountered in this work.

7.3 Future work

Based on this study and the remarks of the previous section, following future work can provide a wider understanding of wear mechanisms as well as the materials investigated:

i) Examining a wider range of the factors that affected the wear performance of Y-TZP using different slurries including pH, viscosity and nutritious additives.

ii) Modelling and investigating the effect of flow of different slurries on dental restorations in the oral cavity.

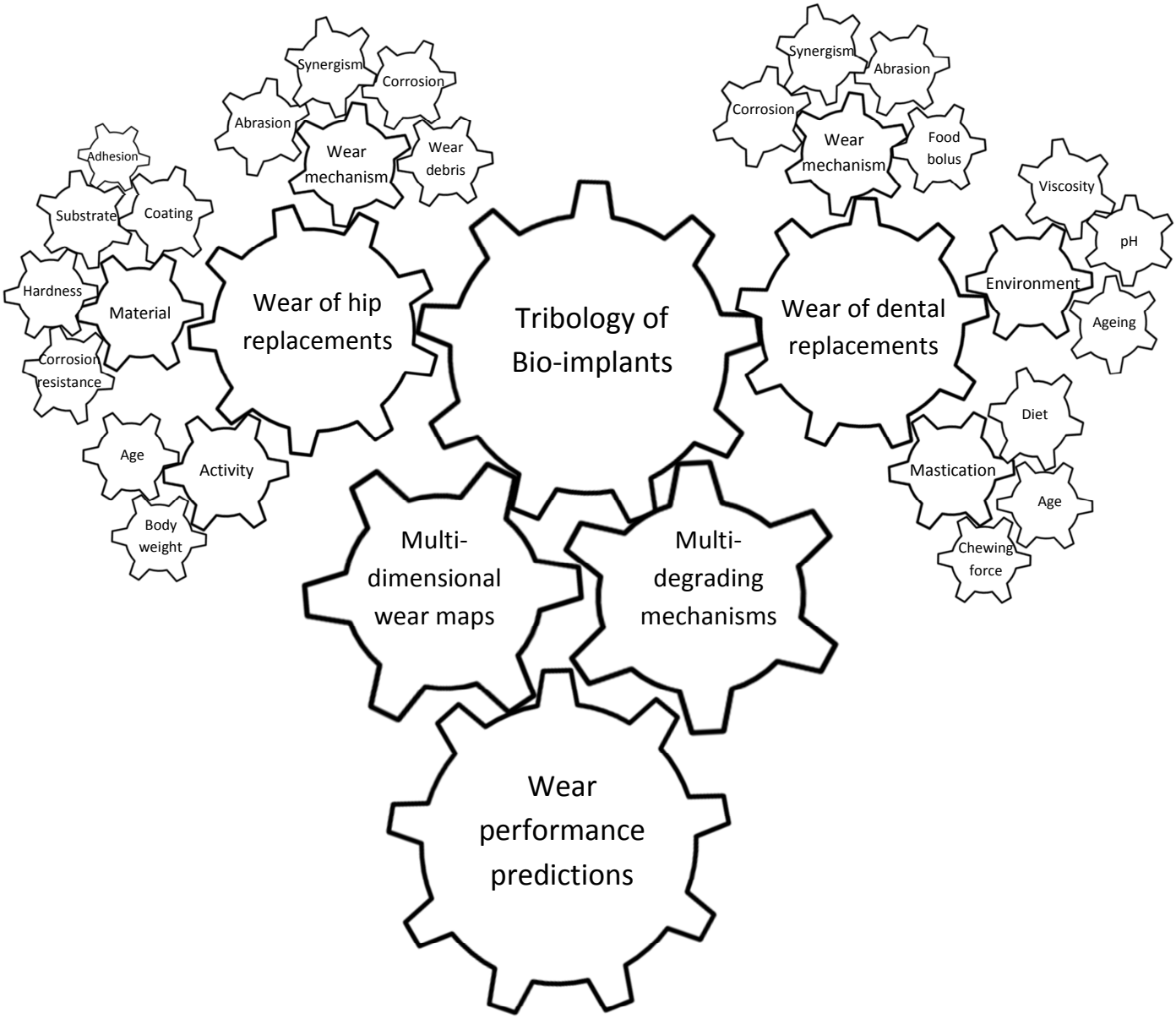

Figure 7.3 – The relationships between different factors and parameters affecting wear of bio-implants

iii) Suggesting standards for the manufacturing processes of the current dental restoration materials.

iv) Suggesting a more detailed standard for abrasive wear mechanisms with two or more interactive bodies.

v) Developing either realistic models or virtual models through the use of computer software to investigate synergistic wear mechanisms with more than two mechanisms.

vi) Generating a body of data as a reference based on the existing wear maps using a multi-dimensional wear map.

References

[1] S. . Teoh, “Fatigue of biomaterials: a review,” *International Journal of Fatigue*, vol. 22, no. 10, pp. 825-837, 2000.

[2] A. R. Lansdown and A. L. Price, *Materials to Resist Wear (Materials Engineering Practice)*. Pergamon, 1986, p. 200.

[3] G. W. Stachowiak, *Wear: Materials, Mechanisms and Practice (Tribology in Practice Series)*. Wiley-Blackwell, 2005, p. 480.

[4] S. Mischler, “Triboelectrochemical techniques and interpretation methods in tribocorrosion: A comparative evaluation,” *Tribology International*, vol. 41, no. 7, pp. 573-583, 2008.

[5] J. F. Archard, “Contact and Rubbing of Flat Surfaces,” *Journal of Applied Physics*, vol. 24, no. 8, p. 981, Aug. 1953.

[6] N. Fillot, I. Iordanoff, and Y. Berthier, “Wear modeling and the third body concept,” *Wear*, vol. 262, no. 7, pp. 949-957, 2007.

[7] H. C. Meng and K. C. Ludema, “Wear models and predictive equations: their form and content,” *Wear*, vol. 181, pp. 443-457, 1995.

[8] I. C. Gebeshuber, “Biotribology inspires new technologies,” *Nano Today*, vol. 2, no. 5, pp. 30-37, 2007.

[9] D. F. Williams, “On the mechanisms of biocompatibility,” *Biomaterials*, vol. 29, no. 20, pp. 2941-2953, 2008.

[10] J. A. Williams and A. M. Hyncica, “Mechanisms of abrasive wear in lubricated contacts,” *Wear*, vol. 152, no. 1, pp. 57-74, 1992.

[11] M. L. Harper, A. Dooris, and P. E. Paré, “The fundamentals of biotribology and its application to spine arthroplasty,” *SAS Journal*, vol. 3, no. 4, pp. 125-132, 2009.

[12] Hutchins and I. Hutchings, *Tribology, Friction and Wear of Engineering Materials*. Elsevier Limited, 1992, p. 284.

[13] R. C. Cozza, D. K. Tanaka, and R. M. Souza, “Friction coefficient and wear mode transition in micro-scale abrasion tests,” *Tribology International*, vol. 44, no. 12, pp. 1878-1889, 2011.

[14] W. Höland et al., “Future perspectives of biomaterials for dental restoration,” *Journal of the European Ceramic Society*, vol. 29, no. 7, pp. 1291-1297, 2009.

[15] L. Wang, Y. Liu, W. Si, H. Feng, Y. Tao, and Z. Ma, “Friction and wear behaviors of dental ceramics against natural tooth enamel,” *Journal of the European Ceramic Society*, vol. 32, no. 11, pp. 2599-2606, Aug. 2012.

[16] P. Vale Antunes and A. Ramalho, “Study of abrasive resistance of composites for dental restoration by ball-cratering,” *Wear*, vol. 255, no. 7, pp. 990-998, 2003.

[17] P. F. Manicone, P. Rossi Iommetti, and L. Raffaelli, “An overview of zirconia ceramics: Basic properties and clinical applications,” *Journal of Dentistry*, vol. 35, no. 11, pp. 819-826, 2007.

[18] C. Hodge and M. M. Stack, “Tribo-corrosion mechanisms of stainless steel in soft drinks,” *Wear*, vol. 270, no. 1-2, pp. 104-114, Dec. 2010.

[19] A. G. Threlfall, L. Pilkington, K. M. Milsom, A. S. Blinkhorn, and M. Tickle, “General dental practitioners’ views on the use of stainless steel crowns to restore primary molars.,” *British dental journal*, vol. 199, no. 7, pp. 453-5; discussion 441, Oct. 2005.

[20] K. V. Sudhakar, “Metallurgical investigation of a failure in 316L stainless steel orthopaedic implant,” *Engineering failure analysis*, no. 2. Elsevier Science, pp. 249-256, 2005.

[21] T. M. Wright and S. B. Goodman, *Implant Wear: Future of Total Joint Replacement (Seminar)*. American Academy of Orthopaedic Surgeons, 1996, p. 150.

[22] L. Mattei, F. Di Puccio, B. Piccigallo, and E. Ciulli, “Lubrication and wear modelling of artificial hip joints: A review,” *Tribology International*, vol. 44, no. 5, pp. 532-549, May 2011.

[23] G. Pezzotti and K. Yamamoto, “Artificial hip joints: The biomaterials challenge.,” *Journal of the mechanical behavior of biomedical materials*, vol. null, no. null, Jun. 2013.

[24] R. Hauert, “An overview on the tribological behavior of diamond-like carbon in technical and medical applications,” *Tribology International*, vol. 37, no. 11, pp. 991-1003, 2004.

[25] T. Haque, D. Ertas, A. Ozekcin, H. W. Jin, and R. Srinivasan, “The role of abrasive particle size on the wear of diamond-like carbon coatings,” *Wear*, vol. 302, no. 1, pp. 882-889, 2013.

[26] T. M. Manhabosco, S. M. Tamborim, C. B. dos Santos, and I. L. Müller, “Tribological, electrochemical and tribo-electrochemical characterization of bare and nitrided Ti6Al4V in simulated body fluid solution,” *Corrosion Science*, vol. 53, no. 5, pp. 1786-1793, 2011.

[27] J. D. Summers-Smith, *An Introductory Guide to Industrial Tribology (Introductory Guide Series (REP))*. Wiley-Blackwell, 1994, p. 218.

[28] J. Halling, *Principles of Tribology*. Macmillan, 1975, p. 415.

[29] S. Prakash, M. B. Karacor, and S. Banerjee, “Surface modification in microsystems and nanosystems,” *Surface Science Reports*, vol. 64, no. 7, pp. 233-254, 2009.

[30] K. C. Ludema, *Friction, Wear, Lubrication: A Textbook in Tribology*. CRC Press, 1996, p. 272.

[31] F. P. Bowden and D. Tabor, *The Friction and Lubrication of Solids (Oxford Classic Texts in the Physical Sciences)*. OUP Oxford, 2001, p. 424.

[32] E. Rabinowicz, *Friction and Wear of Materials*. John Wiley & Sons, 1995, p. 336.

[33] S. . Lim, “The relevance of wear-mechanism maps to mild-oxidational wear,” *Tribology International*, vol. 35, no. 11, pp. 717-723, 2002.

[34] D. C. Evans and G. S. Senior, “Self-lubricating materials for plain bearings,” *Tribology International*, vol. 15, no. 5, pp. 243-248, 1982.

[35] H. E. Sliney, “Solid lubricant materials for high temperatures—a review,” *Tribology International*, vol. 15, no. 5, pp. 303-315, 1982.

[36] M. N. Gardos, “Self-lubricating composites for extreme environment applications,” *Tribology International*, vol. 15, no. 5, pp. 273-283, 1982.

[37] M. H. Jones and D. Scott, *Industrial Tribology: Practical Aspects of Friction, Lubrication and Wear*. Elsevier Science Ltd, 1983, p. 516.

[38] D. Dowson, *History of Tribology*. Wiley-Blackwell, 1998, p. 768.

[39] T. F. J. Quinn, “Tribology,” *Physics Education*, vol. 12, no. 3, pp. 140-143, Apr. 1977.

[40] K. U. Katz and M. G. Katz, “Stevin Numbers and Reality,” *Foundations of Science*, vol. 17, no. 2, pp. 109-123, May 2011.

[41] I. H. Shames, *Mechanics of fluids (McGraw-Hill series in mechanical engineering)*. McGraw-Hill, 1982, p. 773.

[42] M. Nosonovsky and B. Bhushan, “Multiscale friction mechanisms and hierarchical surfaces in nano- and bio-tribology,” *Materials Science and Engineering: R: Reports*, vol. 58, no. 3, pp. 162-193, 2007.

[43] V. L. Popov, *Contact Mechanics and Friction: Physical Principles and Applications*. Springer, 2010, p. 362.

[44] P. J. Blau, *Friction Science and Technology: From Concepts to Applications, Second Edition (Dekker Mechanical Engineering)*. CRC Press, 2008, p. 432.

[45] G. M. Bartenev, *Friction and Wear of Polymers (Composite Materials)*. Elsevier Science Ltd, 1982, p. 338.

[46] R. Chattopadhyay, *Surface Wear: Analysis, Treatment, and Prevention*. ASM International, 2001, p. 307.

[47] T. S. Eyre, "Wear characteristics of metals," *Tribology International*, vol. 9, no. 5, pp. 203-212, 1976.

[48] J. A. Williams, "Wear modelling: analytical, computational and mapping: a continuum mechanics approach," *Wear*, vol. 225, pp. 1-17, 1999.

[49] R. G. Bayer, *Mechanical wear prediction and prevention*. M. Dekker, 1994, p. 657.

[50] W. M. da Silva, H. L. Costa, and J. D. B. de Mello, "Transitions in abrasive wear mechanisms: Effect of the superimposition of interactions," *Wear*, vol. 271, no. 5, pp. 977-986, 2011.

[51] T. S. Eyre, "Abrasive wear," *Tribology International*, vol. 11, no. 1. pp. 4-5, 1978.

[52] J. D. Gates, "Two-body and three-body abrasion: A critical discussion," *Wear*, vol. 214, no. 1, pp. 139-146, Jan. 1998.

[53] M. . Hamblin and G. . Stachowiak, "Characterisation of surface abrasivity and its relation to two-body abrasive wear," *Wear*, vol. 206, no. 1, pp. 69-75, 1997.

[54] G. W. Stachowiak, "Particle angularity and its relationship to abrasive and erosive wear," *Wear*, vol. 241, no. 2, pp. 214-219, 2000.

[55] M. G. Hamblin and G. W. Stachowiak, "A multi-scale measure of particle abrasivity, and its relation to two-body abrasive wear," *Wear*, vol. 190, no. 2, pp. 190-196, 1995.

[56] K. C. Ludema, S. J. Shaffer, R. C. Cozza, J. D. B. de Mello, D. K. Tanaka, and R. M. Souza, "Relationship between test severity and wear mode transition in micro-abrasive wear tests," *Wear*, vol. 263, no. 1, pp. 111-116, 2007.

[57] P. . Shipway and C. J. . Hodge, "Microabrasion of glass – the critical role of ridge formation," *Wear*, vol. 237, no. 1, pp. 90-97, 2000.

[58] M. . Stack and M. Mathew, "Micro-abrasion transitions of metallic materials," *Wear*, vol. 255, no. 1, pp. 14-22, 2003.

[59] K. L. Rutherford and I. M. Hutchings, "A micro-abrasive wear test, with particular application to coated systems," *Surface and Coatings Technology*, vol. 79, no. 1, pp. 231-239, 1996.

[60] T. F. J. Quinn, "Review of oxidational wear," *Tribology International*, vol. 16, no. 5, pp. 257-271, 1983.

[61] T. F. J. Quinn, “Role of oxidation in the mild wear of steel,” *British Journal of Applied Physics*, vol. 13, no. 1, pp. 33-37, Jan. 1962.

[62] B. Bhushan, *Introduction to Tribology*. John Wiley & Sons, 2002, p. 752.

[63] N. Axén, S. Jacobson, and S. Hogmark, “Influence of hardness of the counterbody in three-body abrasive wear — an overlooked hardness effect,” *Tribology International*, vol. 27, no. 4, pp. 233-241, 1994.

[64] K. Adachi and I. M. Hutchings, “Wear-mode mapping for the micro-scale abrasion test,” *Wear*, vol. 255, no. 1, pp. 23-29, 2003.

[65] S. M. Hsu, M. C. Shen, and A. W. Ruff, “Wear prediction for metals,” *Tribology International*, vol. 30, no. 5, pp. 377-383, 1997.

[66] D. A. Rigney, “Comments on the sliding wear of metals,” *Tribology International*, vol. 30, no. 5. pp. 361-367, 1997.

[67] M. A. Masen, M. B. de Rooij, and D. J. Schipper, “Micro-contact based modelling of abrasive wear,” *Wear*, vol. 258, no. 1, pp. 339-348, 2005.

[68] F. H. Stott, “High-temperature sliding wear of metals,” *Tribology International*, vol. 35, no. 8, pp. 489-495, 2002.

[69] Z. M. Jin, M. Stone, E. Ingham, and J. Fisher, “Biotribology,” *Current Orthopaedics*, vol. 20, no. 1, pp. 32-40, Feb. 2006.

[70] D. F. Williams and E. S. for Biomaterials, *Definitions in biomaterials: proceedings of a consensus conference of the European Society for Biomaterials, Chester, England, March 3-5, 1986*. Elsevier, 1987, p. 72.

[71] F. H. Jones, “Teeth and bones: applications of surface science to dental materials and related biomaterials,” *Surface Science Reports*, vol. 42, no. 3, pp. 75-205, 2001.

[72] S. Bauer, P. Schmuki, K. von der Mark, and J. Park, “Engineering biocompatible implant surfaces,” *Progress in Materials Science*, vol. 58, no. 3, pp. 261-326, Apr. 2013.

[73] J. Y. Wong and J. D. Bronzino, *Biomaterials*. CRC Press, 2007, p. 296.

[74] D. H. Kohn, “Metals in medical applications,” *Current Opinion in Solid State and Materials Science*, vol. 3, no. 3, pp. 309-316, 1998.

[75] J. S. Temenoff and A. G. Mikos, *Biomaterials: The Intersection of Biology and Materials Science*. Prentice Hall, 2008, p. 504.

[76] H. J. Conrad, W.-J. Seong, and I. J. Pesun, “Current ceramic materials and systems with clinical recommendations: A systematic review,” *The Journal of Prosthetic Dentistry*, vol. 98, no. 5, pp. 389-404, 2007.

[77] I. Denry and J. R. Kelly, “State of the art of zirconia for dental applications,” *Dental Materials*, vol. 24, no. 3, pp. 299-307, 2008.

[78] A. J. Raigrodski, “Contemporary materials and technologies for all-ceramic fixed partial dentures: A review of the literature,” *The Journal of Prosthetic Dentistry*, vol. 92, no. 6, pp. 557-562, 2004.

[79] R. G. Luthardt, M. S. Holzhüter, H. Rudolph, V. Herold, and M. H. Walter, “CAD/CAM-machining effects on Y-TZP zirconia,” *Dental Materials*, vol. 20, no. 7, pp. 655-662, 2004.

[80] F. Carinci et al., “Zirconium oxide: analysis of MG63 osteoblast-like cell response by means of a microarray technology,” *Biomaterials*, vol. 25, no. 2, pp. 215-228, 2004.

[81] M. Cattani-Lorente, S. S. Scherrer, P. Ammann, M. Jobin, and H. W. A. Wiskott, “Low temperature degradation of a Y-TZP dental ceramic,” *Acta Biomaterialia*, vol. 7, no. 2, pp. 858-865, 2011.

[82] J. Chevalier, “What future for zirconia as a biomaterial?,” *Biomaterials*, vol. 27, no. 4, pp. 535-543, 2006.

[83] J. R. Kelly and I. Denry, “Stabilized zirconia as a structural ceramic: An overview,” *Dental Materials*, vol. 24, no. 3, pp. 289-298, 2008.

[84] J. D. Bronzino, *Biomedical Engineering Handbook, Volume I*. CRC Press, 1999, p. 1656.

[85] R. A. Antunes and M. C. L. de Oliveira, “Corrosion fatigue of biomedical metallic alloys: mechanisms and mitigation.,” *Acta biomaterialia*, vol. 8, no. 3, pp. 937-62, Mar. 2012.

[86] A. Itman Filho, J. M. D. A. Rollo, R. V. Silva, and G. Martinez, “Alternative process to manufacture austenitic–ferritic stainless steel wires,” *Materials Letters*, vol. 59, no. 10, pp. 1192-1194, Apr. 2005.

[87] S. Karimi, T. Nickchi, and A. M. Alfantazi, “Long-term corrosion investigation of AISI 316L, Co–28Cr–6Mo, and Ti–6Al–4V alloys in simulated body solutions,” *Applied Surface Science*, vol. 258, no. 16, pp. 6087-6096, 2012.

[88] C. B. von der Ohe, R. Johnsen, and N. Espallargas, “A multi-degradation test rig for studying the synergy effects of tribocorrosion interacting with 4-point static and cyclic bending,” *Wear*, vol. 271, no. 11, pp. 2978-2990, 2011.

[89] “ASTM G75 - 07 Standard Test Method for Determination of Slurry Abrasivity (Miller Number) and Slurry Abrasion Response of Materials (SAR Number).” .

[90] “ASTM G119 - 09 Standard Guide for Determining Synergism Between Wear and Corrosion.” [Online]. Available: http://www.astm.org/Standards/G119.htm. [Accessed: 26-Sep-2013].

[91] R. . Trezona and I. . Hutchings, “Three-body abrasive wear testing of soft materials,” *Wear*, vol. 233, pp. 209-221, 1999.

[92] S. Mischler and A. I. Muñoz, “Wear of CoCrMo alloys used in metal-on-metal hip joints: A tribocorrosion appraisal,” *Wear*, vol. 297, no. 1, pp. 1081-1094, 2013.

[93] J. Jiang, M. M. Stack, and A. Neville, “Modelling the tribo-corrosion interaction in aqueous sliding conditions,” *Tribology International*, vol. 35, no. 10, pp. 669-679, 2002.

[94] M. M. Stack, M. T. Mathew, and C. Hodge, “Micro-abrasion–corrosion interactions of Ni–Cr/WC based coatings: Approaches to construction of tribo-corrosion maps for the abrasion–corrosion synergism,” *Electrochimica Acta*, vol. 56, no. 24, pp. 8249-8259, 2011.

[95] C. Hodge and M. M. Stack, “Tribo-corrosion mechanisms of stainless steel in soft drinks,” *Wear*, vol. 270, no. 1, pp. 104-114, 2010.

[96] M. M. Stack et al., “Micro-abrasion–corrosion of a Co–Cr/UHMWPE couple in Ringer’s solution: An approach to construction of mechanism and synergism maps for application to bio-implants,” *Wear*, vol. 269, no. 5, pp. 376-382, 2010.

[97] R. Wood, A. Neville, M. R. Thakare, J. A. Wharton, R. J. K. Wood, and C. Menger, “Investigation of micro-scale abrasion–corrosion of WC-based sintered hardmetal and sprayed coating using in situ electrochemical current-noise measurements,” *Wear*, vol. 267, no. 11, pp. 1967-1977, 2009.

[98] K. C. Ludema, S. J. Shaffer, M. R. Thakare, J. A. Wharton, R. J. K. Wood, and C. Menger, “Exposure effects of alkaline drilling fluid on the microscale abrasion–corrosion of WC-based hardmetals,” *Wear*, vol. 263, no. 1, pp. 125-136, 2007.

[99] S. J. Shaffer, J. O. Bello, R. J. K. Wood, and J. A. Wharton, “Synergistic effects of micro-abrasion–corrosion of UNS S30403, S31603 and S32760 stainless steels,” *Wear*, vol. 263, no. 1, pp. 149-159, 2007.

[100] S. . Lim, “Recent developments in wear-mechanism maps,” *Tribology International*, vol. 31, no. 1, pp. 87-97, 1998.

[101] S. Amini and A. Miserez, “Wear and abrasion resistance selection maps of biological materials,” *Acta Biomaterialia*, vol. 9, no. 8, pp. 7895-7907, 2013.

[102] I. D. Marinescu, *Tribology of Abrasive Machining Processes*. William Andrew, 2012, p. 800.

[103] C. G. Telfer, M. M. Stack, and B. D. Jana, “Particle concentration and size effects on the erosion-corrosion of pure metals in aqueous slurries,” *Tribology International*, vol. 53, pp. 35-44, 2012.

[104] M. M. Stack, S. M. Abdelrahman, and B. D. Jana, “A new methodology for modelling erosion–corrosion regimes on real surfaces: Gliding down the galvanic series for a range of metal-corrosion systems,” *Wear*, vol. 268, no. 3, pp. 533-542, 2010.

[105] A. Cantizano, A. Carnicero, and G. Zavarise, “Numerical simulation of wear-mechanism maps,” *Computational Materials Science*, vol. 25, no. 1, pp. 54-60, 2002.

[106] H. Li and Z. R. Zhou, “Wear behaviour of human teeth in dry and artificial saliva conditions,” *Wear*, vol. 249, no. 10-11, pp. 980-984, Nov. 2001.

[107] H.-C. Wang, M. M. Stack, W.-L. Li, T.-F. Hong, and M.-C. Wang, “On the construction of wear maps for Y-TZP dental ceramics in aqueous environments: pH, exposure time and impact angle effects,” *Tribology International*, vol. 43, no. 12, pp. 2258-2267, Dec. 2010.

[108] S. K. Sinha, N. Satyanarayana, S. C. Lim, J. Zheng, and Z. R. Zhou, “Friction and wear behavior of human teeth under various wear conditions,” *Tribology International*, vol. 40, no. 2, pp. 278-284, 2007.

[109] V. Preis, M. Behr, C. Kolbeck, S. Hahnel, G. Handel, and M. Rosentritt, “Wear performance of substructure ceramics and veneering porcelains,” *Dental Materials*, vol. 27, no. 8, pp. 796-804, 2011.

[110] P. Bourdiol and L. Mioche, “Correlations between functional and occlusal tooth-surface areas and food texture during natural chewing sequences in humans,” *Archives of Oral Biology*, vol. 45, no. 8, pp. 691-699, 2000.

[111] P. Sevilla, C. Sandino, M. Arciniegas, J. Martínez-Gomis, M. Peraire, and F. J. Gil, “Evaluating mechanical properties and degradation of YTZP dental implants,” *Materials Science and Engineering: C*, vol. 30, no. 1, pp. 14-19, 2010.

[112] O. Zidan and U. Abdel-Keriem, “The effect of amalgam bonding on the stiffness of teeth weakened by cavity preparation,” *Dental Materials*, vol. 19, no. 7, pp. 680-685, 2003.

[113] J. L. Shi, G. Q. Zhu, and T. R. Lai, “Compressive deformation behaviour of superplastic Y-TZP-based ceramics: Role of grain boundary phases,” *Journal of the European Ceramic Society*, vol. 17, no. 6, pp. 851-858, 1997.

[114] A. Médevielle, F. Thévenot, and D. Tréheux, “Wear resistance of zirconias. Dielectrical approach,” *Wear*, vol. 213, no. 1, pp. 13-20, 1997.

[115] P. Hvizdoš, Á. Mestra, and M. Anglada, “Effect of heat treatment on wear damage mechanisms in 3Y-TZP ceramics,” *Wear*, vol. 269, no. 1, pp. 26-30, 2010.

[116] J. Phelan and J. Rees, “The erosive potential of some herbal teas,” *Journal of Dentistry*, vol. 31, no. 4, pp. 241-246, 2003.

[117] P. A. Brunton and A. Hussain, “The erosive effect of herbal tea on dental enamel,” *Journal of Dentistry*, vol. 29, no. 8, pp. 517-520, 2001.

[118] I. M. Low and A. Alhuthali, “In-situ monitoring of dental erosion in tooth enamel when exposed to soft drinks,” *Materials Science and Engineering: C*, vol. 28, no. 8. pp. 1322-1325, 2008.

[119] M. E. Barbour, M. Finke, D. M. Parker, J. A. Hughes, G. C. Allen, and M. Addy, “The relationship between enamel softening and erosion caused by soft drinks at a range of temperatures,” *Journal of Dentistry*, vol. 34, no. 3, pp. 207-213, 2006.

[120] J. F. Tahmassebi, M. S. Duggal, G. Malik-Kotru, and M. E. J. Curzon, “Soft drinks and dental health: A review of the current literature,” *Journal of Dentistry*, vol. 34, no. 1, pp. 2-11, 2006.

[121] D. Rios, H. M. Honório, A. C. Magalhães, A. Wiegand, M. A. de Andrade Moreira Machado, and M. A. R. Buzalaf, “Light cola drink is less erosive than the regular one: An in situ/ex vivo study,” *Journal of Dentistry*, vol. 37, no. 2. pp. 163-166, 2009.

[122] S. Lawson, “Environmental degradation of zirconia ceramics,” *Journal of the European Ceramic Society*, vol. 15, no. 6, pp. 485-502, 1995.

[123] F. J. Buchanan and P. H. Shipway, “Microabrasion—a simple method to assess surface degradation of UHMWPE following sterilisation and ageing,” *Biomaterials*, vol. 23, no. 1, pp. 93-100, 2002.

[124] J. A. Puértolas, A. Larrea, and E. Gómez-Barrena, “Fracture behavior of UHMWPE in non-implanted, shelf-aged knee prostheses after gamma irradiation in air,” *Biomaterials*, vol. 22, no. 15, pp. 2107-2114, 2001.

[125] D. Xiong, Z. Gao, and Z. Jin, “Friction and wear properties of UHMWPE against ion implanted titanium alloy,” *Surface and Coatings Technology*, vol. 201, no. 15, pp. 6847-6850, Apr. 2007.

[126] S. Ge, S. Wang, N. Gitis, M. Vinogradov, and J. Xiao, “Wear behavior and wear debris distribution of UHMWPE against Si3N4 ball in bi-directional sliding,” *Wear*, vol. 264, no. 7, pp. 571-578, 2008.

[127] K. Marcus and C. Allen, “The sliding wear of ultrahigh molecular weight polyethylene in an aqueous environment,” *Wear*, vol. 178, no. 1, pp. 17-28, 1994.

[128] P. Lambrechts, E. Debels, K. Van Landuyt, M. Peumans, and B. Van Meerbeek, “How to simulate wear? Overview of existing methods.,” *Dental materials : official publication of the Academy of Dental Materials*, vol. 22, no. 8, pp. 693-701, Aug. 2006.

[129] G. J. . Fleming, H. S. Jandu, L. Nolan, and F. . Shaini, “The influence of alumina abrasion and cement lute on the strength of a porcelain laminate veneering material,” *Journal of Dentistry*, vol. 32, no. 1, pp. 67-74, 2004.

[130] Q. Sun, K. Reuter, and M. Scheffler, “Effect of a humid environment on the surface structure of RuO 2 (110),” *Structure*, vol. 2, no. July, 2002.

[131] A. G. Khurshudov, Y. N. Drozdov, and K. Kato, “Transitional phenomena in the lubricated heavily loaded sliding contact of ceramics and steel,” *Wear*, vol. 184, no. 2, pp. 179-186, 1995.

[132] K. Bose and R. J. K. Wood, “Optimum tests conditions for attaining uniform rolling abrasion in ball cratering tests on hard coatings,” *Wear*, vol. 258, no. 1, pp. 322-332, 2005.

[133] M. Albu et al., “Ball cratering an efficient tool for 3 body microabrasion of coated systems,” *Surface and Coatings Technology*, vol. 200, no. 1, pp. 153-156, 2005.

[134] R. V. Camerini, R. B. de Souza, F. de Carli, A. S. Pereira, and N. M. Balzaretti, “Ball cratering test on ductile materials,” *Wear*, vol. 271, no. 5-6, pp. 770-774, Jun. 2011.

[135] L. He, “Mechanical behaviour of human enamel and the relationship to its structural and compositional characteristics.,” University of Sydney, 2008.

[136] G. W. Stachowiak and G. B. Stachowiak, “Environmental effects on wear and friction of toughened zirconia ceramics,” *Wear*, vol. 160, no. 1, pp. 153-162, 1993.

[137] R. S. D.-J. and R. Lewis, “Wear of human teeth: A tribological perspective,” *Journal of Engineering Tribology*, vol. 219, no. 1, pp. 1-18, 2005.

[138] C. and M. M. S. Hodge, “The effect of slurry concentration on the micro-abrasive wear behaviour encountered by pure aluminium in aqueous conditions.” University of Strathclyde, 2009.

[139] M. Turell, A. Wang, and A. Bellare, “Quantification of the effect of cross-path motion on the wear rate of ultra-high molecular weight polyethylene,” *Wear*, vol. 255, no. 7, pp. 1034-1039, 2003.

[140] S. Raghavan, H. Wang, W. D. Porter, R. B. Dinwiddie, and M. J. Mayo, “Thermal properties of zirconia co-doped with trivalent and pentavalent oxides,” *Acta Materialia*, vol. 49, no. 1, pp. 169-179, 2001.

[141] T. Kimura and T. Goto, “Thermal conductivities of yttria-stabilized zirconia films measured by a laser-heating AC method,” *Surface and Coatings Technology*, vol. 198, no. 1, pp. 129-132, 2005.

[142] M. G. Gee et al., “Progress towards standardisation of ball cratering,” *Wear*, vol. 255, no. 1, pp. 1-13, 2003.

[143] G. B. Stachowiak, G. W. Stachowiak, and J. M. Brandt, “Ball-cratering abrasion tests with large abrasive particles,” *Tribology International*, vol. 39, no. 1, pp. 1-11, 2006.

[144] R. I. Trezona, D. N. Allsopp, and I. M. Hutchings, “Transitions between two-body and three-body abrasive wear: influence of test conditions in the microscale abrasive wear test,” *Wear*, vol. 225-229, no. null, pp. 205-214, Apr. 1999.

[145] M. . Stack and M. Mathew, “Micro-abrasion transitions of metallic materials,” *Wear*, vol. 255, no. 1-6, pp. 14-22, Aug. 2003.

[146] K. Adachi, K. Kato, and N. Chen, “Wear map of ceramics,” *Wear*, vol. 203, pp. 291-301, 1997.

[147] S. M. Hsu and M. Shen, “Wear prediction of ceramics,” *Wear*, vol. 256, no. 9, pp. 867-878, 2004.

[148] M. Kalin, S. Novak, and J. Vižintin, “Wear and friction behavior of alumina ceramics in aqueous solutions with different pH,” *Wear*, vol. 254, no. 11, pp. 1141-1146, 2003.

[149] H. J. Smit, M. L. Grady, Y. E. Finnegan, S.-A. C. Hughes, J. R. Cotton, and P. J. Rogers, “Role of familiarity on effects of caffeine- and glucose-containing soft drinks,” *Physiology & Behavior*, vol. 87, no. 2, pp. 287-297, 2006.

[150] J. Chevalier, S. Deville, E. Münch, R. Jullian, and F. Lair, “Critical effect of cubic phase on aging in 3mol% yttria-stabilized zirconia ceramics for hip replacement prosthesis,” *Biomaterials*, vol. 25, no. 24, pp. 5539-5545, 2004.

[151] C. Lorenzo-Martín et al., “Mechanical behaviour of yttria tetragonal zirconia polycrystalline nanoceramics: dependence on the glassy phase content,” *Journal of the European Ceramic Society*, vol. 22, no. 14, pp. 2603-2607, 2002.

[152] S. Sharifi, M. M. Stack, L. Stephen, W.-L. Li, and M.-C. Wang, “Micro-abrasion of Y-TZP in tea,” *Wear*, pp. 713-721, 2013.

[153] V. Sobolık, R. Žitný, V. Tovcigrecko, M. Delgado, and K. Allaf, “Viscosity and electrical conductivity of concentrated solutions of soluble coffee,” *Journal of Food Engineering*, vol. 51, no. 2, pp. 93-98, 2002.

[154] A. U. Guler, F. Yilmaz, T. Kulunk, E. Guler, and S. Kurt, “Effects of different drinks on stainability of resin composite provisional restorative materials,” *The Journal of Prosthetic Dentistry*, vol. 94, no. 2, pp. 118-124, 2005.

[155] R. Wood, A. Neville, W. M. da Silva, and J. D. B. de Mello, “Using parallel scratches to simulate abrasive wear,” *Wear*, vol. 267, no. 11, pp. 1987-1997, 2009.

[156] R. Mattes and M. G. Ferruzzi, “The influence of beverage composition on delivery of phenolic compounds from coffee and tea,” *Physiology & Behavior*, vol. 100, no. 1, pp. 33-41, 2010.

[157] A. J. Gant and M. G. Gee, “A review of micro-scale abrasion testing,” *Journal of Physics D: Applied Physics*, vol. 44, no. 7, p. 073001, Feb. 2011.

[158] M.-L. Jalabert-Malbos, A. Mishellany-Dutour, A. Woda, and M.-A. Peyron, “Particle size distribution in the food bolus after mastication of natural foods,” *Food Quality and Preference*, vol. 18, no. 5, pp. 803-812, 2007.

[159] K. Shiozawa and K. Kohyama, “Effects of Addition of Water on Masticatory Behavior and the Mechanical Properties of the Food Bolus,” *Journal of Oral Biosciences*, vol. 53, no. 2, pp. 148-157, 2011.

[160] L. Mioche, P. Bourdiol, S. Monier, J.-F. Martin, and D. Cormier, “Changes in jaw muscles activity with age: effects on food bolus properties,” *Physiology & Behavior*, vol. 82, no. 4, pp. 621-627, 2004.

[161] A. Mishellany-Dutour et al., “Comparison of food boluses prepared in vivo and by the AM2 mastication simulator,” *Food Quality and Preference*, vol. 22, no. 4, pp. 326-331, 2011.

[162] J. Chen, N. Khandelwal, Z. Liu, and T. Funami, “Influences of food hardness on the particle size distribution of food boluses,” *Archives of Oral Biology*, vol. 58, no. 3, pp. 293-298, 2013.

[163] D.-W. Kim and K.-W. Kim, “Effects of sliding velocity and normal load on friction and wear characteristics of multi-layered diamond-like carbon (DLC) coating prepared by reactive sputtering,” *Wear*, vol. 297, no. 1-2, pp. 722-730, Jan. 2013.

[164] B. K. Prasad, S. Das, A. K. Jha, O. P. Modi, R. Dasgupta, and A. H. Yegneswaran, “Factors controlling the abrasive wear response of a zinc-based alloy silicon carbide particle composite,” *Composites Part A: Applied Science and Manufacturing*, vol. 28, no. 4, pp. 301-308, 1997.

[165] Z. R. Zhou and J. Zheng, “Tribology of dental materials: a review,” *Journal of Physics D: Applied Physics*, vol. 41, no. 11, p. 113001, Jun. 2008.

[166] E. Sajewicz and Z. Kulesza, “A new tribometer for friction and wear studies of dental materials and hard tooth tissues,” *Tribology International*, vol. 40, no. 5, pp. 885-895, 2007.

[167] K. Marcus and C. Allen, “The sliding wear of ultrahigh molecular weight polyethylene in an aqueous environment,” *Wear*, vol. 178, no. 1-2, pp. 17-28, Nov. 1994.

[168] A. M. Korsunsky et al., “Increasing wear resistance of UHMWPE by mechanical activation and chemical modification combined with addition of nanofibers,” *Procedia Engineering*, vol. 1, no. 1, pp. 67-70, 2009.

[169] S. D. Heintze, G. Zellweger, I. Grunert, C. A. Muñoz-Viveros, and K. Hagenbuch, “Laboratory methods for evaluating the wear of denture teeth and their correlation with clinical results,” *Dental Materials*, vol. 28, no. 3, pp. 261-272, 2012.

[170] Z. H. Baqain, W. Y. Moqbel, and F. A. Sawair, “Early dental implant failure: risk factors,” *British Journal of Oral and Maxillofacial Surgery*, vol. 50, no. 3, pp. 239-243, 2012.

[171] G. F. Ferrazzano, I. Amato, A. Ingenito, A. De Natale, and A. Pollio, “Anti-cariogenic effects of polyphenols from plant stimulant beverages (cocoa, coffee, tea),” *Fitoterapia*, vol. 80, no. 5, pp. 255-262, 2009.

[172] A. B. Sharangi, “Medicinal and therapeutic potentialities of tea (Camellia sinensis L.) – A review,” *Food Research International*, vol. 42, no. 5, pp. 529-535, 2009.

[173] M. Shabanian and L. C. Richards, “In vitro wear rates of materials under different loads and varying pH,” *The Journal of Prosthetic Dentistry*, vol. 87, no. 6, pp. 650-656, 2002.

[174] M. M. Stack, W. Huang, G. Wang, and C. Hodge, “Some views on the construction of bio-tribo-corrosion maps for Titanium alloys in Hank’s solution: Particle concentration and applied loads effects,” *Tribology International*, vol. 44, no. 12, pp. 1827-1837, 2011.

[175] J. S. Ren et al., “Tea, coffee, carbonated soft drinks and upper gastrointestinal tract cancer risk in a large United States prospective cohort study,” *European Journal of Cancer*, vol. 46, no. 10, pp. 1873-1881, 2010.

[176] H.-C. Wang, M. M. Stack, W.-L. Li, T.-F. Hong, and M.-C. Wang, “On the construction of wear maps for Y-TZP dental ceramics in aqueous environments: pH, exposure time and impact angle effects,” *Tribology International*, vol. 43, no. 12, pp. 2258-2267, 2010.

[177] M. M. Stack, J. A. Williams, H. Jawan, and M. T. Mathew, “On the construction of micro-abrasion maps for a steel/polymer couple in corrosive environments,” *Tribology International*, vol. 38, no. 9, pp. 848-856, 2005.

[178] H. P. Papanagiotou, S. M. Morgano, R. A. Giordano, and R. Pober, “In vitro evaluation of low-temperature aging effects and finishing procedures on the flexural strength and structural stability of Y-TZP dental ceramics,” *The Journal of Prosthetic Dentistry*, vol. 96, no. 3, pp. 154-164, 2006.

[179] L. Hallmann, P. Ulmer, E. Reusser, M. Louvel, and C. H. F. Hämmerle, “Effect of dopants and sintering temperature on microstructure and low temperature degradation of dental Y-TZP-zirconia,” *Journal of the European Ceramic Society*, vol. 32, no. 16, pp. 4091-4104, 2012.

[180] A. H. a Sabrah, N. B. Cook, P. Luangruangrong, A. T. Hara, and M. C. Bottino, “Full-contour Y-TZP ceramic surface roughness effect on synthetic hydroxyapatite wear.,” *Dental materials : official publication of the Academy of Dental Materials*, vol. 29, no. 6, pp. 666-73, Jun. 2013.

[181] V. Preis, M. Behr, G. Handel, S. Schneider-Feyrer, S. Hahnel, and M. Rosentritt, "Wear performance of dental ceramics after grinding and polishing treatments," *Journal of the Mechanical Behavior of Biomedical Materials*, vol. 10, pp. 13-22, 2012.

[182] A. Kocijan, D. K. Merl, and M. Jenko, "The corrosion behaviour of austenitic and duplex stainless steels in artificial saliva with the addition of fluoride," *Corrosion Science*, vol. 53, no. 2, pp. 776-783, Feb. 2011.

[183] S. Pourhashem and A. Afshar, "Double layer bioglass-silica coatings on 316L stainless steel by sol–gel method," *Ceramics International*, vol. null, no. null, Jul. 2013.

[184] M. . Fathi, M. Salehi, A. Saatchi, V. Mortazavi, and S. . Moosavi, "In vitro corrosion behavior of bioceramic, metallic, and bioceramic–metallic coated stainless steel dental implants," *Dental Materials*, vol. 19, no. 3, pp. 188-198, May 2003.

[185] E. Sajewicz, "Effect of saliva viscosity on tribological behaviour of tooth enamel," *Tribology International*, vol. 42, no. 2, pp. 327-332, Feb. 2009.

[186] J. Gibson and J. Beeley, "Natural and synthetic saliva: a stimulating subject," *Biotechnology and Genetic Engineering Reviews*, vol. 12, pp. 39-62, 1994.

[187] D. Ziskind, E. Venezia, I. Kreisman, and E. Mass, "Amalgam type, adhesive system, and storage period as influencing factors on microleakage of amalgam restorations," *The Journal of Prosthetic Dentistry*, vol. 90, no. 3, pp. 255-260, Sep. 2003.

[188] B. B. Zhang, Y. F. Zheng, and Y. Liu, "Effect of Ag on the corrosion behavior of Ti-Ag alloys in artificial saliva solutions.," *Dental materials : official publication of the Academy of Dental Materials*, vol. 25, no. 5, pp. 672-7, May 2009.

[189] C. M. A. Brett and F. Trandafir, "The corrosion of dental amalgam in artificial salivas: an electrochemical impedance study," *Journal of Electroanalytical Chemistry*, vol. 572, no. 2, pp. 347-354, Nov. 2004.

[190] K. Elagli, M. Traisnel, and H. F. Hildebrand, "Electrochemical behaviour of titanium and dental alloys in artificial saliva," *Electrochimica Acta*, vol. 38, no. 13, pp. 1769-1774, Sep. 1993.

[191] J. C. M. Souza, S. L. Barbosa, E. Ariza, J.-P. Celis, and L. A. Rocha, "Simultaneous degradation by corrosion and wear of titanium in artificial saliva containing fluorides," *Wear*, vol. 292-293, no. null, pp. 82-88, Jul. 2012.

[192] A. C. Vieira, A. R. Ribeiro, L. A. Rocha, and J. P. Celis, "Influence of pH and corrosion inhibitors on the tribocorrosion of titanium in artificial saliva," *Wear*, vol. 261, no. 9, pp. 994-1001, Nov. 2006.

[193] I. M. Hutchings, *Tribology: Friction and Wear of Engineering Materials (Metallurgy & Materials Science)*. Butterworth-Heinemann Ltd, 1992, p. 280.

[194] S. Ge, S. Wang, N. Gitis, M. Vinogradov, and J. Xiao, “Wear behavior and wear debris distribution of UHMWPE against Si3N4 ball in bi-directional sliding,” *Wear*, vol. 264, no. 7-8, pp. 571-578, Mar. 2008.

[195] S. Affatato, M. Spinelli, M. Zavalloni, C. Mazzega-Fabbro, and M. Viceconti, “Tribology and total hip joint replacement: current concepts in mechanical simulation.,” *Medical engineering & physics*, vol. 30, no. 10, pp. 1305-17, Dec. 2008.

[196] S. Kurtz, K. Ong, E. Lau, F. Mowat, and M. Halpern, “Projections of primary and revision hip and knee arthroplasty in the United States from 2005 to 2030.,” *The Journal of bone and joint surgery. American volume*, vol. 89, no. 4, pp. 780-5, Apr. 2007.

[197] S. J. Mellon, A. D. Liddle, and H. Pandit, “Hip replacement: landmark surgery in modern medical history.,” *Maturitas*, vol. 75, no. 3, pp. 221-6, Jul. 2013.

[198] R. M. Hall, M. J. K. Bankes, and G. Blunn, “Biotribology for joint replacement,” *Current Orthopaedics*, vol. 15, no. 4. pp. 281-290, 2001.

[199] M. P. Gispert, A. P. Serro, R. Colaço, E. Pires, and B. Saramago, “Wear of ceramic coated metal-on-metal bearings used for hip replacement,” *Wear*, vol. 263, no. 7-12, pp. 1060-1065, Sep. 2007.

[200] S. Williams, G. Isaac, P. Hatto, M. H. Stone, E. Ingham, and J. Fisher, “Comparative wear under different conditions of surface-engineered metal-on-metal bearings for total hip arthroplasty,” *The Journal of Arthroplasty*, vol. 19, no. 8, pp. 112-117, Dec. 2004.

[201] R. Hauert, “An overview on the tribological behavior of diamond-like carbon in technical and medical applications,” *Tribology International*, vol. 37, no. 11-12, pp. 991-1003, Nov. 2004.

[202] M. T. Mathew, T. Uth, N. J. Hallab, R. Pourzal, A. Fischer, and M. A. Wimmer, “Construction of a tribocorrosion test apparatus for the hip joint: Validation, test methodology and analysis,” *Wear*, vol. 271, no. 9. pp. 2651-2659, 2011.

[203] T. P. Schmalzried, P. C. Peters, B. T. Maurer, C. R. Bragdon, and W. H. Harris, “Long-duration metal-on-metal total hip arthroplasties with low wear of the articulating surfaces,” *The Journal of Arthroplasty*, vol. 11, no. 3, pp. 322-331, 1996.

[204] A. Grill, “Review of the tribology of diamond-like carbon,” *Wear*, vol. 168, no. 1, pp. 143-153, 1993.

[205] C. Donnet and A. Erdemir, *Tribology of Diamond-like Carbon Films: Fundamentals and Applications*. Springer, 2010, p. 664.

[206] P. E. Sinnett-Jones, J. A. Wharton, and R. J. K. Wood, “Micro-abrasion–corrosion of a CoCrMo alloy in simulated artificial hip joint environments,” *Wear*, vol. 259, no. 7, pp. 898-909, 2005.

[207] S. Sharifi and M. M. Stack, “A comparison of the tribological behaviour of Y-TZP in tea and coffee under micro-abrasion conditions,” *Journal of Physics D: Applied Physics*, vol. 46, no. 40, p. 404008, Oct. 2013.

[208] J. Hesketh, Q. Meng, D. Dowson, and A. Neville, “Biotribocorrosion of metal-on-metal hip replacements: How surface degradation can influence metal ion formation,” *Tribology International*, vol. 65, no. null, pp. 128-137, Sep. 2013.

[209] E. P. J. Watters, P. L. Spedding, J. Grimshaw, J. M. Duffy, and R. L. Spedding, “Wear of artificial hip joint material,” *Chemical Engineering Journal*, vol. 112, no. 1, pp. 137-144, 2005.